

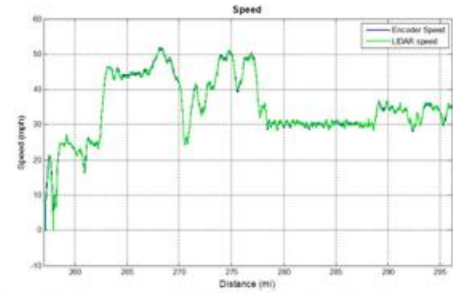
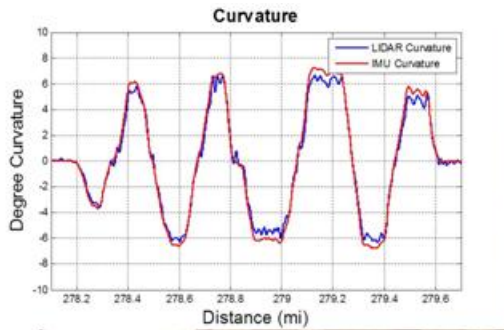


U.S. Department of
Transportation

Federal Railroad
Administration

Multifunction LIDAR Sensors for Noncontact, Speed, and Complex Rail Dynamics

Office of Research
and Development
Washington, DC 20590



NOTICE

This document is disseminated under the sponsorship of the Department of Transportation in the interest of information exchange. The United States Government assumes no liability for its contents or use thereof. Any opinions, findings and conclusions, or recommendations expressed in this material do not necessarily reflect the views or policies of the United States Government, nor does mention of trade names, commercial products, or organizations imply endorsement by the United States Government. The United States Government assumes no liability for the content or use of the material contained in this document.

NOTICE

The United States Government does not endorse products or manufacturers. Trade or manufacturers' names appear herein solely because they are considered essential to the objective of this report.

REPORT DOCUMENTATION PAGE			<i>Form Approved</i> <i>OMB No. 0704-0188</i>
Public reporting burden for this collection of information is estimated to average 1 hour per response, including the time for reviewing instructions, searching existing data sources, gathering and maintaining the data needed, and completing and reviewing the collection of information. Send comments regarding this burden estimate or any other aspect of this collection of information, including suggestions for reducing this burden, to Washington Headquarters Services, Directorate for Information Operations and Reports, 1215 Jefferson Davis Highway, Suite 1204, Arlington, VA 22202-4302, and to the Office of Management and Budget, Paperwork Reduction Project (0704-0188), Washington, DC 20503.			
1. AGENCY USE ONLY (Leave blank)	2. REPORT DATE July 2014	3. REPORT TYPE AND DATES COVERED Technical Report 4/13/11–11/31/12	
4. TITLE AND SUBTITLE Multifunction LIDAR Sensors for Noncontact, Speed, and Complex Rail Dynamics		5. FUNDING NUMBERS	
6. AUTHOR(S) and FRA COTR Mehdi Ahmadian, Michael Craft, Cameron Stuart (FRA – COTR)			
7. PERFORMING ORGANIZATION NAME(S) AND ADDRESS(ES) Virginia Tech 3103 Commerce St Blacksburg, VA 24061		8. PERFORMING ORGANIZATION REPORT NUMBER Final Report #1	
9. SPONSORING/MONITORING AGENCY NAME(S) AND ADDRESS(ES) U.S. Department of Transportation Federal Railroad Administration Office of Research and Development Washington, DC 20590		10. SPONSORING/MONITORING AGENCY REPORT NUMBER DOT/FRA/ORD-14/26	
11. SUPPLEMENTARY NOTES COTR: Cameron Stuart			
12a. DISTRIBUTION/AVAILABILITY STATEMENT This document is available to the public through the FRA Web site at www.fra.dot.gov/us/content/185 , or by calling 202-493-1300.		12b. DISTRIBUTION CODE	
13. ABSTRACT (Maximum 200 words) The results of an extensive series of tests are presented to evaluate the viability and applicability of LIDAR systems for measuring track speed, distance, and curvature in revenue service. The tests indicate that a LIDAR system can successfully provide multifunctional, noncontact measurements with a higher degree of accuracy than encoders and IMUs, at speeds ranging from 0.5 to 100 mph. The tests are conducted onboard FRA's R4 Hy-Rail vehicle and a track geometry measurement railcar. The railcar tests involve a field-hardy, unmanned system that is successfully operated over several months and thousands of revenue service miles. The results indicate that, with further development, the LIDAR technology would be suitable for implementation in FRA's ATGMS and track geometry measurement systems. Additional studies are recommended to further establish the LIDAR system's measurement accuracy, ability to generate a foot pulse (similar to encoder's TTL signal), and potential for measuring track geometry. The LIDAR system must be tested on a trial basis as a retrofit to wheel-mounted encoders to better assess its potential for integration into track geometry cars. A plausible commercialization plan is needed to prepare the technology for revenue service and integration into FRA's ATGMS.			
14. SUBJECT TERMS LIDAR, noncontact velocity measurement, curvature, alignment, ATGMS, track geometry, Railway Technologies Laboratory, Virginia Tech		15. NUMBER OF PAGES 86	16. PRICE CODE
17. SECURITY CLASSIFICATION OF REPORT Unclassified	18. SECURITY CLASSIFICATION OF THIS PAGE Unclassified	19. SECURITY CLASSIFICATION OF ABSTRACT Unclassified	20. LIMITATION OF ABSTRACT

METRIC/ENGLISH CONVERSION FACTORS

ENGLISH TO METRIC

LENGTH (APPROXIMATE)

- 1 inch (in) = 2.5 centimeters (cm)
- 1 foot (ft) = 30 centimeters (cm)
- 1 yard (yd) = 0.9 meter (m)
- 1 mile (mi) = 1.6 kilometers (km)

AREA (APPROXIMATE)

- 1 square inch (sq in, in²) = 6.5 square centimeters (cm²)
- 1 square foot (sq ft, ft²) = 0.09 square meter (m²)
- 1 square yard (sq yd, yd²) = 0.8 square meter (m²)
- 1 square mile (sq mi, mi²) = 2.6 square kilometers (km²)
- 1 acre = 0.4 hectare (he) = 4,000 square meters (m²)

MASS - WEIGHT (APPROXIMATE)

- 1 ounce (oz) = 28 grams (gm)
- 1 pound (lb) = 0.45 kilogram (kg)
- 1 short ton = 2,000 pounds (lb) = 0.9 tonne (t)

VOLUME (APPROXIMATE)

- 1 teaspoon (tsp) = 5 milliliters (ml)
- 1 tablespoon (tbsp) = 15 milliliters (ml)
- 1 fluid ounce (fl oz) = 30 milliliters (ml)
- 1 cup (c) = 0.24 liter (l)
- 1 pint (pt) = 0.47 liter (l)
- 1 quart (qt) = 0.96 liter (l)
- 1 gallon (gal) = 3.8 liters (l)
- 1 cubic foot (cu ft, ft³) = 0.03 cubic meter (m³)
- 1 cubic yard (cu yd, yd³) = 0.76 cubic meter (m³)

TEMPERATURE (EXACT)

$$[(x-32)(5/9)] \text{ } ^\circ\text{F} = y \text{ } ^\circ\text{C}$$

METRIC TO ENGLISH

LENGTH (APPROXIMATE)

- 1 millimeter (mm) = 0.04 inch (in)
- 1 centimeter (cm) = 0.4 inch (in)
- 1 meter (m) = 3.3 feet (ft)
- 1 meter (m) = 1.1 yards (yd)
- 1 kilometer (km) = 0.6 mile (mi)

AREA (APPROXIMATE)

- 1 square centimeter (cm²) = 0.16 square inch (sq in, in²)
- 1 square meter (m²) = 1.2 square yards (sq yd, yd²)
- 1 square kilometer (km²) = 0.4 square mile (sq mi, mi²)
- 10,000 square meters (m²) = 1 hectare (ha) = 2.5 acres

MASS - WEIGHT (APPROXIMATE)

- 1 gram (gm) = 0.036 ounce (oz)
- 1 kilogram (kg) = 2.2 pounds (lb)
- 1 tonne (t) = 1,000 kilograms (kg) = 1.1 short tons

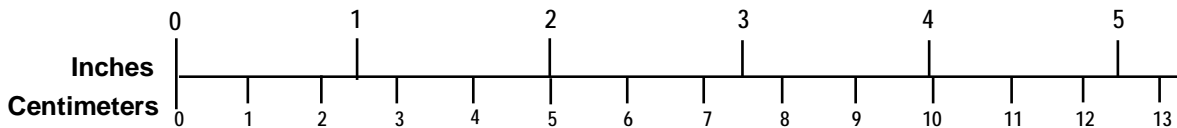
VOLUME (APPROXIMATE)

- 1 milliliter (ml) = 0.03 fluid ounce (fl oz)
- 1 liter (l) = 2.1 pints (pt)
- 1 liter (l) = 1.06 quarts (qt)
- 1 liter (l) = 0.26 gallon (gal)
- 1 cubic meter (m³) = 36 cubic feet (cu ft, ft³)
- 1 cubic meter (m³) = 1.3 cubic yards (cu yd, yd³)

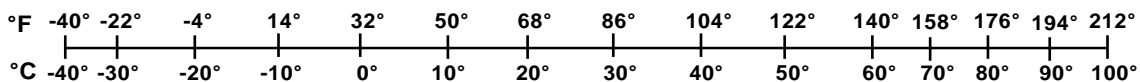
TEMPERATURE (EXACT)

$$[(9/5) y + 32] \text{ } ^\circ\text{C} = x \text{ } ^\circ\text{F}$$

QUICK INCH - CENTIMETER LENGTH CONVERSION



QUICK FAHRENHEIT - CELSIUS TEMPERATURE CONVERSION



For more exact and or other conversion factors, see NIST Miscellaneous Publication 286, Units of Weights and Measures. Price \$2.50 SD Catalog No. C13 10286

Updated 6/17/98

Acknowledgements

The financial support provided by the FRA Office of Research and Development under the direction of Mr. Cameron Stuart is gratefully acknowledged. The continuous support of Cam Stuart and Gary Carr (also of FRA) was critical to the success of this program. We are also indebted to the Norfolk Southern (NS) Research and Tests Department for their tremendous technical support and many invaluable discussions. Most of the tests and findings discussed in this report could not have been completed without the help of many at NS, including Brad Kerchof, Sean Woody, Scott Hailey, James Harris, Lee Turner, Mike Hedrick, Noah Robinson, Barry Radford, Steve Smith, and Tim Childress. The system support provided by Carvel Holton (independent consultant), and Mark Beaubien and Craig Versek of Yankee Environmental Systems, Inc. (YES) is also greatly appreciated.

All views expressed in this publication are those of the authors and do not necessarily reflect the views of our sponsors and technical partners.

Contents

Executive Summary	1
1. Introduction	2
1.1 Background on LIDAR Technology	2
1.2 LIDAR Technology Benefits and Risks.....	4
1.3 Project Frame Work	6
1.3.1 Research Personnel.....	6
1.3.2 Project Funding	6
1.3.3 Testing Plan.....	6
1.4 Project Goals	7
1.5 Approach	7
1.6 Project Tasks and Timeline	8
1.6.1 Project Tasks	8
1.6.2 Project Timeline	8
2. Initial System Testing (R4)	11
2.1 System Installation	11
2.2 Test Results	14
2.2.1 Post-Processing	14
2.2.2 Speed Comparisons	16
2.2.3 Distance Comparisons.....	18
2.2.4 R4 Curvature Measurements.....	19
2.2.5 Wet Rail Testing.....	20
3. Initial Rail Geometry Car Testing	23
3.1 Test Setup and System Installation	24
3.2 Test Route.....	24
3.3 Distance Calibration	25
3.3.1 Tangent Track, GPS-Determined Distance Calibration	25
3.3.2 Ground-Truth Distance Calibration.....	26
3.4 Test Results	28
3.4.1 Curved Track Testing.....	29
3.4.2 Inclement Weather Testing	36
3.4.3 Effect of Special Track Work.....	38
4. Semi-Autonomous PXI LIDAR Railway Geometry Car Testing.....	39
4.1 System Installation	40
4.1.1 Ruggedized Enclosures for Optical Lenses.....	41
4.2 Test Route.....	42
4.3 Test Results	42

4.3.1	Tangent Track Testing.....	43
4.3.2	Curved Track Testing.....	46
4.3.3	Foot Pulse Feasibility	50
5.	Carbody-Mounted LIDAR System Revenue Service Testing.....	53
5.1	Test Setup	53
5.2	Test Results	54
5.2.1	Speed Testing	54
5.2.2	Curvature Track Testing.....	56
5.2.3	Individual Left and Right Rail Track Measurements	57
6.	Summary.....	59
Appendices 62		
Appendix A.	LIDAR Beam Configurations.....	62
Appendix B.	Analysis of Encoder Noise in Encoder Measurements.....	66
Appendix C.	Rail Geometry Car Testing—Weather Summary Table.....	67
Appendix D.	PXI System Testing—Frequency Content Analysis.....	68
Abbreviations and Acronyms		73

Illustrations

Figure 1: LIDAR concept for measuring speed in a noncontact manner for railroad applications	2
Figure 2: System-level block diagram of multifunction LIDAR sensors for noncontact speed and complex rail dynamics measurements	3
Figure 3: Project timeline overview	9
Figure 4: Different options for beam alignment were tested. TOR, gauge face, and web alignments were compared with one another to select the best performing configuration ..	12
Figure 5: LIDAR lens mounting for TOR, gauge corner, and web face and fiber routing on the R4	12
Figure 6: Encoder attached to the right rear (passenger side) truck axle	13
Figure 7: Water-dispensing system used to wet the rail attached to R4	13
Figure 8: Hy-Rail LIDAR testing was performed along a section of the Western Maryland Scenic Railroad (highlighted in blue)	14
Figure 9: A comparison of raw LIDAR speed from right and left rail vs. time of a Hy-Rail test	15
Figure 10: A comparison of raw LIDAR speed from right and left rail vs. time of a Hy-Rail test, with the dropout corrected	15
Figure 11: A comparison of filtered, LIDAR speed from right and left rail vs. time of a Hy-Rail test	16
Figure 12: A comparison of encoder, GPS, foot data, and LIDAR speed data vs. time	16
Figure 13: A comparison of encoder, GPS, foot data, and LIDAR speed data vs. time during the first 60 seconds of test	17
Figure 14: A comparison of encoder, GPS, foot data, and LIDAR speed data vs. time at the start of a Hy-Rail data run showing low spatial resolution of the “foot” data collected and oscillations from the encoder signal	17
Figure 15: The distance traveled was measured by LIDAR, encoder, foot data, and GPS data (with and without considering altitude) on the Hy-Rail, and compared with one another vs. time	18
Figure 16: Distance comparison of LIDAR, encoder, foot data, and GPS data (with and without considering altitude) vs. time from 12 to 15.1 seconds	18
Figure 17: A comparison of LIDAR, encoder, foot data, and GPS speed data vs. time show variation of the speed signal from the encoder. Foot data is provided by the R4 instruments, derived from the encoder and IMU	19
Figure 18: Initial curvature measurements using the LIDAR system on the Hy-Rail against GPS curvature measurements	20
Figure 19: Wet rail test setup	21
Figure 20: A comparison of wet and dry rail speed signals for both Gauge Face and TOR	21

Figure 21: LIDAR signal intensity signatures are shown before, during, and after the wet rail test section. The intensity readings exhibit normal fluctuations that are most commonly associated with surface roughness (smoother surfaces result in lower intensity) or beam orientation changes. Note that the wetted TOR beam records a -3 dB change in signal intensity, lower than the substantial changes in signal intensity on dry rail for the Gauge Face Beam.....	22
Figure 22: LIDAR system installation onboard the rail geometry car.....	24
Figure 23: LIDAR computer installed onboard the track geometry car and linked to KVM system	24
Figure 24: A comparison of calculated speeds vs. distance along 1.5 miles of tangent track calibration	25
Figure 25: A comparison of speed vs. distance with filtered encoder and LIDAR	26
Figure 26: 1000 ft being walked out for ground-truth calibration run.....	26
Figure 27: The encoder vs. LIDAR distances scaled to match ground measurement (Calibration Run #1).....	27
Figure 28: An assessment of the encoder vs. LIDAR speeds during calibration run (Calibration Run #1).....	27
Figure 29: The encoder vs. LIDAR distance measurements based on scaling during calibration from Run #1 (Calibration Run #2).....	28
Figure 30: An assessment of the encoder vs. LIDAR speeds during calibration run (Calibration Run #2).....	28
Figure 31: The encoder and LIDAR speed vs. distance over a 15-mile piece of track	29
Figure 32: GPS position and direction of travel for 5.8-degree curve.....	30
Figure 33: Curvature vs. distance for a 5.8-degree left-hand curve. The negative values imply a left-hand curve	31
Figure 34: Train speed signals recorded from LIDAR, encoder, and GPS sensors during a 5.8-degree curve show high variation of the encoder signal due to wheel slip, flanging, and contact point lateral position movement.....	32
Figure 35: During a 5.8-degree curve, the calculated distances measured by LIDAR, encoder, and GPS systems were compared, and LIDAR and encoder showed good agreement (Encoder and LIDAR readings are essentially overlaid)	33
Figure 36: LIDAR curvature in comparison to track chart curvature.....	34
Figure 37: LIDAR and rail geometry car measurements: (a) curvature; (b) speed	35
Figure 38: Comparison of LIDAR and rail geometry car data for a 3 mile track segment: (a) track curvature; (b) speed.....	36
Figure 39: The LIDAR maintained the ability to accurately measure speed continuously through a heavy rain over a nearly 35-mile distance.....	37

Figure 40: In inclement weather, the LIDAR maintains its ability to accurately measure distances. Here, the encoder and LIDAR left rail measurements were 34.136 mi and 34.237 mi, respectively.....	37
Figure 41: Consistent LIDAR signal over an 88-mile stretch including special track work with no dropouts.....	38
Figure 42: Truck mounted LIDAR lenses, pointing at gauge corner	40
Figure 43: Installation of LIDAR lenses, oriented toward Top of Rail (TOR)	41
Figure 44: PXI system mounted onboard the track geometry car	41
Figure 45: Explosion-proof protective housing securing the LIDAR lenses onboard the track geometry car.....	42
Figure 46: Coordinates for an example tangent track near Chicago, IL.....	43
Figure 47: A comparison of distance vs. time measurements by the encoder and the LIDAR system on tangent track (Encoder and LIDAR are essentially overlaid).....	44
Figure 48: Difference in distance measurement between the encoder and the LIDAR system for tangent track.....	45
Figure 49: A comparison of train speed vs. distance from the LIDAR system and the raw (unfiltered) encoder data on tangent track	45
Figure 50: A comparison of LIDAR speed measurements with GPS and encoder data for tangent tracks	46
Figure 51: A comparison between the LIDAR track curvature measurements with the track geometry car (IMU) data	47
Figure 52: A comparison of LIDAR track curvature measurements east- and westbound, to show repeatability.....	48
Figure 53: A comparison of LIDAR and encoder train speed through a 3.1-degree left-hand curve.....	49
Figure 54: Train speed measured by the LIDAR system and the encoder in the main body of a 3.1-degree left-hand curve	50
Figure 55: Simulated LIDAR foot pulse signal versus encoder foot pulse for 50 ft of travel.....	51
Figure 56: A close-up of simulated LIDAR foot pulse signal versus encoder signal for 5 ft of travel	52
Figure 57: Body-mounted LIDAR system onboard the track geometry car with the gauge corner beam alignment.....	53
Figure 58: LIDAR lens housing attached to an air supply to create positive air pressure inside the housing.....	54
Figure 59: A comparison of encoder and LIDAR speed measurements for 40 miles of revenue service track	55
Figure 60: A close-up of encoder and LIDAR speed measurements from 1 mile of revenue service track	55

Figure 61: A comparison of IMU vs. LIDAR curvature measurements on 40 miles of revenue service track 56

Figure 62: A comparison between LIDAR and Inertial Measurement Unit (IMU) curvature measurements on approximately 1 mile of revenue service track 57

Figure 63: A comparison between LIDAR and Inertial Measurement Unit (IMU) alignment measurements on approximately 1 mile of revenue service track 58

Figure A-1: Comparison of the truck mounted LIDAR facing TOR vs. track geometry car readings of curvature and left and right rail curvature readings (alignments) from May 2012 63

Figure A-2: Comparison of the body mounted LIDAR facing gauge corner vs. the track geometry car readings of curvature and left and right rail curvature readings (alignments) from July 2012 64

Figure A-3: A comparison of the truck mounted, TOR LIDAR and the body mounted, gauge corner LIDAR curvature measurements (approximately two months between readings).... 65

Figure B-1: Speed variation over track speed for the encoder and the LIDAR system..... 66

Figure B-2: Encoder filtered with third-order Butterworth with 0.5 Hz cutoff frequency 66

Figure D-1: LIDAR and encoder train speed on a tangent 3.1-degree left-hand curve tangent section of track (low-pass, third-order Butterworth filtered at 0.15 Hz): (a) the FFT frequency spectrum analysis of this filtered data; (b) showing a higher frequency content in the encoder data at all but the lowest frequencies..... 69

Figure D-2: LIDAR and encoder train speed on a 3.1-degree left-hand curve tangent section of track (low-pass, third-order Butterworth filtered at 2 Hz): (a) the FFT frequency spectrum analysis of this filtered data; (b) again showing a higher frequency content in the encoder data at all but the lowest frequencies 71

Figure D-3: A close-up of the frequency spectrum of LIDAR and encoder speed data along a 0.5-mile section of track including a 3.1-degree left-hand curve, unfiltered. This frequency analysis shows that the broadband frequency content is significantly higher for the encoder sensor (from 1 Hz upwards)..... 72

Tables

Table 1: Test sequence for LIDAR system.....	10
Table C-1: NOAA weather summary (Farmville) for the 4-hour inclement weather test period.	67

Executive Summary

The applicability of a Light Detection and Ranging (LIDAR) system for measuring track speed, distance, and curvature is evaluated through an extensive series of revenue service tests that represent the railroad environment. The test results indicate that LIDAR systems can be used as multifunctional noncontact sensors with a high degree of accuracy over a broad range of speeds that span from 0.5 to more than 100 mph. As opposed to conventional wheel-mounted encoders, a noncontact LIDAR system eliminates the mechanical failures and need for frequent calibration that are caused by vibrations and change in wheel diameter due to wear. Whereas Inertial Measurement Units (IMUs) generally cannot be relied on at speeds below 10 mph, the LIDAR system can measure track curvature down to crawling speeds.

Two different LIDAR systems are tested on the Federal Railroad Administration's (FRA) R4 Hy-Rail vehicle and on a track geometry measurement railcar operated by Norfolk Southern (NS). The R4 tests evaluate the feasibility of using a laboratory-grade LIDAR system for the intended track measurements. They are also used to determine suitable installation configurations for the LIDAR lenses. The tests onboard the track geometry car include a field-hardy system and are intended to further evaluate the suitability of LIDAR systems for railroad environments over an extended range of revenue service tracks. Additionally, ground-truth tests are performed to establish the absolute accuracy of the LIDAR systems in comparison with encoders.

The test results indicate that the LIDAR system can (1) measure distance traveled with high accuracy and without the high-frequency noise that is commonly present in encoder measurements; (2) provide accurate curvature measurements at and below speeds possible with IMUs; and (3) with further development, demonstrate suitability for integration into FRA's Autonomous Track Geometry Measurement System (ATGMS).

Additional efforts are needed to further investigate some of the findings of the study and to advance the system architecture towards a commercially viable system for integration into ATGMS and geometry railcars operated by U.S. railroads. Specifically, it is recommended that the LIDAR system's accuracy in measuring track distance and curvature be examined against ground-truth and cordal-length measurements. Methods currently used to convert the distance measurements to a Transistor-Transistor Logic (TTL) foot pulse signal need to be evaluated in order to make the output of the LIDAR system compatible with the protocol used in track measurement systems. Finally, the LIDAR system must be used, on a trial basis, as a retrofit to encoders in a track geometry measurement railcar operated by FRA or one of the U.S. railroads so that it can lead to a development plan for a commercially viable system.

1. Introduction

1.1 Background on LIDAR Technology

LIDAR is a noncontact measurement sensor that determines speed with high accuracy. LIDAR sensors use the Doppler technology in which a laser pulse is emitted at a specific wavelength and is then reflected back at a different wavelength to a receiver system. Based on the travel time of the laser pulse and the Doppler shift in wavelength, the speed of a moving object can be determined (in this case, a moving railcar relative to the track). Incidentally, this is the same technology that law enforcement uses to catch speeding drivers.

Figure 1 displays the concept of using LIDAR sensors to determine rail speed. The Doppler LIDAR sensors can be attached to the underside of a track geometry car with two laser beams facing the left and right rails. The dashed arrow indicates the outgoing LIDAR beam, and the dotted-dashed arrow shows the same beam reflected back to the sensors, which detect the Doppler shift for each rail.

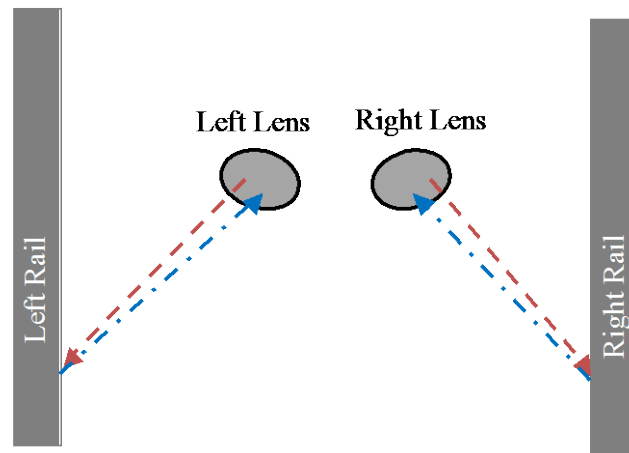


Figure 1: LIDAR concept for measuring speed in a noncontact manner for railroad applications

As shown in Figure 2, the Doppler shift is passed to a central processing unit (CPU) through a high-fidelity RF device. The CPU that is used for our study is a National Instruments (NI) PXI Computer that can be configured and used for applications such as the LIDAR system. For mass production, we envision replacing the PXI computer with an Application Specific Integrated Circuit Board (ASIC) that is far more compact, less costly, and draws less power. The development of such a system is intended for a follow-up study. The PXI computer performs a number of tasks in real time, including computing the Fast Fourier Transform (FFT) of the two LIDAR signals, establishing the left and right rail velocities, and performing the necessary calculations to determine track speed (based on the average speed of the two rails) and track curvature (based on the speed and distance difference between the two rails).

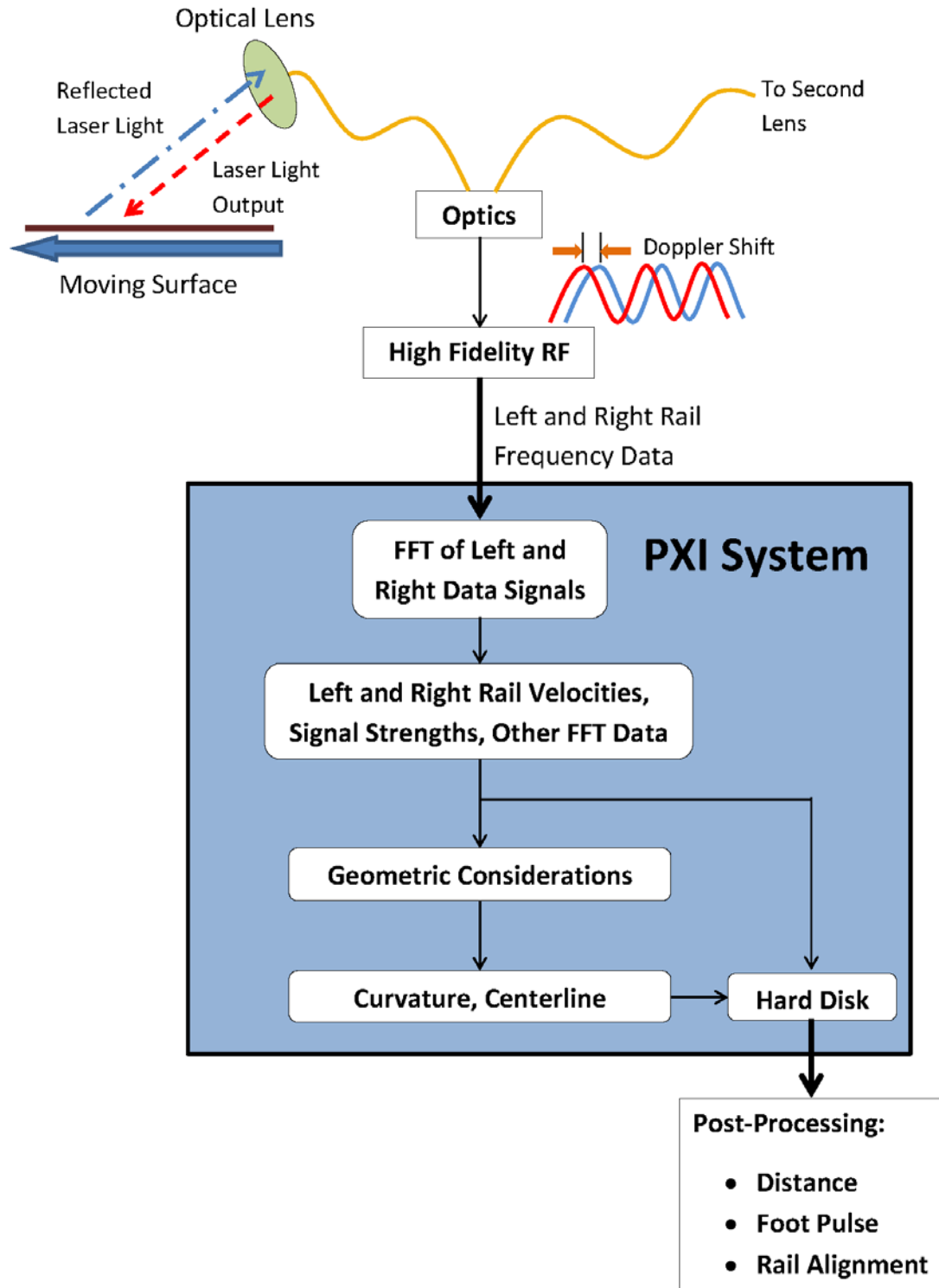


Figure 2: System-level block diagram of multifunction LIDAR sensors for noncontact speed and complex rail dynamics measurements

The speed and distance measurements are analog outputs of the PXI computer. The data is stored to a hard drive or solid-state drive (SSD) at a user-defined storage rate. In addition to track curvature and speed determination, the post-processing of the data includes a travel distance calculation that can provide the basis for generating a foot pulse, much in the same way as a conventional encoder. The system shown in Figure 2 is intended to be a direct retrofit to an encoder in a track geometry car, without any changes to other instruments that use the foot pulse signal.

1.2 LIDAR Technology Benefits and Risks

The benefits of LIDAR technology, particularly for high speeds and/or elevated safety environments, are:

1. A noncontact measurement technology that eliminates the speed-dependent design complexity, reliability, maintenance, and accuracy (slip) issues and limitations (e.g., vibration) of mechanically contacting or axle-mounted tachometers (analog or digital).
2. A noncontact, Doppler measurement technology with:
 - a. Inherently high accuracy and speed independence; absolute scale factor (580 KHz/mph) is not subject to wear, track speed (slip and data rate), spatial resolution or standoff (radar), environment, etc.;
 - b. Continuous, consistent operation over a wide range of track speeds from creep to more than 100 mph, exceeding any current technology (analog/digital tachometers, radar, GPS, etc.);
 - c. Consistent track curvature measurement at speeds at or slower than those possible with IMUs that are commonly used in track geometry railcars;
 - d. Suitability for autonomous operation in generic revenue service or high-precision track metrology applications (e.g., Autonomous Track Geometry Measurement Systems (ATGMS)); and
 - e. Capability of detecting auxiliary parameters critical to autonomous, in-motion safety and just-in-time maintenance in High Speed Rail or Intercity Passenger Trains (e.g., instantaneous curvature, GPS position correction (PTC), and possibly rail condition and stability).
3. A noncontact, optical measurement technology that uses the following:
 - a. Telecommunications wavelengths at 1.5 micrometer, providing
 - i. Highest, inherent eye safety;
 - ii. Ten thousand times higher spatial precision and speed accuracy relative to radar;
 - iii. Demonstrated performance in rain against wet, icy, and/or snow surfaces;
 - iv. Reduced cost components with increased Mean Time to Failure (MTTF); and
 - v. Functionality in environmental extremes as compared with typical laser optics.

- b. Telecommunications optical fibers with
 - i. Flexible, arbitrary mounting locations for easier system integration, and
 - ii. Fixed, no-maintenance internal optical alignments.
- c. Coherent detection, resulting in larger dynamic detection ranges than conventional intensity-based optical metrology sensors used for rail applications, enabling
 - i. Reduced maintenance—tolerance of dirtier lenses and windows, rain, mist, etc.;
 - ii. Reduced diameter optics (¼–1 in) and/or increased noncontact ranges (millimeters to meters); and
 - iii. Detection of scattered light sensing on all surface materials (e.g., rock, steel, ice and snow, etc.), roughness (e.g., shiny or coarse), and colors (e.g., light or dark) while rejecting sun or artificial lighting (e.g., headlamps, etc.).

The challenges and risks of the LIDAR technology are:

1. We have not previously attempted to measure track geometry to the extent that is planned here. It remains to be determined what aspects of the track geometry can be measured repeatedly and accurately with the two-channel LIDAR system that the Railway Technologies Laboratory (RTL) is currently using. Including additional channels will add costs and increase software complexity. Additionally, separating track geometry parameters from the rest of the information contained in the data will require data analysis beyond what RTL has previously performed. But, ultimately, such an analysis must be made and implemented.
2. Measuring track curvature and geometry at low speeds requires some adjustments to our current software. Successfully extending the range of the system to make measurements at very low and very high speeds will require an adaptive FFT that will need to be developed and implemented. It is, however, feasible to have separate systems that are suitable for low-speed operation (such as Low Speed Track Geometry Measurement System (LTGMS) at Virginia Tech (VT)) and high-speed operation (HSR and Intercity Passenger Trains).
3. Successfully integrating the LIDAR system with foot pulse demarcation into existing track geometry measurement systems will likely generate integration issues that must be meticulously managed. The software and hardware challenges are unknown at this time, but RTL intends to undertake the work in the near future.
4. Current system architecture requires significant power (500 watts), limiting utility in autonomous, freight-based operations.

1.3 Project Frame Work

1.3.1 Research Personnel

Personnel at VT have extensive experience in railroad operations and have conducted numerous programs pertaining to LIDAR applications in rail operations over the last 6 years under the auspices of TTCI and AAR Tech Scanning. VT has successfully demonstrated the use of custom Doppler LIDARs (with respect to speed, friction, vibration, rail stability, etc.) in actual operational field tests. Furthermore, we have been actively involved in research related to insulated rail joints, acoustic diagnostics, friction wedge modeling and development, and a large number of related rail programs. With respect to the current programs, VT holds multiple patents in LIDAR speed sensing, including the recently issued *Doppler Sensor for the Derivation of Torsional Slip, Friction and Related Parameters*, US Patent No. 7705972, April 27, 2010, that includes measurement of friction and instantaneous curvature. An extensive list of publications is available on request.

This research was performed by a number of VT researchers, faculty, and students. Dr. Mehdi Ahmadian (PI), Michael Craft (Senior Research Associate), Josh Munoz (graduate student researcher), Shannon Wrobel (graduate student researcher), and Tarek Shalaby (undergraduate student researcher) provided the bulk of the research effort. Dr. Alireza Farjoud (post-doc researcher) and Clement Nagode (graduate student researcher) also contributed to the research.

1.3.2 Project Funding

Financial support for this research was provided by the FRA Track Research Division under BAA 2010-01, in accordance with FAR Part 35. Our industrial partner, NS, and our collaborating partner, YES, provided additional funding through cost sharing.

NS provided access to two of its rail-bound track geometry measurement railcars. The value of this in-kind contribution is estimated to be approximately \$60,000, accounting for the 20 days that VT personnel had access to the NS railcar to install the LIDAR system and to travel onboard the train and fine-tune the system. This amount does not include the more than 130 days of unattended testing that was performed onboard the rail geometry car. The total mileage on NS rail cars exceeded 4,000 miles on revenue service tracks throughout the United States.

YES, located in Turners Falls, MA, is a collaborating partner that wants to be a designer and supplier of VT LIDAR technology to the rail industry. YES has licensed VT patents in this area and is currently the supplier of autonomous systems for trackside rail wheel inspection. YES is a small business as defined by the Small Business Administration and provided software and hardware design and integration support for this project.

1.3.3 Testing Plan

The goal for the initial demonstration of the LIDAR system was to prove its feasibility as a speedometer and instantaneous curvature instrument. VT, YES, FRA, and ENSCO (operating the FRA R4 Hy-Rail) collaborated on the demonstration.

The second part of the demonstration was to prove the use of the LIDAR system in an autonomous capacity. The LIDAR autonomous system can be run in an “un-attended” mode in which the system is observed once or twice a day for any unexpected software or hardware

glitches. This testing was performed by VT in collaboration with YES and NS on rail-bound research cars. The tests were run at speeds considerably higher than what was achievable on the Hy-Rail vehicle. The successful completion of this research task was a very important step towards the complete integration of the LIDAR system into an autonomous track measurement system such as ATGMS. The test results significantly contributed to creating a field-ready, autonomous system. Additionally, the data available on the rail car was crucial for comparing the LIDAR data with the standards measurement technologies currently used by U.S. railroads for speed, distance, and curvature measurement.

1.4 Project Goals

The primary objectives of this project were:

1. to demonstrate the viability and applicability of LIDAR systems for measuring speed, distance, and track curvature for railroad applications;
2. to determine if LIDAR systems can be used to replace wheel-mounted encoders and IMUs that are used for track distance and curvature measurements in track geometry cars;
3. to establish the accuracy of LIDAR systems in measuring track speed, curvature, and distance as compared with encoders and IMUs;
4. to highlight the practical advantages and disadvantages of LIDAR systems for railroad applications in order to determine the needs regarding future development efforts toward a production-viable, noncontact, multifunctional sensor; and
5. to design and build a prototype system that can survive the demanding railroad environment and operate in an unmanned manner.

1.5 Approach

The following steps were taken toward achieving the project goals:

1. A laboratory-grade LIDAR system, already available at VT's RTL, was tested onboard the FRA Hy-Rail vehicle, R4. The results of the tests were used to provide an initial assessment of the LIDAR system's functionality in various rail environments (such as wet and dry rail) and in the presence of special track work (frogs, switches, etc.). The results were also used to determine the most suitable orientation of the LIDAR lenses toward the two rails.
2. The Hy-Rail vehicle tests were performed on a track geometry measurement railcar operating on revenue service track. The laboratory-grade LIDAR system was installed onboard the railcar and tested on short runs in order to gain a better understanding of the critical issues that could potentially arise from operating the system in revenue service. The tests were also intended to evaluate the performance of the system at speeds much higher than that of the Hy-Rail vehicle.
3. The information gathered from testing the laboratory-grade system onboard R4 and the track geometry railcar was used to design and build a field-hardy prototype system that can better withstand the rigors of field testing and can be operated with minimal operator attention in a nearly unmanned manner.

4. Tests were performed onboard the track geometry railcar to accumulate a large number of miles in revenue service and to expose the system to various types of track and weather conditions. The tests were aimed at assessing how well the components mounted outside the railcar (e.g., the LIDAR lenses) withstand the vibrations, jarring, and dirt and grime present in a revenue service environment. The tests were also used to ensure that the system can work in different installation configurations (e.g., attached to the railcar truck or body).
5. The data accumulated during the tests were processed using different signal processing techniques to obtain the measurements of interest: track speed, distance, and curvature. A comparison was made between the LIDAR measurements and the encoder's and IMU's data to establish the relative accuracy of the system.

1.6 Project Tasks and Timeline

1.6.1 Project Tasks

Table 1 includes a summary of the tests performed during this program, including the test location and platform, the start and end dates, the distance traveled, and the LIDAR mounting and beam configuration. The details of each test will be covered in Sections 2–5 of the report.

1.6.2 Project Timeline

Figure 3 shows a timeline of the project's main events from kickoff to final review at VT's RTL.

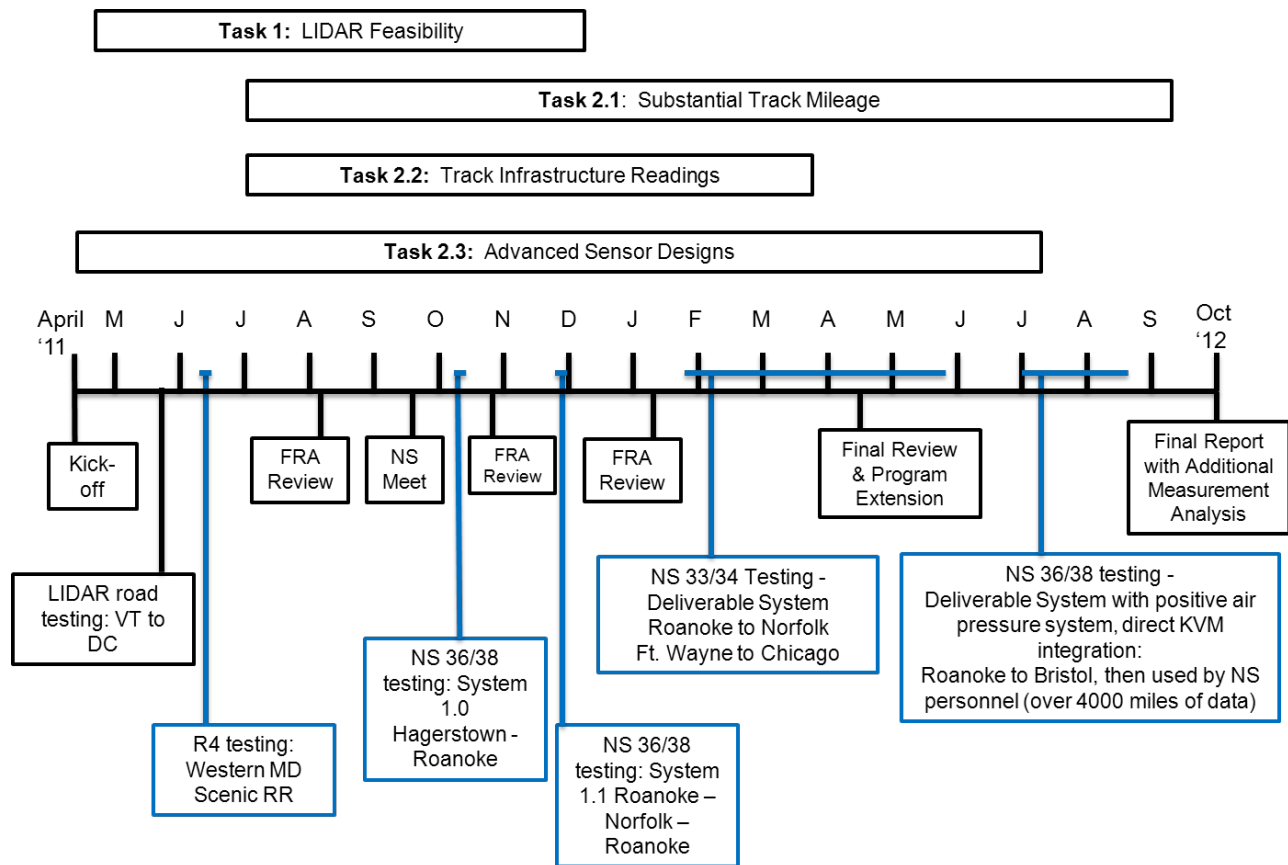


Figure 3: Project timeline overview

Table 1: Test sequence for LIDAR system

LIDAR Test Number	Test Platform	Test Locations	Test Partner	Start Date	End Date	Approximate Miles of Data	LIDAR Lens Mount	LIDAR Beam Location	Comments
1	FRA R4 Hy-Rail	Western Maryland Scenic RR	ENSCO	15-Jun-11	15-Jun-11	4	Truck Frame	TOR/Web/ Gauge Corner	Test non-autonomous LIDAR (w/o encoder data) on R4
2	NS 36/38	Hagerstown, MD to Roanoke, VA	Norfolk Southern	10-Oct-11	10-Oct-11	220	Body Mount	Gauge Corner	LIDAR System (Rev 1), Testing on Track
3	NS 36/38	Roanoke, VA to Norfolk, VA round trip	Norfolk Southern	28-Nov-11	29-Nov-11	500	Body Mount	Gauge Corner	LIDAR System (Rev 1), Ground Calibration
4	NS 33/34	Roanoke, VA to Bluefield, VA, round trip / Roanoke to Norfolk, VA, round trip	Norfolk Southern	27-Jan-12	1-Feb-12	515	Truck Mount	Gauge Corner	PXI LIDAR (Rev 2), Testing on Track
5	NS 33/34	Roanoke, VA to Narrows, VA round trip / Ft. Wayne, IN to Chicago, IL round trip / additional testing with NS personnel	Norfolk Southern	2-Feb-12	30-May-12	470	Truck Mount	TOR	PXI LIDAR (Rev 3), Testing on Track
6	NS 36/38	Roanoke, VA to Bristol, TN / additional testing with NS personnel	Norfolk Southern	6-Jul-12	16-Aug-12	4080	Body Mount	Gauge Corner	PXI LIDAR (Rev 3) system, with air curtain lens

2. Initial System Testing (R4)

The significant findings from the R4 tests include:

1. Doppler LIDAR measures and records accurate speed and distances in a noncontact manner, providing an alternative to encoder or GPS systems.
2. The gauge corner was determined to be the most suitable location to aim the beams.
3. The presence of water on the rail does not degrade the accuracy of the LIDAR speed, distance traveled, or curvature data.
4. The LIDAR system can be used for curvature measurement, although these measurements could not be verified against other typical means of curvature measurement.

Specifically, the tests were intended to:

- Demonstrate the broad capability of the system on a Hy-Rail vehicle,
- Collect data on LIDAR performance in the presence of documented track infrastructure (switches, frogs, crossings, etc.),
- Investigate LIDAR beam orientation relative to the rail for speed and curvature measurements, and
- Investigate the efficacy of the LIDAR system in the presence of wet rail.

2.1 System Installation

A LIDAR system was installed on FRA's R4 Hy-Rail vehicle; it was operated by ENSCO and used to gather "foot" data. The LIDAR CPU was installed inside the cab and six lenses were installed on an adjustable frame underneath the truck chassis. Figure 4 shows the different LIDAR beam configurations: top of rail (TOR), gauge corner, and the web of rail. Data was collected for each of these configurations to evaluate the signal quality off the surface of each section of rail, the effect of special track work on the signal, and signal continuity in curves. The beam location tests determined that gauge corner or TOR locations provided good readings and were not adversely affected by special track work (see Appendix A for more information on beam configurations).

Figure 5 shows a close-up of the LIDAR beam lenses attached to the R4 chassis. In the upper left-hand corner, the TOR lens for the left rail is shown. Web of rail and gauge corner lenses are present in the foreground. All beams are oriented at an angle of 60 degrees with respect to the forward velocity of the train.

The encoder signal was collected by a VT data acquisition laptop, and "foot count" data was collected by the R4's onboard computer. The encoder on the R4 is located on the rear drive axle of the truck on the passenger side (right side), as shown in Figure 6. The VT LIDAR computer recorded the LIDAR signal data along with GPS location. The R4's IMU data was not recorded.

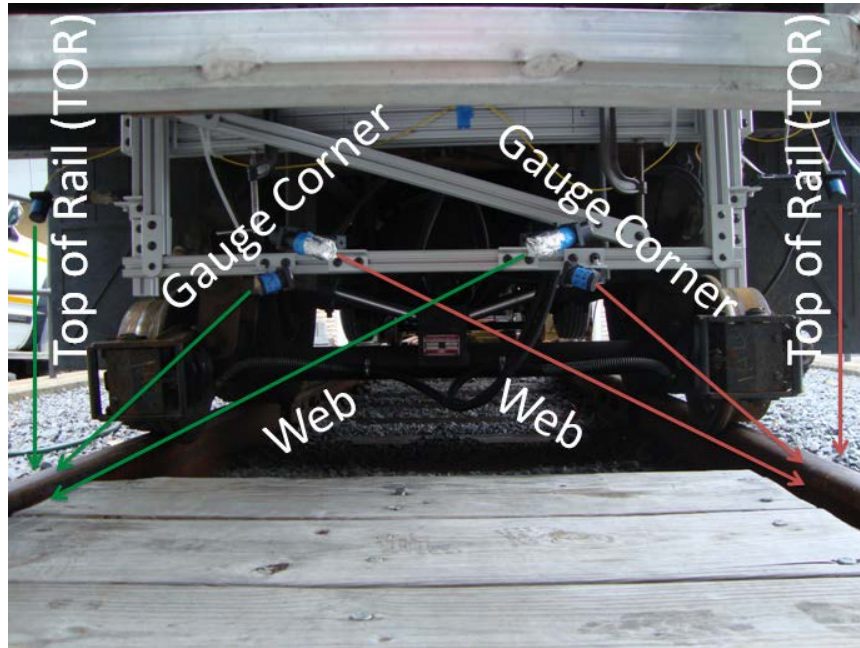


Figure 4: Different options for beam alignment were tested. TOR, gauge face, and web alignments were compared with one another to select the best performing configuration

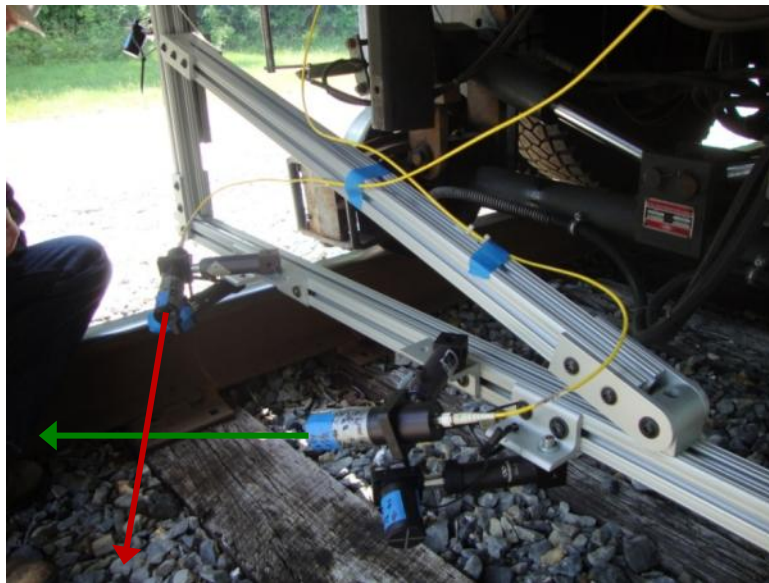


Figure 5: LIDAR lens mounting for TOR, gauge corner, and web face and fiber routing on the R4

A water dispensing system was also installed on the R4 to test the LIDAR signal strength on a wet rail condition. Figure 7 shows the dispensing nozzle for the water system, located just behind the rear Hy-Rail wheel and connected to a small water tank by a hose.



Figure 6: Encoder attached to the right rear (passenger side) truck axle



Figure 7: Water-dispensing system used to wet the rail attached to R4

The Hy-Rail testing was performed at Western Maryland Scenic Railroad shown below in Figure 8. The rail consisted of older joint bars with no continuously welded rail. A 300-foot calibration run was performed to determine if the foot data was accurate. VT was told that ± 1 ft was typical of the encoder accuracy (for a 300-foot, measuring wheel distance calibration).

Three track sections were chosen for testing. The first section, used for testing the wet rail condition, consisted of tangent track. The second test section, chosen to test the curvature

readings, included one left-hand curve, one right-hand curve, a level crossing, a steel-framed bridge, and a section of tangent track. The final test section, chosen to determine the effect of special track work on the various LIDAR beam configurations, included a turnout and a level grade crossing.



Figure 8: Hy-Rail LIDAR testing was performed along a section of the Western Maryland Scenic Railroad (highlighted in blue)

2.2 Test Results

2.2.1 Post-Processing

The following plots represent a typical speed signal and post-processing that is performed to eliminate temporary signal loss. While not common, these dropouts may occur because of dirty lenses, improper focal length set up, or special track work (depending on the beam focal location). Figure 9 shows a dropout due to a level crossing when using LIDAR beams aimed at the gauge face. Such dropouts, however, can be detected during post-processing of the raw data, and the software can automatically correct the data to ensure that no speed information is lost and the speed data remains contiguous, as shown in Figure 10.

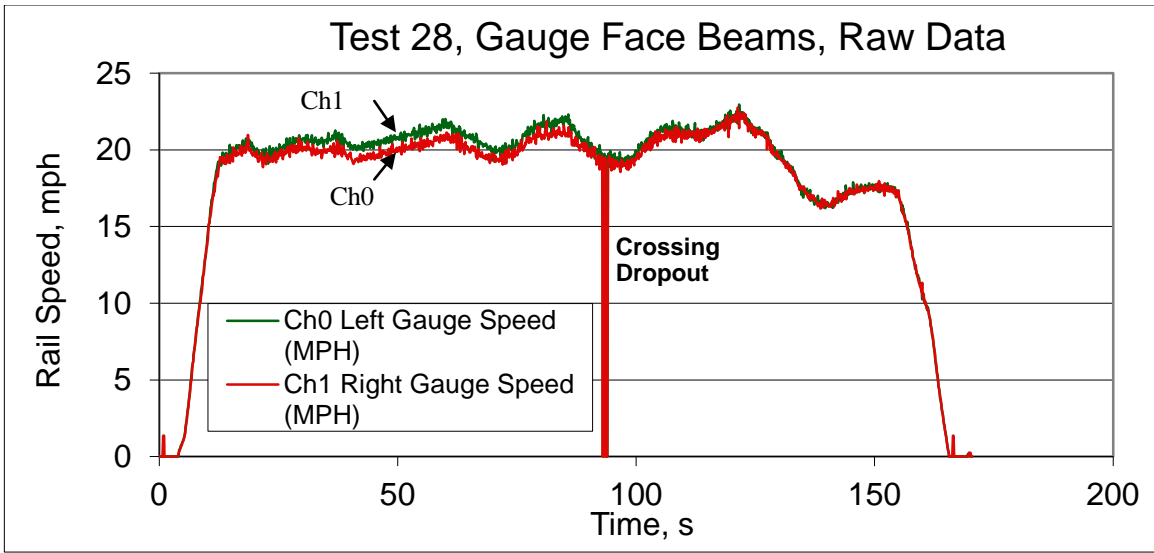


Figure 9: A comparison of raw LIDAR speed from right and left rail vs. time of a Hy-Rail test

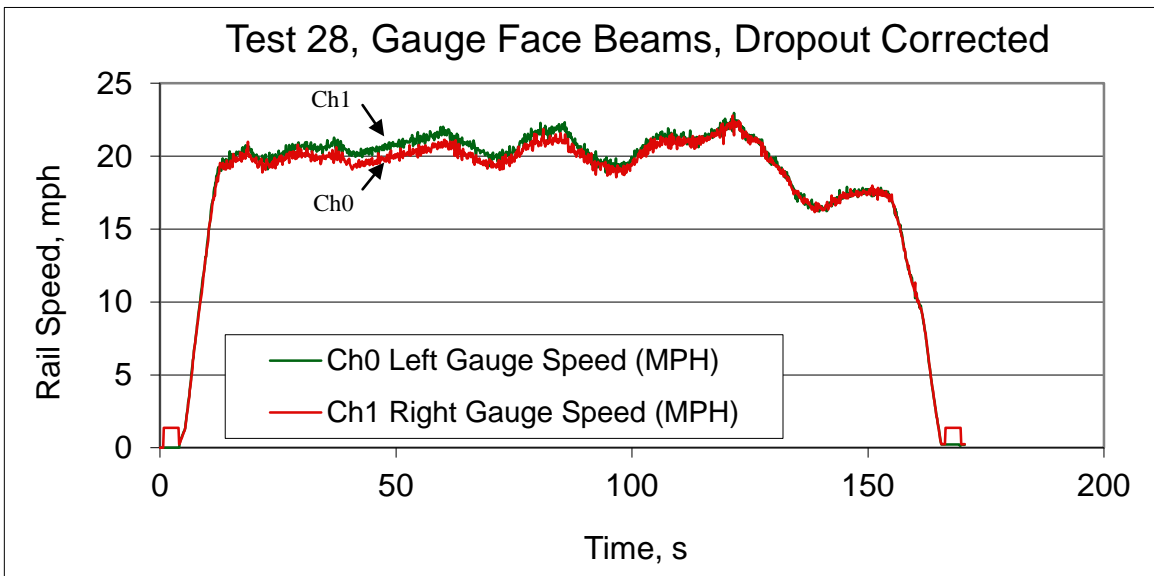


Figure 10: A comparison of raw LIDAR speed from right and left rail vs. time of a Hy-Rail test, with the dropout corrected

Furthermore, the post-processing includes using a low-pass filter to better isolate rail curvature and track alignment readings, as shown in Figure 11. In comparing Figure 10 and Figure 11, one is able to see that the filtered data maintains the data trends (i.e., there is no loss of information), while the noise present in the data has been eliminated.

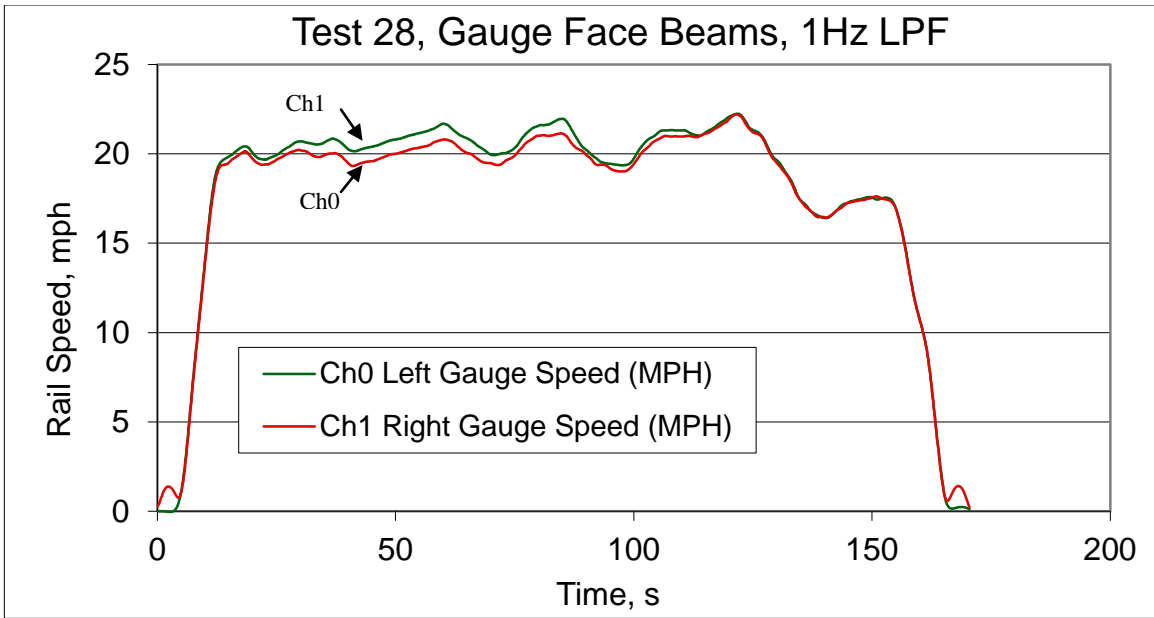


Figure 11: A comparison of filtered, LIDAR speed from right and left rail vs. time of a Hy-Rail test

2.2.2 Speed Comparisons

Figure 12 compares typical speed measurements by LIDAR and other means that are commonly used in the railroad industry. The figure indicates similar readings for encoder and LIDAR data, and inconsistencies and a delay in the GPS (Garmin) signal. Commercial GPS, in contrast to military GPS, is commonly desensitized to reduce its accuracy.

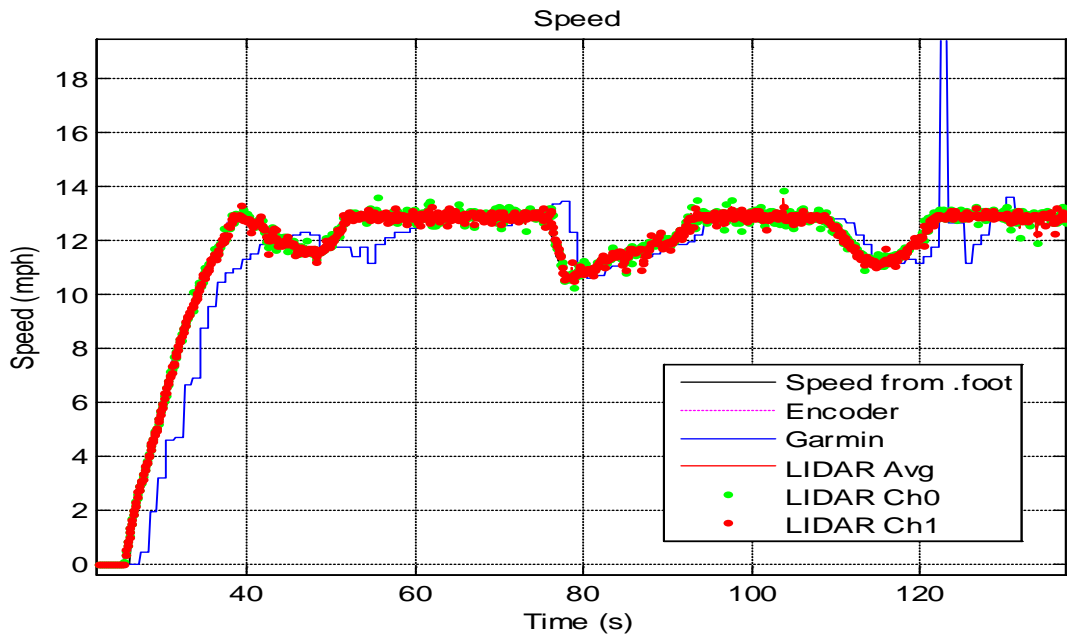


Figure 12: A comparison of encoder, GPS, foot data, and LIDAR speed data vs. time

Figure 13 and Figure 14 show close-ups of the data from Figure 12 for the first 60 seconds and during seconds 25–27.1, respectively. The figures illustrate that the recorded R4 velocity data (the “foot” data, which is a composite of information from the encoder and IMU) has a high spatial threshold at low velocities, too coarse for comparison with LIDAR at very low speeds. However, the raw encoder count data was also collected and compared with the LIDAR data.

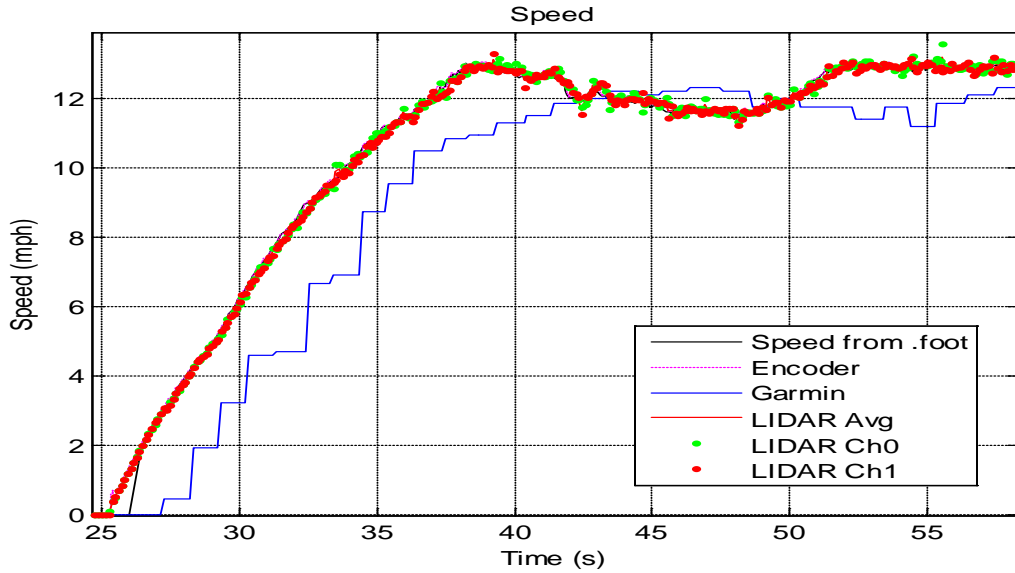


Figure 13: A comparison of encoder, GPS, foot data, and LIDAR speed data vs. time during the first 60 seconds of test

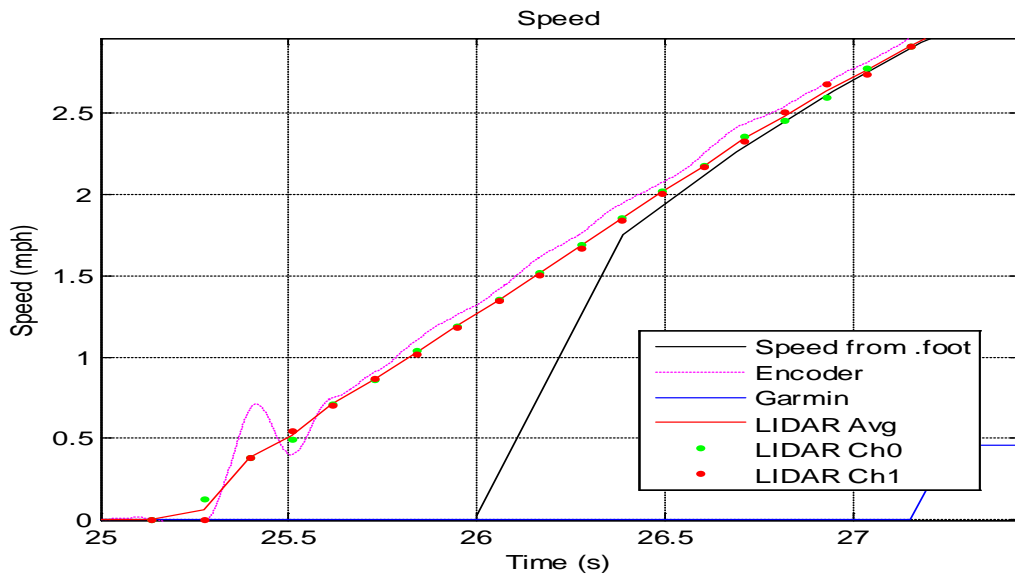


Figure 14: A comparison of encoder, GPS, foot data, and LIDAR speed data vs. time at the start of a Hy-Rail data run showing low spatial resolution of the “foot” data collected and oscillations from the encoder signal

2.2.3 Distance Comparisons

Figure 15 shows that “foot data” (Encoder + IMU readings) gives readings that agree closely with the LIDAR calculated distances. The “Encoder” data, however, is an aliased signal due to insufficient data acquisition speeds and therefore has some inaccuracies. Additionally, the GPS (Garmin) signal also shows distance discrepancies due to signal loss (The Garmin unit is not an IMU.).

Figure 16 shows a close-up of the previous data run from 12–15.1 seconds. A slight but perceivable oscillation on the “foot” signal indicates the inaccurate distance recording of the encoder system.

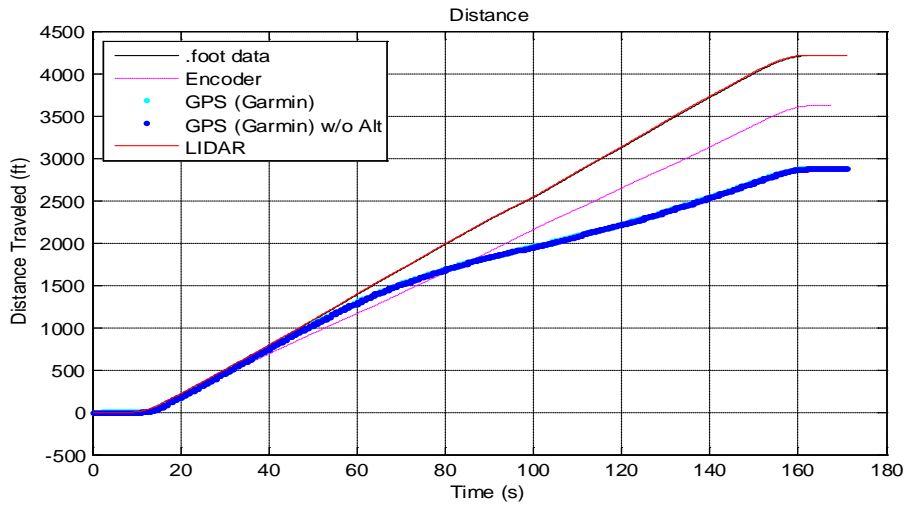


Figure 15: The distance traveled was measured by LIDAR, encoder, foot data, and GPS data (with and without considering altitude) on the Hy-Rail, and compared with one another vs. time

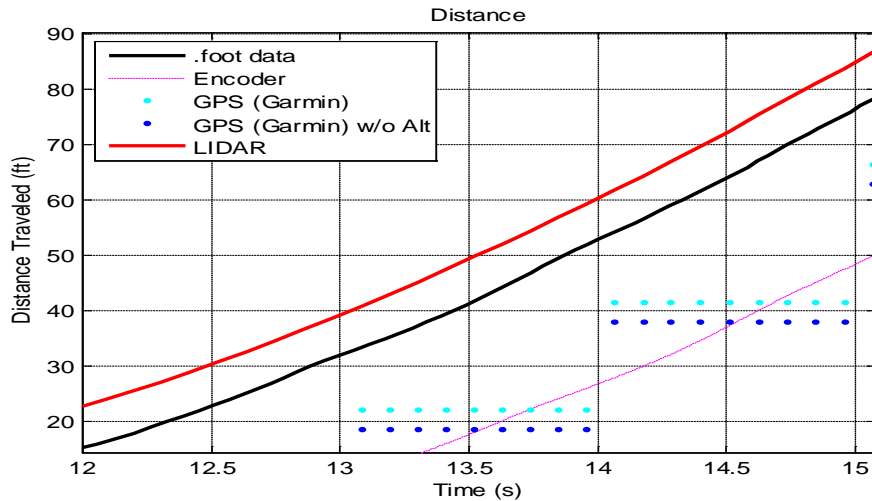


Figure 16: Distance comparison of LIDAR, encoder, foot data, and GPS data (with and without considering altitude) vs. time from 12 to 15.1 seconds

These small oscillations in the distance plot equate to a large variation in speed when compared with the LIDAR signal, as shown in Figure 17. This variation is a result of the encoder mounting location on the truck drive axle. On the drive axle with rubber tires, the tire contacts the rail, but is subject to variation in radius and suspension movement that can change the forward velocity of the wheel and the rail speed detected by the encoder.

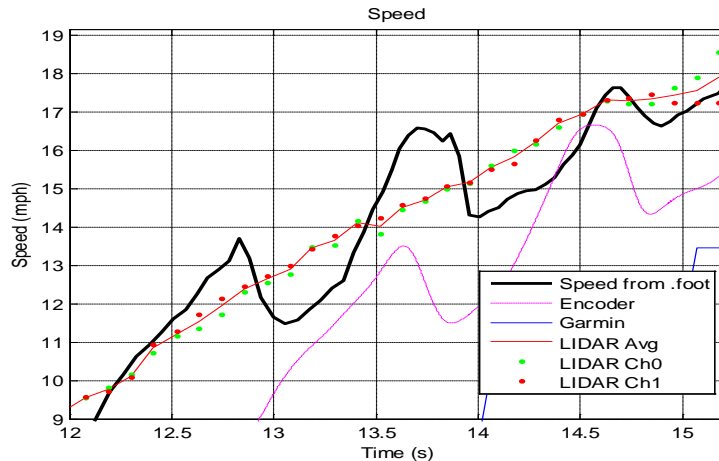


Figure 17: A comparison of LIDAR, encoder, foot data, and GPS speed data vs. time show variation of the speed signal from the encoder. Foot data is provided by the R4 instruments, derived from the encoder and IMU.

2.2.4 R4 Curvature Measurements

On the R4, VT performed initial curvature measurements based on the LIDAR data, as shown in Figure 18. While no track charts or other typical curvature measurements were available to compare with the LIDAR curvature readings, these measurements were compared with low-accuracy GPS coordinate-based curvature estimates. Both measurements show approximate agreement and indicate the potential for using LIDAR for curvature measurements.

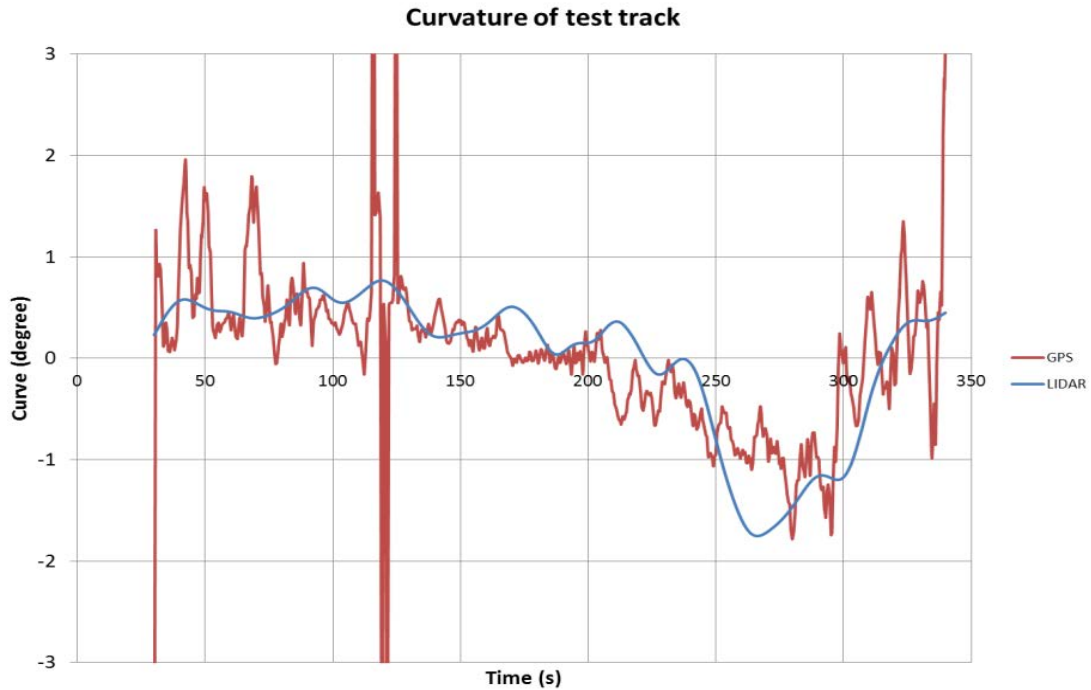


Figure 18: Initial curvature measurements using the LIDAR system on the Hy-Rail against GPS curvature measurements

2.2.5 Wet Rail Testing

Testing was performed to demonstrate LIDAR signal continuity on wet rail and to quantify the effect of wet rail on LIDAR signal intensity. The water-dispensing unit shown in Figure 19 was used to conduct the wet rail tests. With the R4 at a constant speed, the dry rail was wetted for a period of time and then the water valve was closed. The LIDAR recorded signal data continuously on both the wet and dry rails. Every attempt was made to maintain a nearly constant speed, as shown in Figure 20.

Figure 20 indicates that the addition of water on the rail did not interfere with obtaining correct, continuous velocity readings despite absolute TOR signal intensity reduction on wet rail. The quality of the velocity data was unaffected by the wet rail, despite a 3 decibel (dB) drop in LIDAR signal intensity. The frequency in the Doppler signal contains the velocity and speed information, not the intensity of the returned signal. As a result of this functionality, beams on polished, wet, iced, or snow-covered surfaces still scatter light because of the difference in the index of refraction between the air and the surface, as indicated by the LIDAR raw signal in Figure 21.

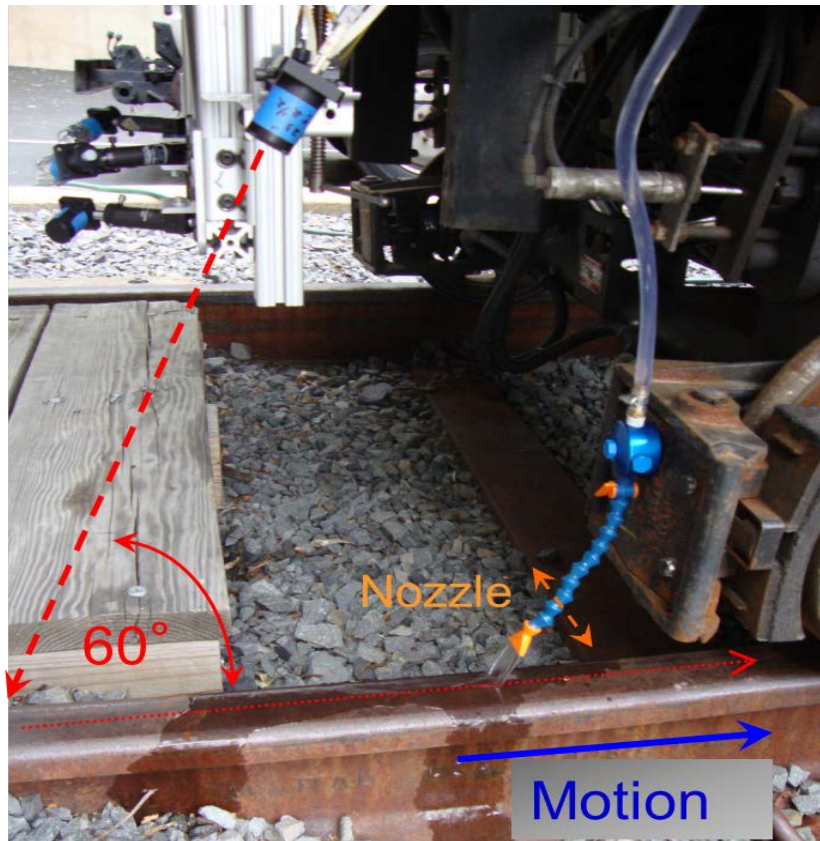


Figure 19: Wet rail test setup

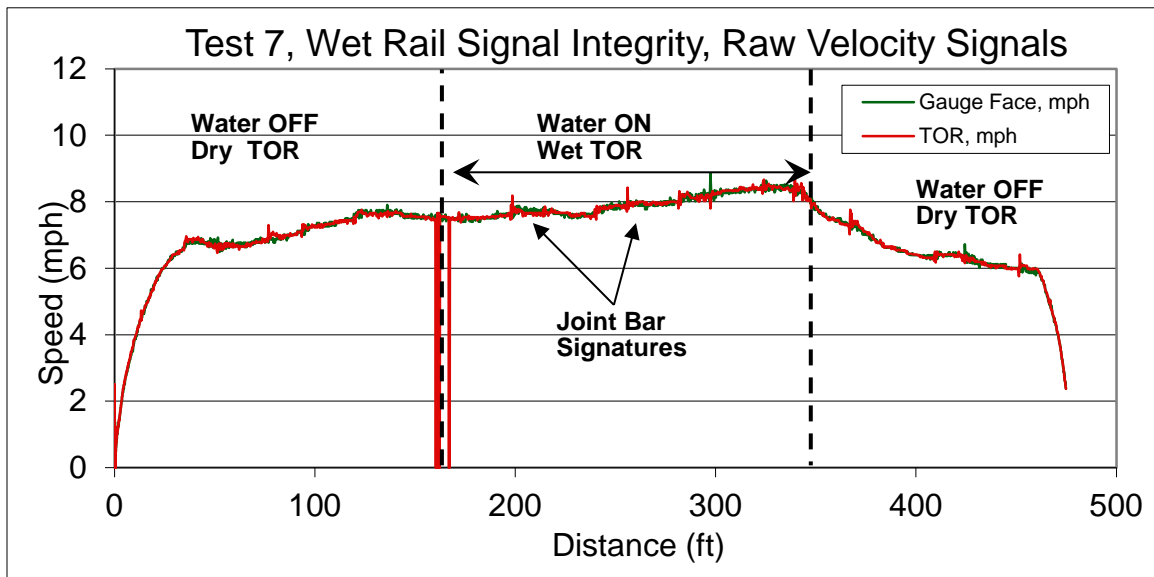


Figure 20: A comparison of wet and dry rail speed signals for both Gauge Face and TOR

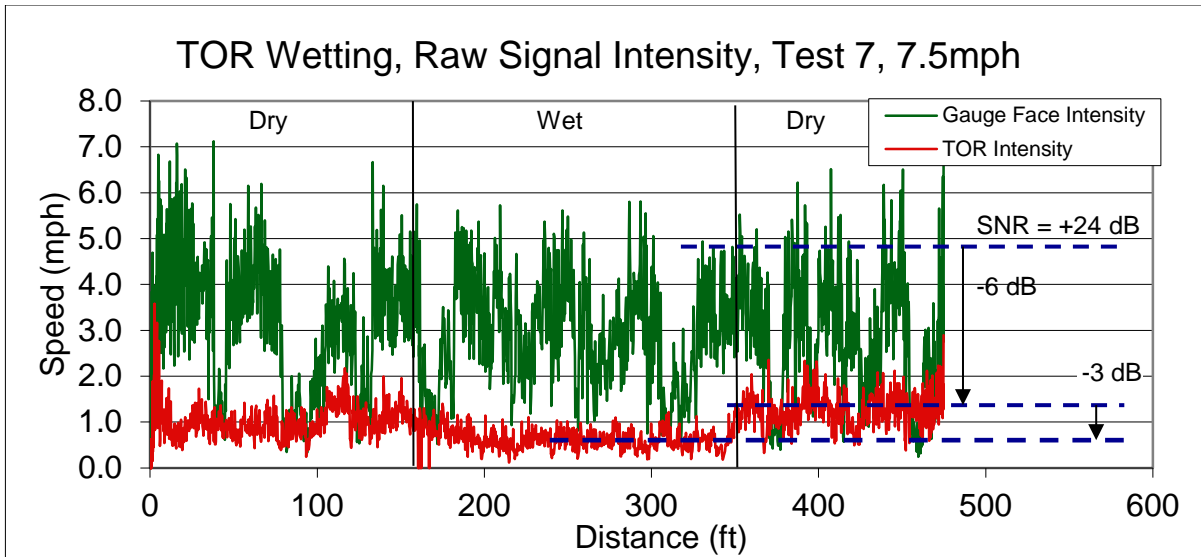


Figure 21: LIDAR signal intensity signatures are shown before, during, and after the wet rail test section. The intensity readings exhibit normal fluctuations that are most commonly associated with surface roughness (smoother surfaces result in lower intensity) or beam orientation changes.

Note that the wetted TOR beam records a -3 dB change in signal intensity, lower than the substantial changes in signal intensity on dry rail for the Gauge Face Beam.

3. Initial Rail Geometry Car Testing

Below are the primary observations and conclusions ascertained from the LIDAR system's initial rail geometry car testing:

1. The system proved effective in accurately measuring both track speed and curvature on revenue service mainlines onboard a rail geometry car traveling over several hundred miles.
2. The LIDAR system proved to be more accurate than encoders that are commonly used for distance measurements, as indicated by the comparison of the two systems in a ground-truth test.
3. The LIDAR system is able to accurately measure track curvature, although the measurements show more high-frequency content than the IMU onboard the rail geometry car. The higher frequency content may be due to the carbody motion in the curves of track geometry measurements. Further analysis of the data (beyond this study) is needed to conclusively determine the sources of the higher-frequency content. Filtered LIDAR data matches the IMU data closely. An advantage of the LIDAR system is that it can measure track curvature at speeds far lower than possible with IMUs and with potentially far higher spatial resolution.

The LIDAR system was installed on a rail geometry measurement railcar for a round of initial testing. The tests, denoted as "Test 2" in Table 1, were made possible by the Research and Testing Department of NS.

The primary goals of the tests were to:

- Demonstrate LIDAR system capabilities on a weight-loaded railcar,
- Compare LIDAR data with the speeds measured by the encoder signal used on the rail geometry car, and
- Gather data on LIDAR's ability to measure curvature and determine the accuracy of the data, particularly in the presence of documented track infrastructure special track work (switches, frogs, crossings, etc.).

Another round of tests was performed on the same rail geometry car at a later date, mainly for the purpose of:

- Comparing LIDAR and encoder signal to ground-truth distance measurements,
- Covering significant mileage in order to significantly build on the total miles of track tested on the system, and
- Testing system functionality over longer time periods.

NS was very accommodating to VT during the planning, setup, testing, and system removal processes. The following section will describe the system installation, test route, and distance calibrations, as well as provide a detailed analysis of the test results.

3.1 Test Setup and System Installation

The LIDAR system was body-mounted on the track geometry car, as shown in Figure 22. The gauge corner beam alignment was chosen for this phase of testing during which the LIDAR beams were pointed at the corner of the gauge at 45 degrees from the horizontal and at 60 degrees from the longitudinal axis of the train.



Figure 22: LIDAR system installation onboard the rail geometry car

The system installation included a video and keyboard interface ported to the inside of the railcar and using the on-board KVM system, as is depicted in Figure 23. The encoder was mounted on the left rail of the lead truck middle axle and its signal was also collected by the LIDAR computer system.



Figure 23: LIDAR computer installed onboard the track geometry car and linked to KVM system

3.2 Test Route

Data was taken along a route from Hagerstown, MD, to Roanoke, VA, on October 10, 2011. The same setup was also used on the return trip from Roanoke, VA, to Norfolk, VA, on November 28 and 29, 2011. During the tests:

- More than 300 miles of data were recorded and analyzed
- Left and right rail speeds were recorded
- Encoder counts were recorded and compared against LIDAR
- System ground-truth calibration was performed
- Inclement weather testing was performed

3.3 Distance Calibration

3.3.1 Tangent Track, GPS-Determined Distance Calibration

GPS locations were used to calibrate the encoder and LIDAR measurements (post-processing). LIDAR and encoder readings on the rail geometry car were compared on a 1.5-mile section of tangent track where the train accelerated from a resting position to approximately 45 mph. The calculated distances were then calibrated to the GPS distance readings. The speeds correspond quite well with the encoder measurements, although the latter included a significant amount of signal noise, as is indicated in Figure 24. The encoder data shown here is shown at a 20Hz sample frequency (digital counter is sampled 20 times per second) and, typically, encoder data is filtered with a low-pass filter when used with a geometry system. A more detailed analysis of the noise observed in the encoder data is included in Appendix B.

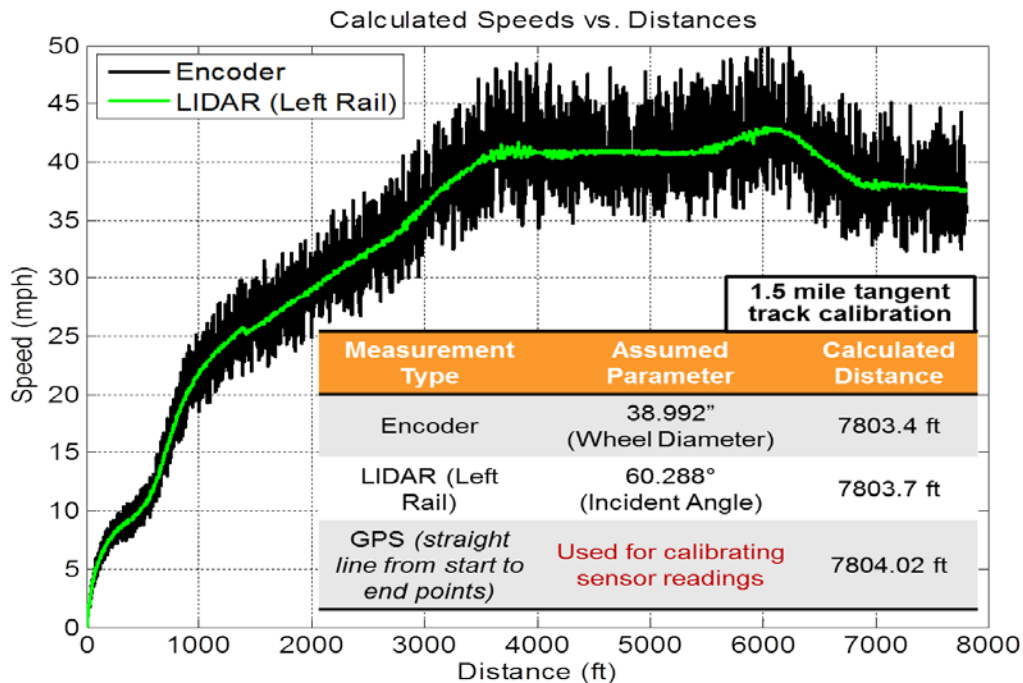


Figure 24: A comparison of calculated speeds vs. distance along 1.5 miles of tangent track calibration

The encoder and LIDAR speed signals are filtered identically to allow direct comparison (Figure 25). The signals correlate well, although the LIDAR still shows significantly less signal noise and variation.

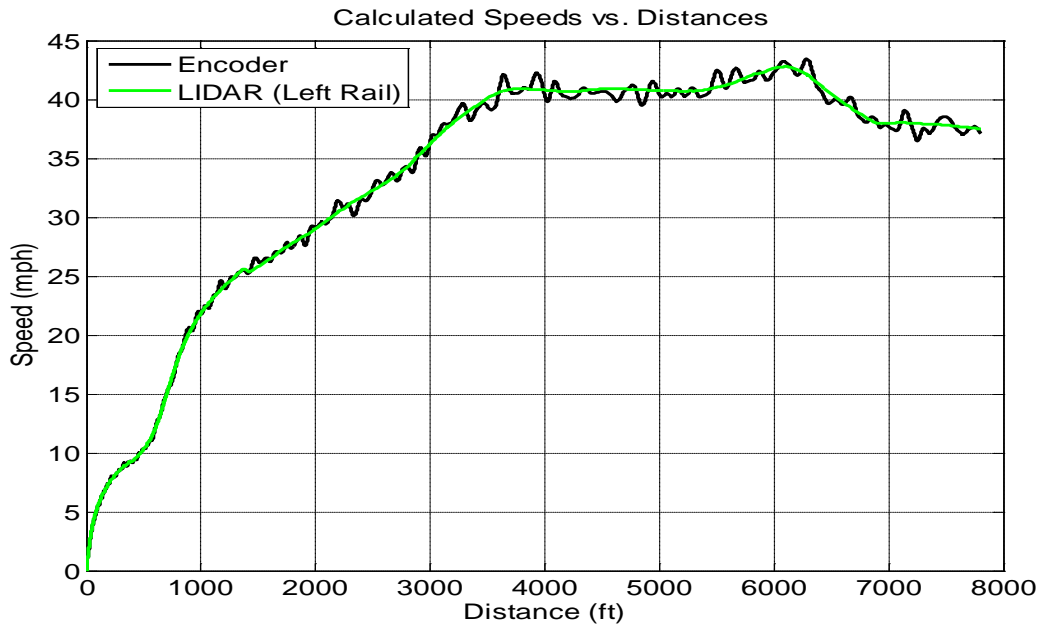


Figure 25: A comparison of speed vs. distance with filtered encoder and LIDAR

3.3.2 Ground-Truth Distance Calibration

Two ground-truth distance measurements were made near Crewe, VA, to calibrate the LIDAR and encoder. These ground-truth distance measurements were made with a measuring wheel. The two test sections, each 1,000 ft long, were marked for the calibration runs, as seen in Figure 26 below.



Figure 26: 1000 ft being walked out for ground-truth calibration run

The encoder and LIDAR distance measurements were scaled to match the initial 1,000-foot ground measurement. The distance versus time results of this calibration are shown in Figure 27. The speed measurements taken during the test are shown in Figure 28. While the encoder and LIDAR speeds correlate closely, the encoder shows more variance throughout the test run. This

is likely due to the mechanical vibration of the encoder (which increases with speed) and the variance in wheel-rail contact mechanics.

Two calibration runs were used to assess the ground-truth accuracy of the LIDAR system. The first run was used to set the LIDAR scaling factors required to convert the raw LIDAR signal data to the physical velocity measurement. The second calibration run was used to assess the accuracy of the LIDAR system.

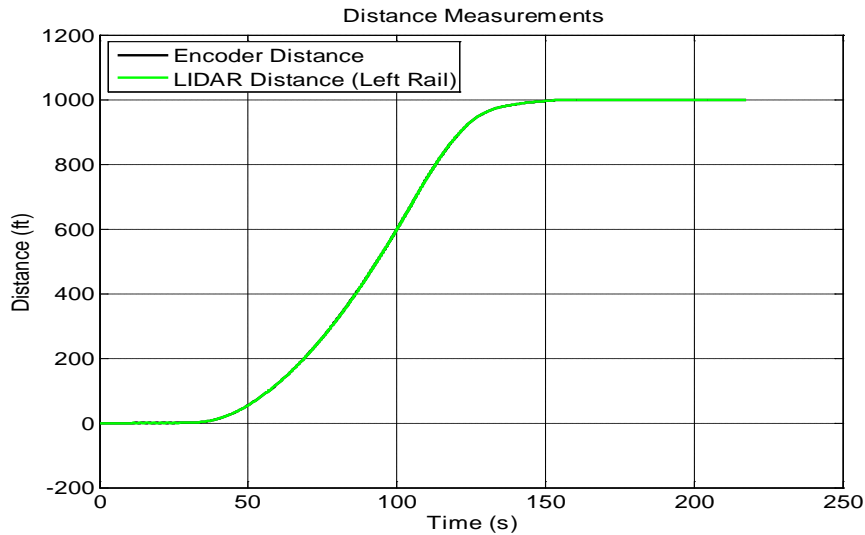


Figure 27: The encoder vs. LIDAR distances scaled to match ground measurement (Calibration Run #1)

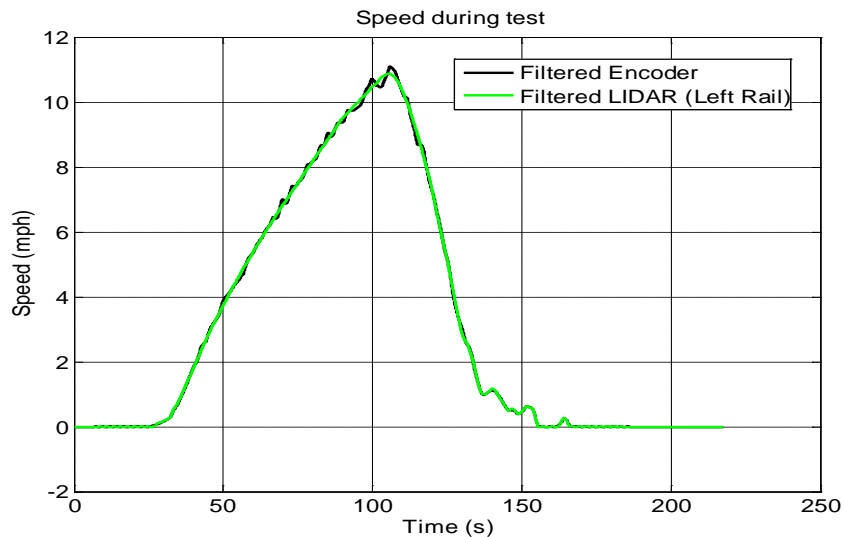


Figure 28: An assessment of the encoder vs. LIDAR speeds during calibration run (Calibration Run #1)

Figure 29 shows the results from the second calibration run. These results are based on the scaling determined from the first calibration run. The performance of the LIDAR is better than

that of the encoder in measuring the distance and closely matching the ground-truth established by the measuring wheel. The LIDAR measured within 0.2 percent of the ground-truth, compared with the encoder, which measured within 0.5 percent. The velocity measurements are shown in Figure 30.

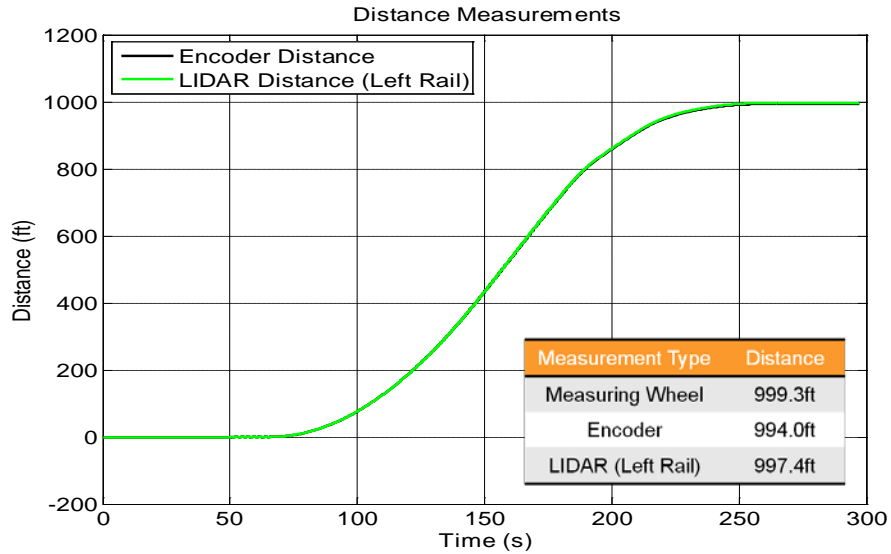


Figure 29: The encoder vs. LIDAR distance measurements based on scaling during calibration from Run #1 (Calibration Run #2)

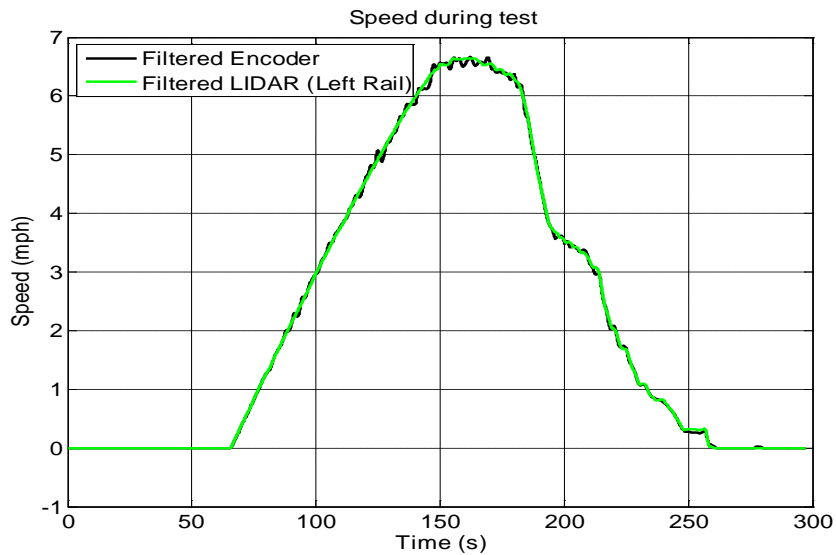


Figure 30: An assessment of the encoder vs. LIDAR speeds during calibration run (Calibration Run #2)

3.4 Test Results

Velocity data was collected over several hundred miles while the system was installed on the rail geometry car. A substantial amount of data was collected for tangent track and curved track in

both dry and inclement weather conditions. The data was post-processed and analyzed to better understand and further develop the performance of the system. Figure 31 shows an example of the LIDAR and encoder speed data across 15 miles of track. The encoder and LIDAR speeds match closely, with no visible dropouts by the LIDAR system. The LIDAR and encoder data were compared with each other in order to quantify the performance and capabilities of the LIDAR system.

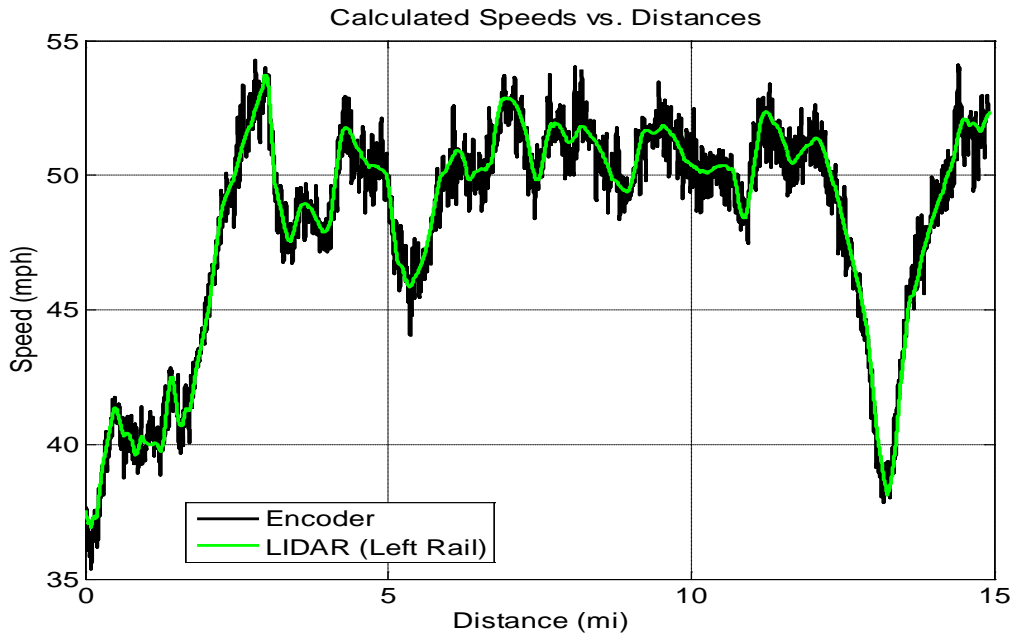


Figure 31: The encoder and LIDAR speed vs. distance over a 15-mile piece of track

3.4.1 Curved Track Testing

One of the primary objectives of this program was to determine the capabilities of the LIDAR system in terms of instantaneously measuring track curvature. A large number of curves traveled on revenue service mainlines were analyzed. To compare the LIDAR lens and beam setup, various curves were isolated and compared with the track chart data. Figure 32 plots an example of one of these curves, a 5.8-degree left-hand curve. VT uses curvature units similar to the U.S. railroad system standard: degrees of turn over an arc length of 100 ft. Each curve was measured by the LIDAR, and the average curvature was computed with and without the spline considered; these measurements were compared with the track chart.

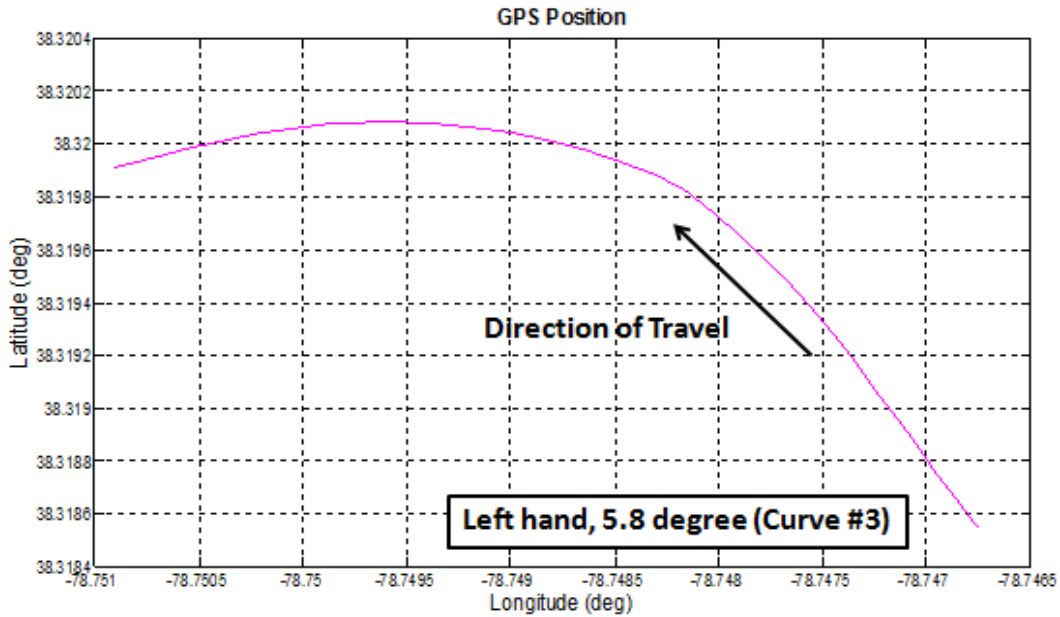


Figure 32: GPS position and direction of travel for 5.8-degree curve

Figure 33 shows the track curvature measurements by the LIDAR system for a 5.8-degree left-hand curve. The system accurately measures the track curvature, as well as the entry and exit spiral. The variations that are observed in the signal are most likely due to the change in carbody position as the railcar negotiates the curve. Given that the LIDAR system is mounted to the carbody, the variations may also be a result of track geometry changes in the curve. Further investigation is needed to conclusively determine the source of the variation. For the purpose of this study, however, one can confidently conclude that the LIDAR system has the ability to accurately measure the track curvature, in this case 5.8 degrees, which is the curvature noted on the track chart.

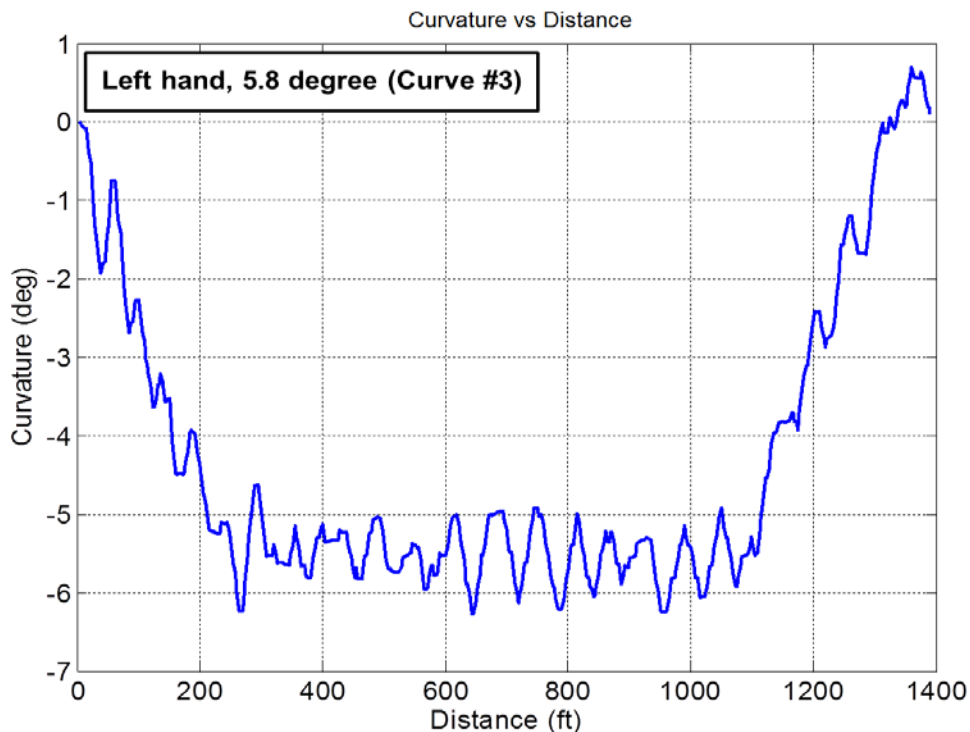


Figure 33: Curvature vs. distance for a 5.8-degree left-hand curve. The negative values imply a left-hand curve

In addition to studying the curvature recorded by the LIDAR, it is useful to compare the speeds it records with those measured by the encoder and the GPS during a curve. Figure 34 provides an illustration of train speed going through the 5.8-degree left-hand curve. During a curve, LIDAR signals are consistently smoother than encoder or GPS signals. The encoder signal has high signal variation (greater than 0.5 mph from the mean) because of wheel slip, flanging, and contact point lateral position movement on the rail wheel. Thus, the true speed of the car during a curve is not known when measuring with a mechanical encoder system. A commercial GPS unit also indicates inconsistent velocity readings while a change in heading is occurring. The figure clearly illustrates the smoothness of the LIDAR signal compared with the encoder velocity reading.

The LIDAR system is more precise than encoders and GPS systems. This precision is the result of the noncontact nature of the LIDAR railhead velocity measurements and the fact that the LIDAR is measuring both railhead velocities and reporting the average, centerline velocity.

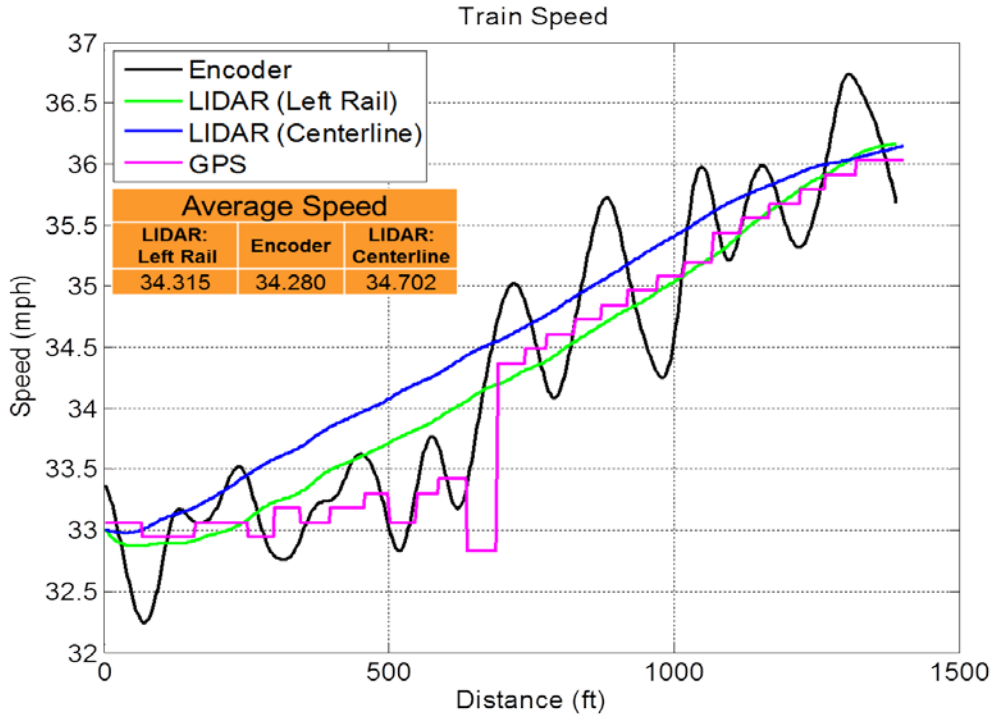


Figure 34: Train speed signals recorded from LIDAR, encoder, and GPS sensors during a 5.8-degree curve show high variation of the encoder signal due to wheel slip, flanging, and contact point lateral position movement

Further analysis was performed to calculate the travel distance measured within each curve by each sensor type (Figure 35). LIDAR- and encoder-calculated distances show a reasonable agreement within the same 5.8-degree curve, while the GPS calculated distance shows significant error.

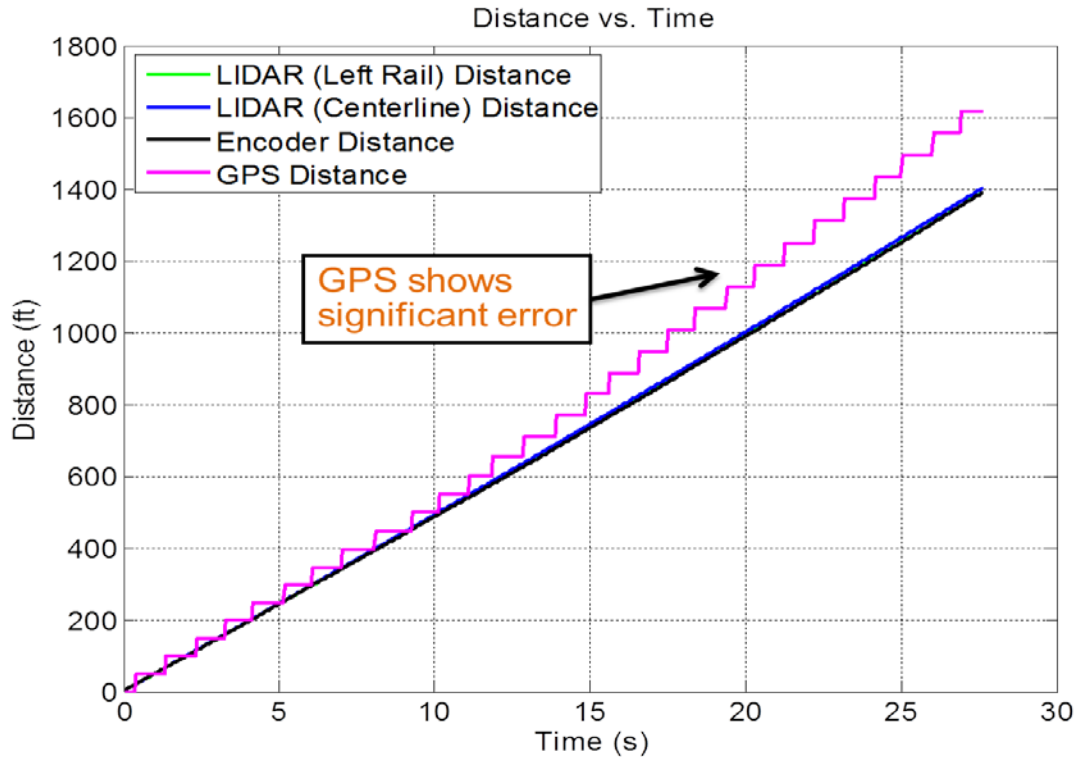


Figure 35: During a 5.8-degree curve, the calculated distances measured by LIDAR, encoder, and GPS systems were compared, and LIDAR and encoder showed good agreement (Encoder and LIDAR readings are essentially overlaid)

This analysis was completed on a total of 28 curves recorded during this test car setup, including the curve presented above. Each of the individual curves was identified on the track chart for comparison with the data for the individual curves. Figure 36 is an overview of all the curves analyzed, showing the curvature as documented on the available track chart

Using track chart curvature information, the LIDAR curvature readings were collected. The average LIDAR curvature measurement and the maximum LIDAR curvature measurement of each curve was calculated and plotted against the track chart curvature. The average curvature measurement from the LIDAR system closely corresponds to the track chart information throughout this series of curves. It is useful to note that the maximum LIDAR curvature readings usually exceed the track chart recordings.

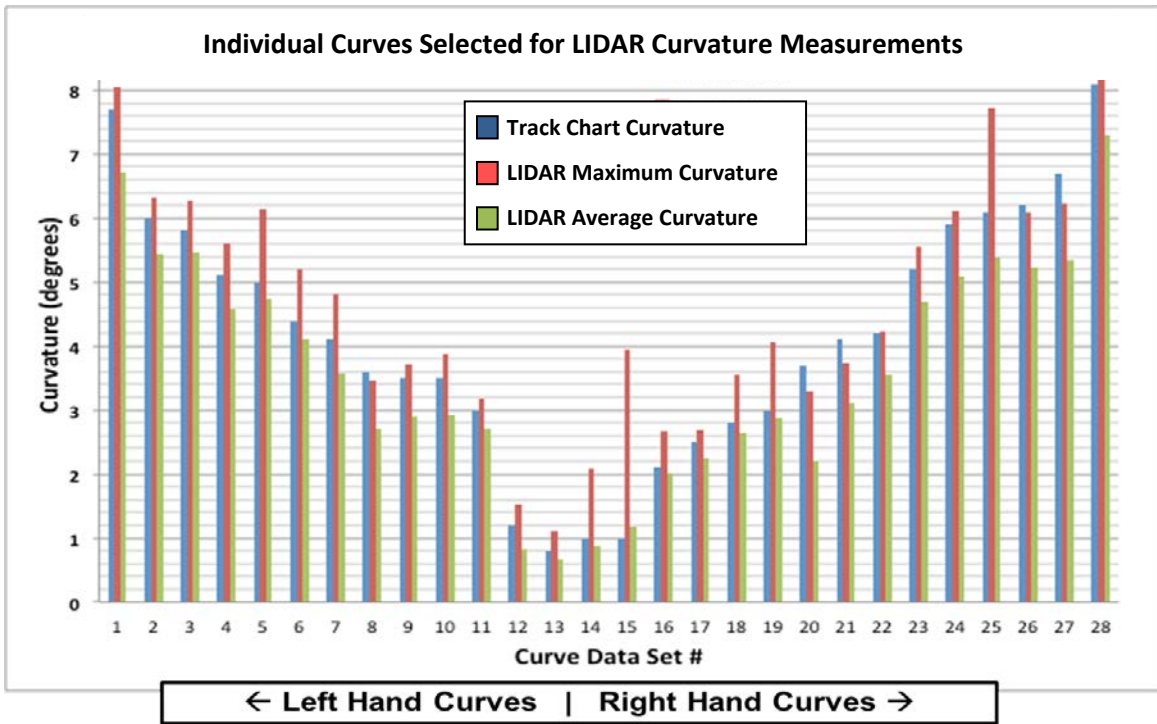


Figure 36: LIDAR curvature in comparison to track chart curvature

In addition to comparing the LIDAR track curvature measurements with the track chart, the LIDAR curvature data was compared with the rail geometry car measurements recorded by an IMU. Figure 37(a) shows the comparison between LIDAR and railcar IMU measurements, while Figure 37(b) shows the measured speed from the LIDAR and encoder systems along the same section of track. Both the LIDAR curvature and speed measurements show good agreement with the rail geometry car measurements, proving that the LIDAR system is capable of accurately determining such measurements.

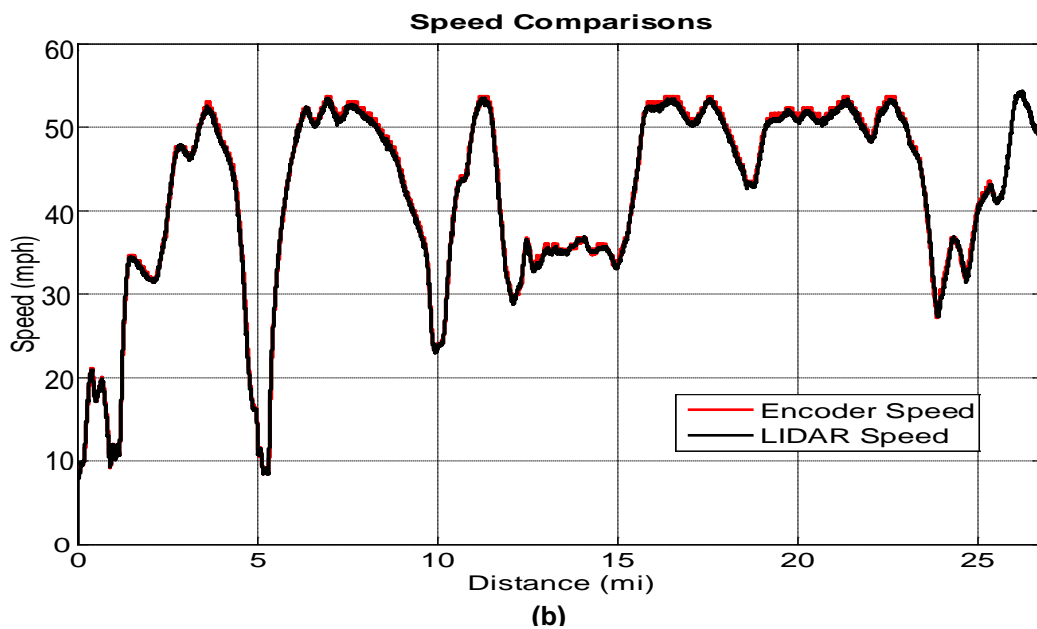
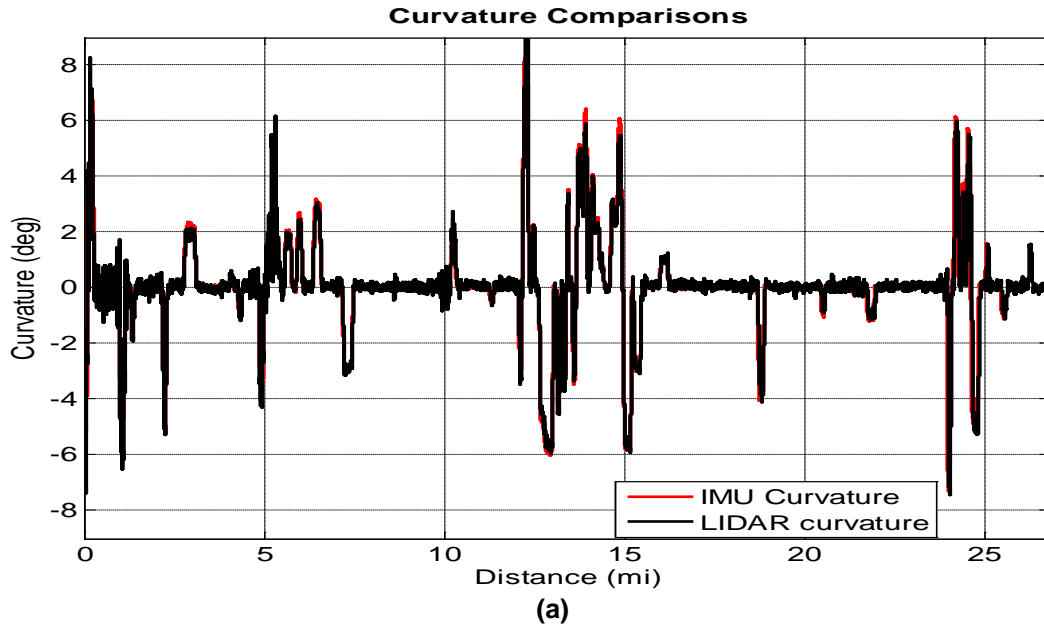


Figure 37: LIDAR and rail geometry car measurements: (a) curvature; (b) speed

A close-up look at the data indicates that the LIDAR measurements show slightly more variation than the rail geometry car measurements at low train speeds (Figure 38). This variation between the LIDAR average and maximum curvature readings is attributed to the ability of the LIDAR system to make measurements at very short intervals on the track. One can think of the LIDAR measurements as instantaneous, whereas railcar measurements are broad-trend data.

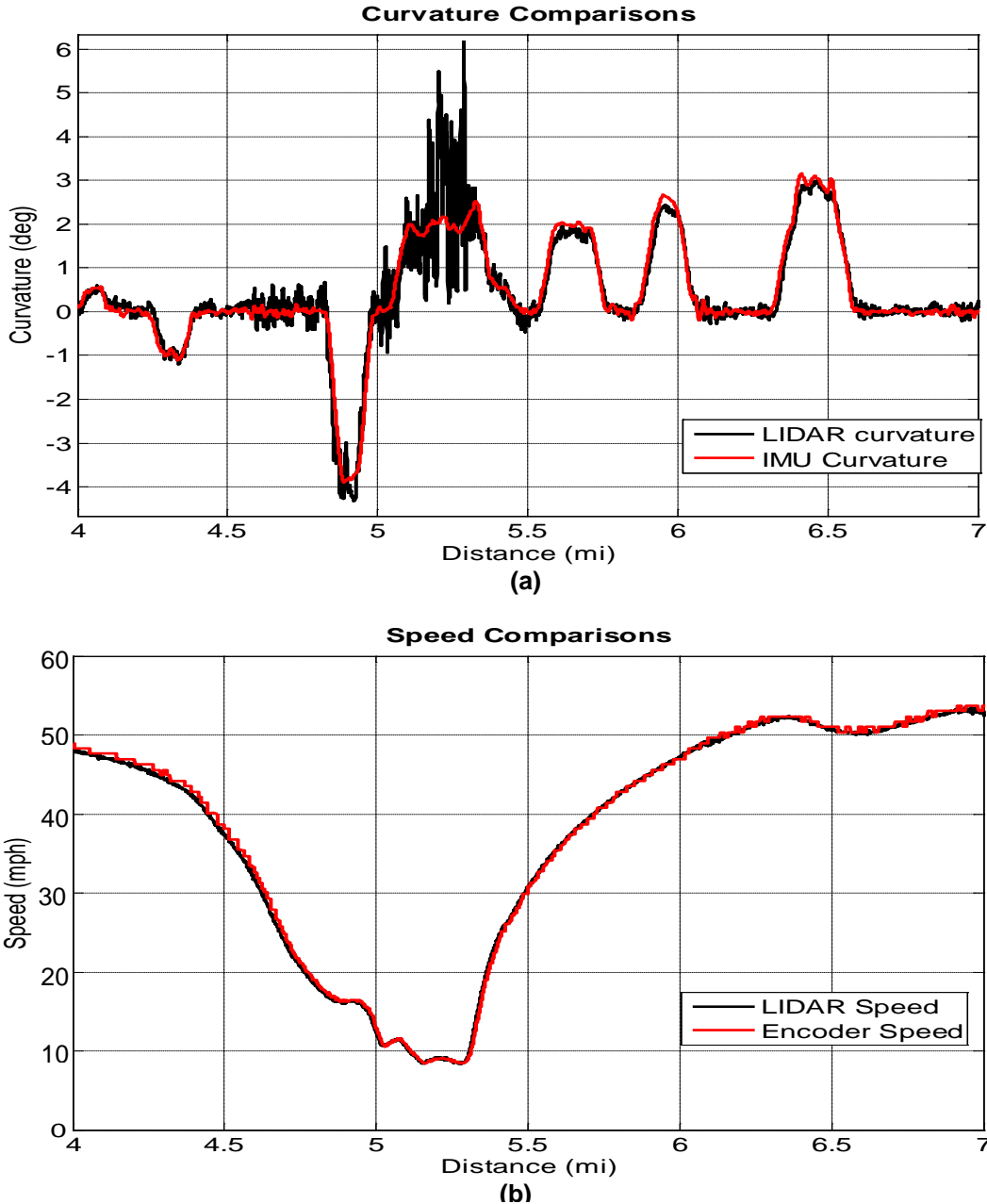


Figure 38: Comparison of LIDAR and rail geometry car data for a 3 mile track segment: (a) track curvature; (b) speed

3.4.2 Inclement Weather Testing

During one of the test days, the LIDAR system went through a significant performance evaluation while faced with heavy winds and rainfall. The system collected data and functioned without any errors, despite the severely inclement weather. The tests began near Crewe, VA, in heavy rain and with wind gusts as high as 25 mph. LIDAR signals were unaffected by the rain, and the system performance was not degraded during the inclement weather. The system collected data during a 4-hour period of rainfall. Table C-1 in Appendix C shows the weather summary for the test period.

Figures 39 and 40 show that the system was still able to measure train speed and distance traveled over a long period with no signal dropouts. The LIDAR data correlates well with the encoder's data from the rail geometry car. The LIDAR data for the left rail (the same side on which the encoder is mounted) is shown, along with the "centerline" LIDAR data (an average of the left and right LIDAR signals).

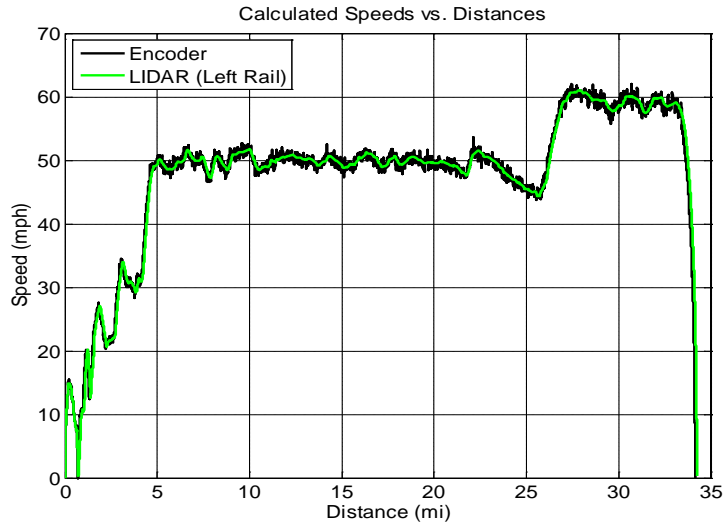


Figure 39: The LIDAR maintained the ability to accurately measure speed continuously through a heavy rain over a nearly 35-mile distance

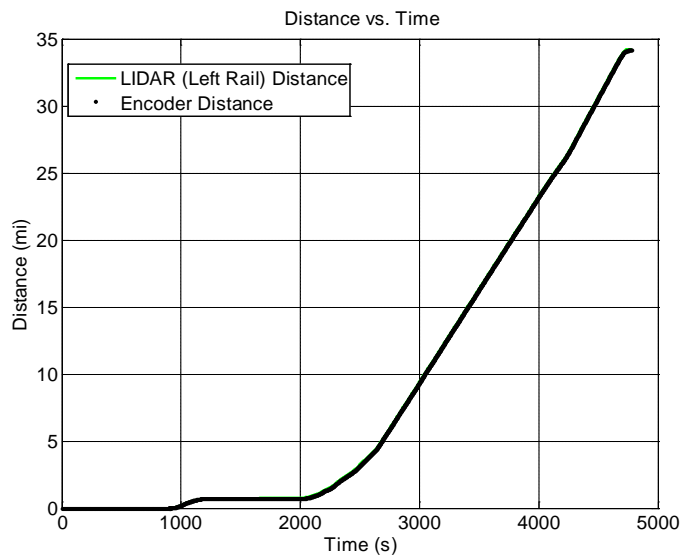


Figure 40: In inclement weather, the LIDAR maintains its ability to accurately measure distances. Here, the encoder and LIDAR left rail measurements were 34.136 mi and 34.237 mi, respectively

3.4.3 Effect of Special Track Work

Although no specific tests were conducted on special track work (i.e., switches, frogs, crossings, etc.) using this test setup, there have been test runs that went on for significantly long distances containing multiple special track work within every mile. Figure 41 shows an 88-mile run on which there were no dropouts or issues with the signal. The plot also indicates a slight difference, similar to what was observed during the ground-truth calibrations, in the total distance measured by the encoder and the LIDAR system.

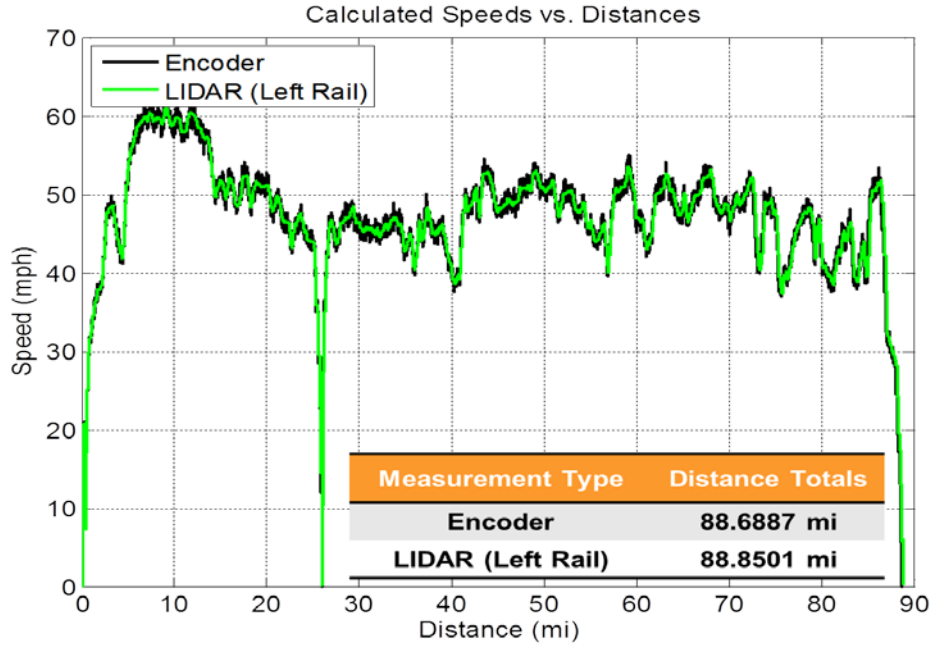


Figure 41: Consistent LIDAR signal over an 88-mile stretch including special track work with no dropouts

4. Semi-Autonomous PXI LIDAR Railway Geometry Car Testing

For this phase of testing, VT introduced new hardware to the system: the NI PXI CPU with updated software, optics, and RF circuits from YES. This system was designed to run in an unmanned mode so that once started, it could collect data continuously without user intervention for as long as 2 to 3 weeks. The data is saved on a conventional hard drive, to be downloaded and erased periodically. The continuous length of each test is dictated by the size of the hard drive. One needs to erase the stored data from the hard drive (approximately every 2 to 3 weeks) before its capacity is exceeded.

Prior to installation on the rail geometry car, the system underwent extensive bench-top tests in the lab. Once installed on the rail geometry car, its functionality and performance were further tested before it was left to operate without user intervention.

Other improvements to the system included:

1. Adaption of polarization-maintaining optical components to further improve the LIDAR signal intensity,
2. Installation of the laser diodes and RF hardware in an isolated chassis in close proximity to the PXI CPU in order to better protect them from vibrations,
3. Increased computational speed of the system, enabling it to sample at more than twice the recorded data frequency, while performing other tasks such as collecting additional data, and
4. Use of ruggedized, explosion-proof housings for the optical lenses to better protect them from the demanding environment that commonly exists in revenue service.

The second round of tests included a new field-hardy system that was built based on the same principles of the laboratory-grade system evaluated during the initial round of testing (described in the previous section). The main conclusions derived as a result of the extensive field-testing performed with the new system include:

1. The new field-hardy LIDAR system worked remarkably well onboard a track geometry car operated by one of the U.S. railroads for 5 months and over several thousand miles of revenue service track, all while operated in an unmanned manner.
2. The LIDAR system proved more accurate than the encoder in ground-truth calibration runs.
3. The wheel-mounted encoder signal is susceptible to significant variations (noise) that are not seen in the LIDAR signal.
4. The LIDAR system is able to measure track curvature in real time, with the same (or greater) accuracy as IMUs that are commonly used in track geometry cars.
5. The LIDAR system is able to measure curvature while traveling at crawling speeds (as low as 1 mph) far below what is possible with IMUs (commonly more than 10 mph).
6. The LIDAR curvature measurements indicated more variation than the IMUs; the variation may have been caused by the truck dynamics in the curve, track geometry differences, or both. Additional studies are needed to determine the exact source of

variations and to assess if the LIDAR system can be used for track geometry measurements while simultaneously measuring track speed and curvature.

7. The output of the LIDAR system can be modified to simulate the TTL foot pulse signal by the encoders that are used in track geometry cars. Further investigation is needed to assess the effectiveness of the LIDAR system in replacing the encoder in a track geometry car as a direct retrofit.

4.1 System Installation

The installation of the LIDAR optics was changed to a truck-mounted configuration, a departure from the earlier tests that adopted a carbody mounting, as shown in Figures 42 and 43. A frame made of extruded aluminum, secured to the truck through redundant fasteners, was used to install the LIDAR optics housings. Initially, the LIDAR lenses were pointed to the gauge corner (similar to what worked well when the lenses were body-mounted), but this orientation proved to be suboptimal for measuring track curvature where the truck experienced significant yaw. To eliminate this problem, the lenses were moved to an alternate configuration in which they were placed almost directly above the TOR. This orientation proved to be effective for both track speed and curvature measurements, although it was noisier than the body-mounted configuration. The TOR orientation is shown in Figure 43. Appendix A presents a more detailed comparison of the LIDAR beam configurations.



Figure 42: Truck mounted LIDAR lenses, pointing at gauge corner

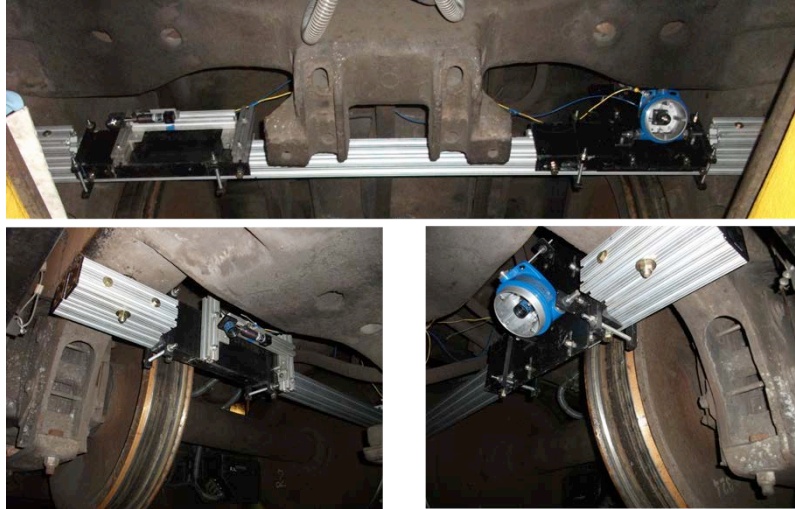


Figure 43: Installation of LIDAR lenses, oriented toward Top of Rail (TOR)

After some initial validation of the new geometry system onboard the track geometry car, it was tested unmanned for a period of 4 months on revenue service mainline. The test (determined by the track geometry car schedule) involved traveling from Roanoke, VA, to Narrows, VA, then to Fort Wayne, IN, and continuing to Chicago, IL.

Figure 44 shows the installation of the PXI system, the chassis containing the RF hardware and laser diodes, and the auxiliary laptop used to remotely access the system. By using the onboard KVM network, one could remotely access and monitor the system through an Internet connection and the auxiliary laptop shown.

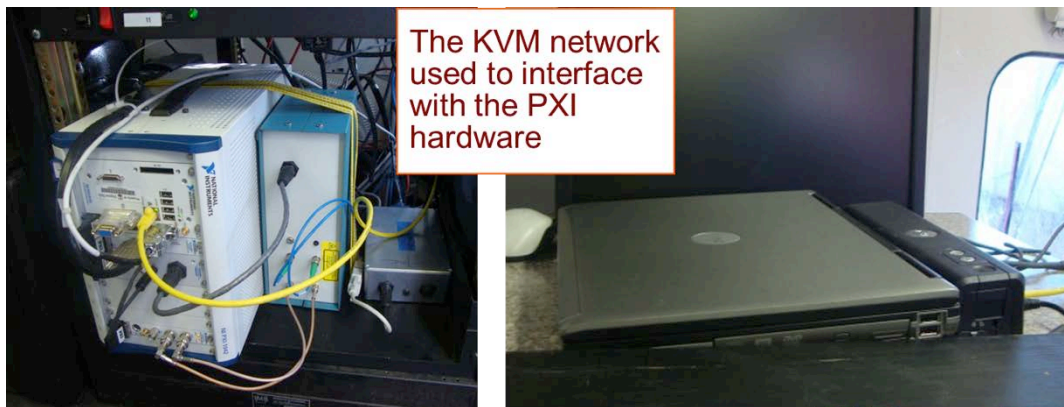


Figure 44: PXI system mounted onboard the track geometry car

4.1.1 Ruggedized Enclosures for Optical Lenses

Another addition to the system during the PXI testing phase was the hardened, explosion-proof protective housings used to enclose the optical lenses. The housing was initially used with its standard glass window; however, testing revealed that the glass provided with the housing absorbed a significant portion of the laser light, resulting in reduced signal strength and leading to increased signal dropouts. A new glass was specified and integrated into the housing to

increase the signal strength. The housing cover was modified to incorporate a window made of borosilicate glass; laboratory testing subsequently showed an improvement of at least 45 percent in signal strength. Figure 45 shows the enclosure after the window modification. In order to assess the optics performance and the optimal housing configuration, the field tests were performed with a glass window in only one of the two housings. The glass window was left out of the other housing so as to compare the signal intensity of the two signals over time. This comparison provides data on the clouding (due to debris and contaminant accumulation) of the lenses over time. The tests proved that the glass lens can be removed from the housing if positive air pressure is supplied to the housing, as will be discussed later.



Figure 45: Explosion-proof protective housing securing the LIDAR lenses onboard the track geometry car

4.2 Test Route

The PXI system has undergone a significant amount of testing and has accumulated substantial test miles on revenue service tracks. The routes that the system was tested on included:

- Roanoke, VA, to Narrows, VA (early February 2012)
- Ft. Wayne, IN, to Chicago, IL, and back (mid-February 2012)
- Various locations on the Eastern seaboard and in the Midwest (February to May 2012)

During the field tests onboard the track geometry car, no modifications or changes were made to the system, indicating the system's durability and sustainability for testing over long distances and long periods of time and in various track conditions and inclement weather.

4.3 Test Results

The data collected on revenue service tracks from the Eastern seaboard to the Midwest included long sections of tangent track, simple and compound curved track, sidings, switches, and other special track work. The following sections will provide a detailed analysis of the results from tangent track and curvature testing. The analysis is intended to highlight the system:

- Accuracy,

- Satisfactory performance in the presence of special track work, and
- Ability to generate a foot pulse marker in a similar manner to wheel-mounted encoders that are used onboard track geometry cars.

4.3.1 Tangent Track Testing

Earlier tests showed that, compared with ground-truth measurements, the LIDAR system provides higher accuracy than a wheel-mounted encoder (see Section 3.3.2). To further assess its performance, the LIDAR system was tested over numerous tangent tracks during the time it was installed onboard the track geometry car. Although an analysis of all the tangent track data would be too voluminous and falls outside the scope of this document, a sample of the distance and speed measurements is provided.

As an example comparison, a 1.3-mile section of tangent track near Chicago, IL was selected. The GPS coordinates, shown in Figure 46, indicate the long stretch of tangent track, followed by a left-hand curve, as the train travels northeast (the direction noted on the figure).

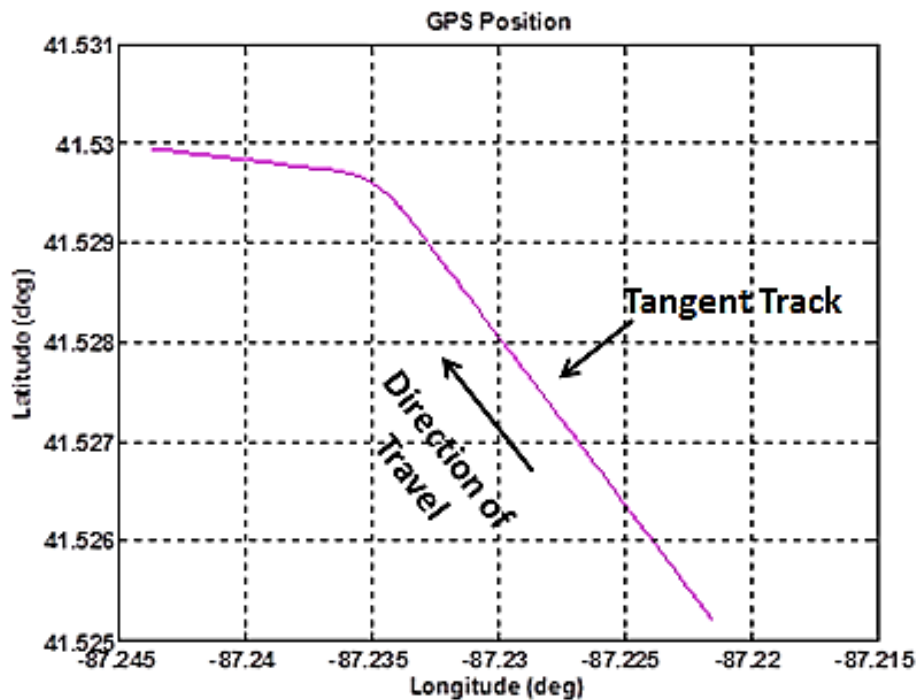


Figure 46: Coordinates for an example tangent track near Chicago, IL

Figure 47 displays distance traveled versus time for the right- and left-rail LIDAR measurements, as well as the encoder and track centerline. The centerline measurement is calculated from the left- and right-rail data by simply taking their average. It is worth noting that the centerline and the left- and right-rail measurements are the same because on tangent track the distance traveled on the two rails is identical. Additionally, the figure indicates that the measurements by the encoder and LIDAR system are nearly identical. To better highlight the similarity of the measurements, Figure 48 shows the difference in measured distance between the encoder and the left rail LIDAR. The left rail LIDAR is selected since the encoder is installed on

the left side of the railcar. The distance difference shown in Figure 48 is believed to be a result of any slippage that happened at the wheel and was measured by the encoder, as was evident during the ground-truth calibrations. Nonetheless, the LIDAR system is able to provide distance measurements with higher accuracy, or as accurately, as the encoders that are currently used on the track geometry cars. Furthermore, it is important to note that the LIDAR system accurately measures distance at much lower speeds than is possible with encoders.

Figure 49 provides a comparison between the train speeds measured by the LIDAR system and those calculated from the encoder distance. (Recall that encoders measure distance through the number of revolutions of the wheel, which can be differentiated to calculate speed.) Once again, the left rail LIDAR measurements are selected for the comparison because the encoder is mounted on the same side. Because the measurements are on a tangent track, the right rail and track centerline measurements are expected to be identical to the left rail.

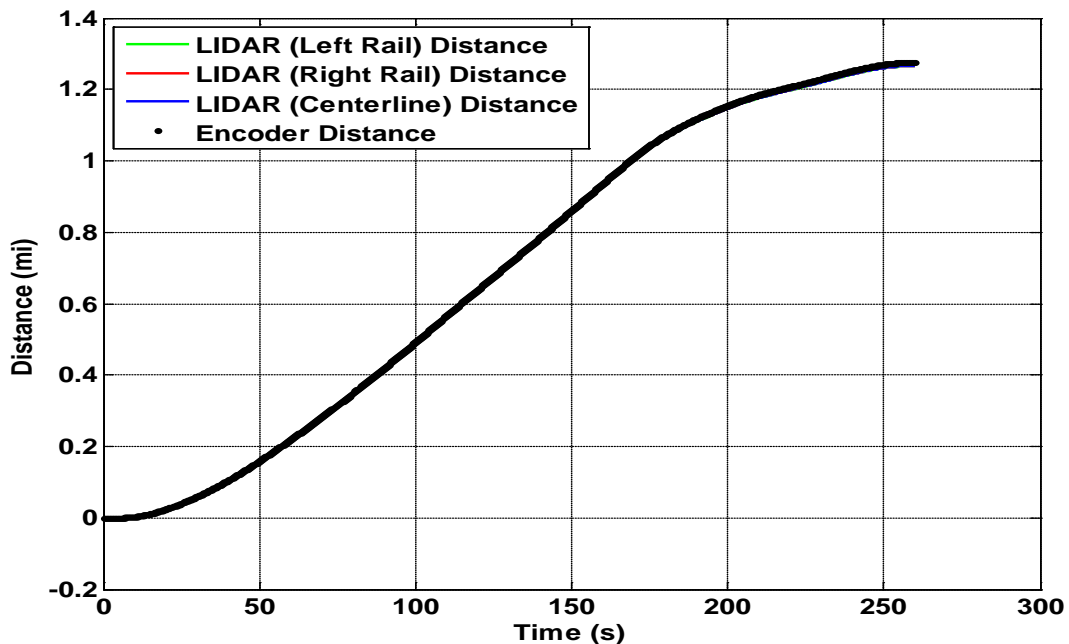


Figure 47: A comparison of distance vs. time measurements by the encoder and the LIDAR system on tangent track (Encoder and LIDAR are essentially overlaid)

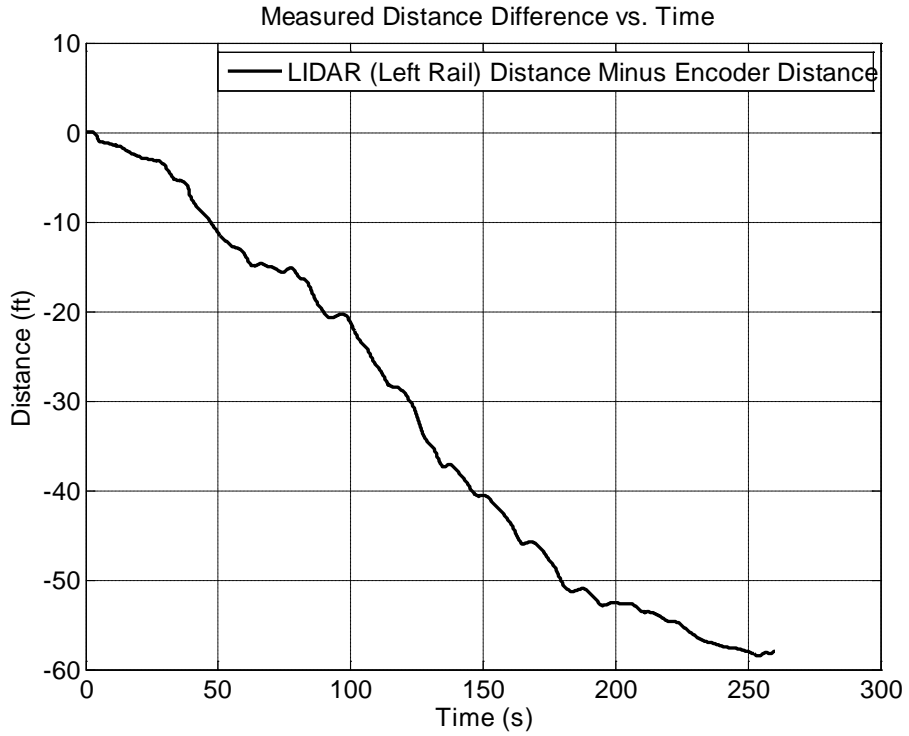


Figure 48: Difference in distance measurement between the encoder and the LIDAR system for tangent track

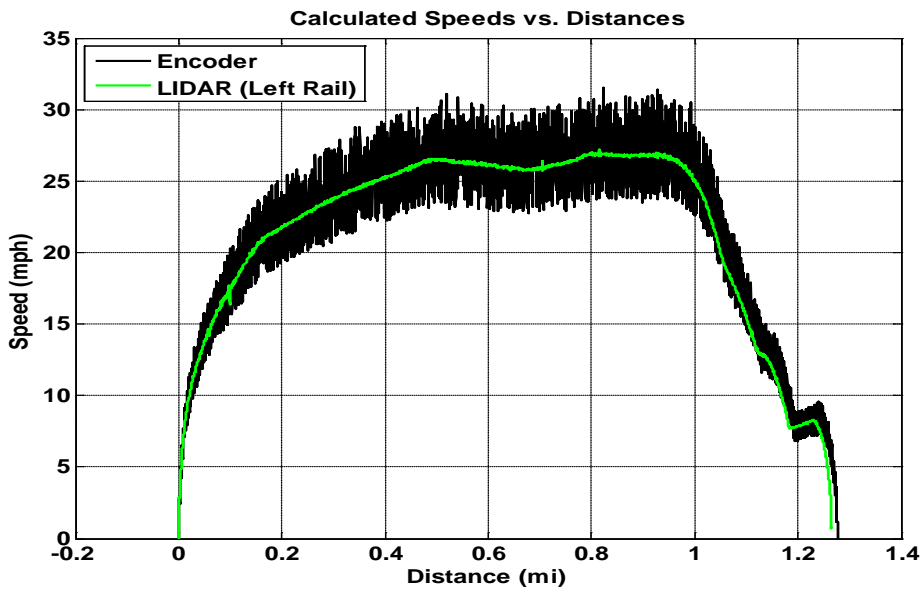


Figure 49: A comparison of train speed vs. distance from the LIDAR system and the raw (unfiltered) encoder data on tangent track

The data presented in Figure 49 is the raw encoder and LIDAR data. Although both plots have the same trend (indicating the similarity in the measurements), the encoder calculated speed shows far more high-frequency content. Track geometry cars commonly use highly sensitive encoders capable of generating as many as 10,000 pulses per wheel revolution. This high sensitivity makes the encoder output susceptible to increased signal noise, although it greatly improves the spatial resolution (accuracy) of the measurements. Common practice is to highly filter the encoder raw data to capture the general trend or average. The encoder's high resolution helps with the ability to generate foot pulses more accurately. It is possible to further filter the encoder data to eliminate the high-frequency (noise) content, although this will make its processing incompatible with the LIDAR measurements. The results shown in Figure 49 sufficiently illustrate the accuracy of the LIDAR speed measurements, compared with the existing practices (i.e., encoders).

An additional assessment of the LIDAR speed measurement is provided in Figure 50, where the filtered data for both rails is co-plotted with GPS data and encoder (calculated) and track centerline (calculated) measurements. The encoder and centerline calculated speeds are the same as described previously. For the encoder, the derivatives of the distance measurements are used to calculate speed, while the average of speed from the two rails gives the track centerline speed. Appendix D provides a frequency content analysis using FFT of the data presented in Figure 50.

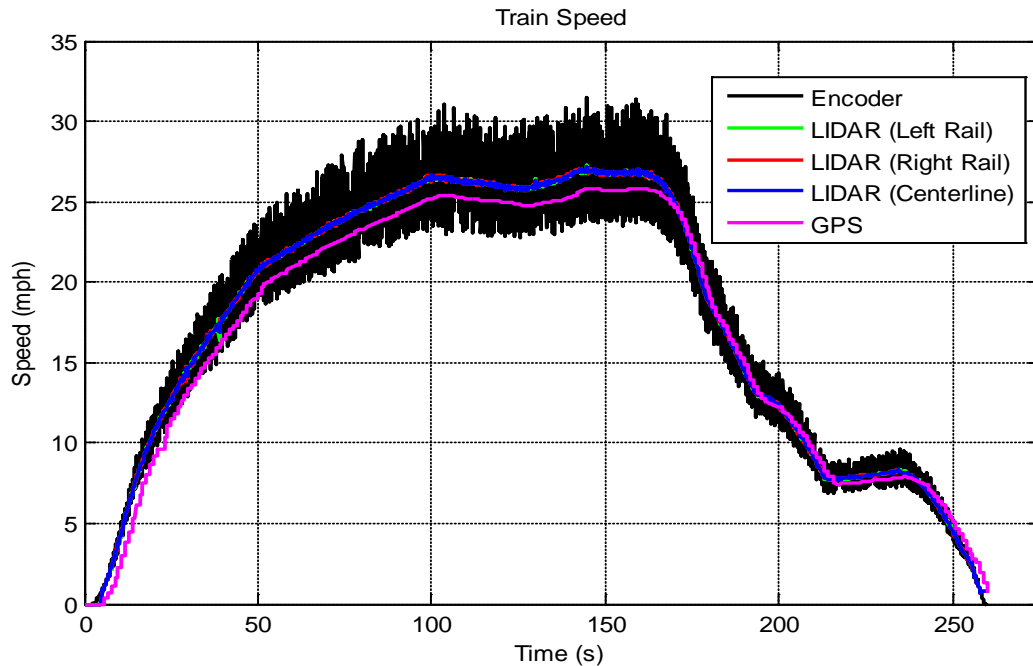


Figure 50: A comparison of LIDAR speed measurements with GPS and encoder data for tangent tracks

4.3.2 Curved Track Testing

The LIDAR system's ability and accuracy in measuring track curvature was evaluated in a manner similar to the tangent track analysis discussed in the previous section. A stretch of mainline track with a few right- and left-hand curves was selected, as is shown in Figure 51. Positive curvature indicates right-hand curves, whereas negative curvatures are left-hand curves.

A comparison is made between the curvature measurements from the LIDAR system and the data from the IMU onboard the track geometry car. The data from both systems closely match each other, although the LIDAR measurements have more fluctuations in the main body of the curves. These fluctuations are attributed to one of two sources, or both:

1. The varying truck yaw movement in the curve can change the relative angle between the LIDAR beams and truck, therefore introducing a variance in the curvature measurements.
2. The ability of the LIDAR system to measure track curvature with very high spatial resolution enables it to detect track geometry variations that may exist in curves. Note that an IMU operates based on the lateral forces generated by the centripetal forces and primarily measures the broad track curvature, not local variations in track geometry. The LIDAR data can be filtered to reduce the effect of the local track variations in order to put it more in line with the inertial filtering that is inherently present in IMU (see Figures 53 and).

It is also possible that both factors mentioned above contribute jointly to the fluctuations observed in the LIDAR data.

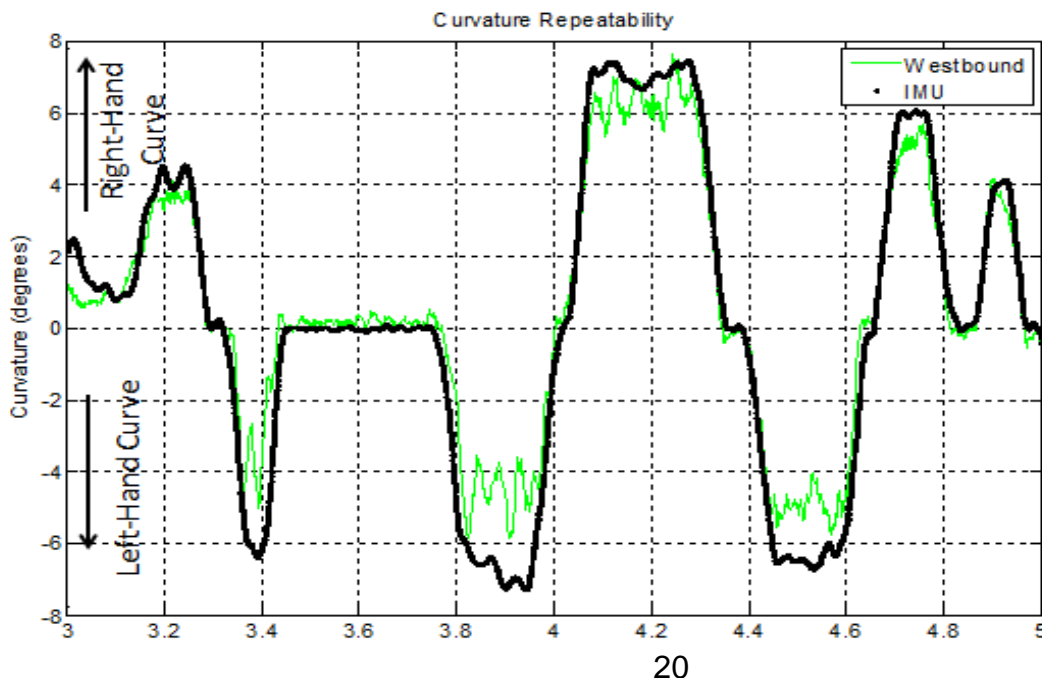


Figure 51: A comparison between the LIDAR track curvature measurements with the track geometry car (IMU) data

Determining the exact source of the fluctuations is the subject of a follow-up study that has been proposed to FRA. Beyond being scientifically intriguing, understanding the main source of the fluctuations can have significant practical implications. If it is determined that the fluctuations in the data are mainly due to the local track geometry changes, then it will be possible to extend the application of the LIDAR system beyond track speed and curvature measurements. Such a discovery will enable the development of a multi-purpose system that can be used for measuring both track speed and curvature and track geometry.

In order to determine the repeatability of the LIDAR curvature measurements, a comparison was made on the same section of track traveling in two different directions, as shown in Figure 52. The eastbound and westbound curvature measurements very closely align, with the exception of the 6-degree left-hand curve (at a distance of 3.9 miles) where westbound curvature measurements are different from the eastbound measurements. A similar, but less significant, discrepancy is seen at 3.4 miles for a short 6-degree curve. At this time, the source of the discrepancy has not been conclusively determined. The best estimate is that the three-axle truck that is on the track geometry car yaws differently during the westbound and eastbound travel, resulting in a change in curvature measurements. This theory, however, is not entirely supported by the measurements for the right-hand curves and the 6-degree left-hand curve at the 4.5-mile marker. Further investigation into this matter is necessary to determine the error source. It is believed that this behavior is primarily found in the truck-mounted LIDAR system with the selected beam alignment. Changing the beam alignment or the LIDAR lens mounting to the carbody could entirely eliminate the variations seen for some of the curves in Figure 52.

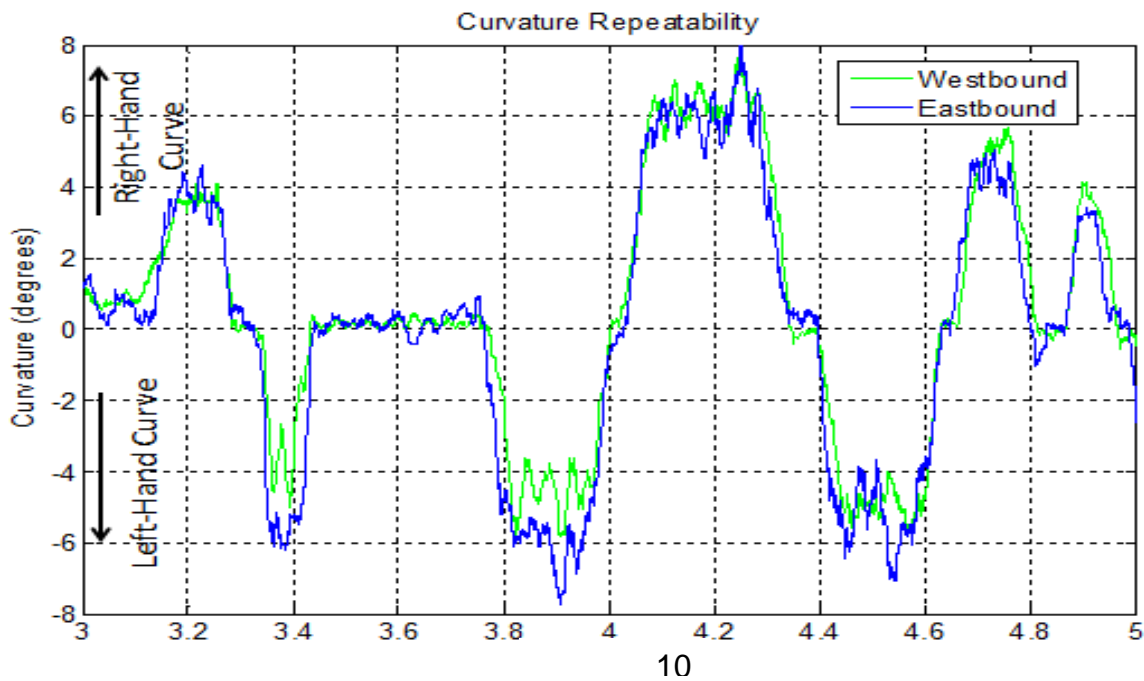


Figure 52: A comparison of LIDAR track curvature measurements east- and westbound, to show repeatability

Whereas earlier figures showed the system performance over a long stretch of track, the next two figures are intended to highlight the LIDAR system results for specific curves. Figure 53 and Figure 54 show the speed versus distance traveled in a 3.1-degree left-hand curve. The slight speed differences between the right- and left-hand curves in Figure 53 are further highlighted in Figure 54. This speed difference indicates the varying distances that the left and right wheels travel in the main body of the curve. The high-rail wheel (in this case, the right side) must travel a longer distance than the low-rail wheel (in this case, the left side). Because the wheels are

rigidly mounted to the solid axle with no differential rotational velocity, the wheel on the high rail (right side) must travel faster than the other wheel, as is clearly shown in Figure 54.

The fluctuations observed in the encoder measurements are believed to be due to the wheel slippage that is on the left side (low-rail side). Slip occurs since the rotational speed of the two wheels is the same throughout the axle even when one wheel (high-rail) travels farther than the other wheel through a curve. Both Figure 53 and Figure 54 effectively capture this intriguing wheel dynamic through the encoder data.

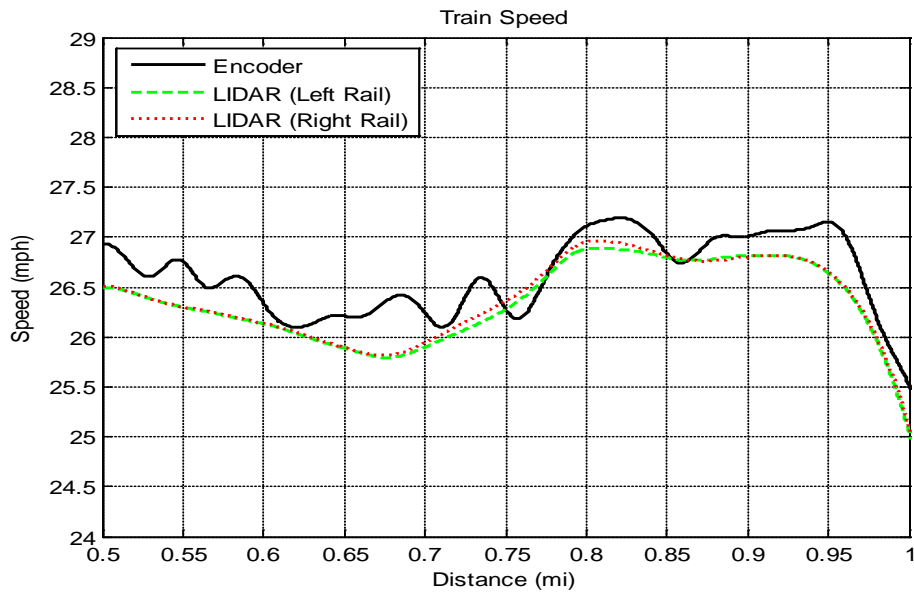


Figure 53: A comparison of LIDAR and encoder train speed through a 3.1-degree left-hand curve

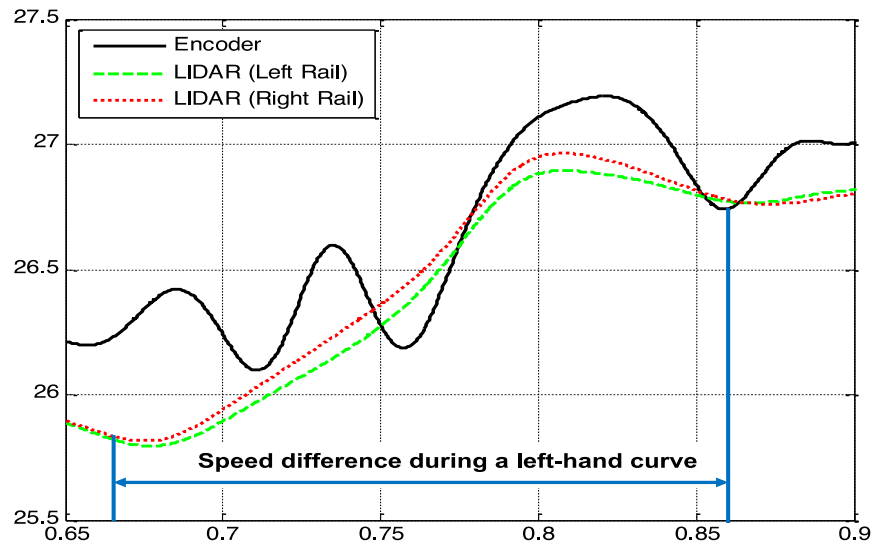


Figure 54: Train speed measured by the LIDAR system and the encoder in the main body of a 3.1-degree left-hand curve

4.3.3 Foot Pulse Feasibility

The feasibility of using the LIDAR distance measurements as a replacement for the encoder-generated “foot pulse” was explored. The wheel encoder signal is currently used to drive a circuit that outputs a digital TTL signal for every foot of travel along the track. This signal is used by a variety of track geometry measurement systems on a track geometry car. A software foot pulse signal was generated to simulate the foot demarcations for the LIDAR distances traveled. This footmark was compared with the footmarks from the encoder pulses. Figures 55 and 56 show a comparison of these two simulated pulses for 50 and 5 ft, respectively.

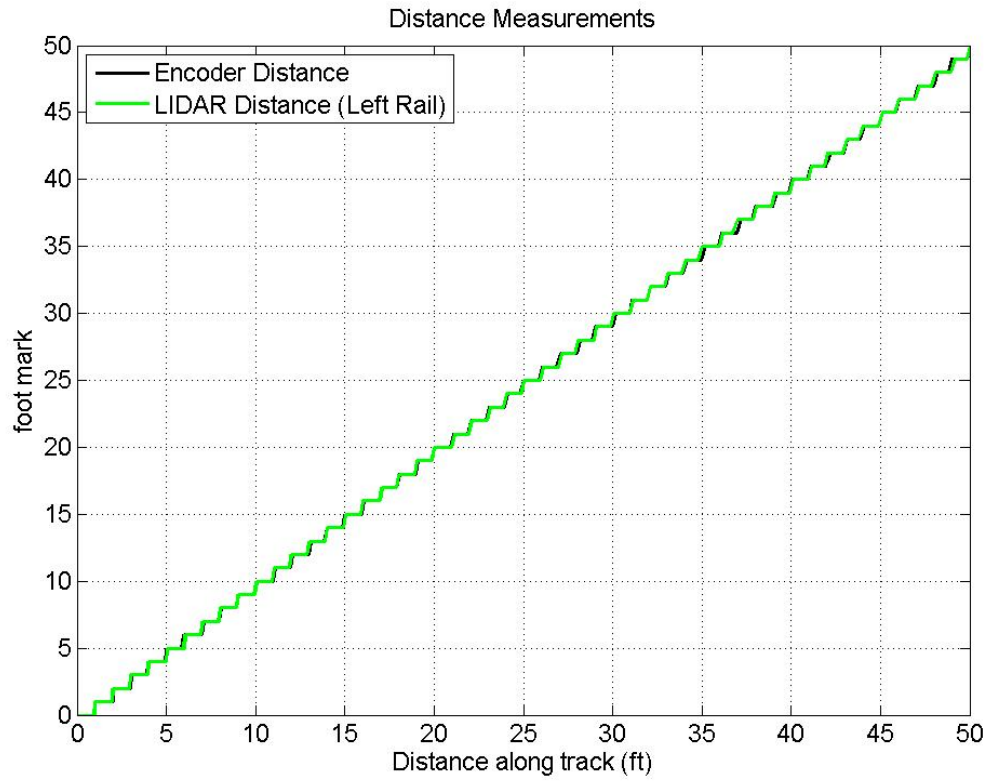


Figure 55: Simulated LIDAR foot pulse signal versus encoder foot pulse for 50 ft of travel

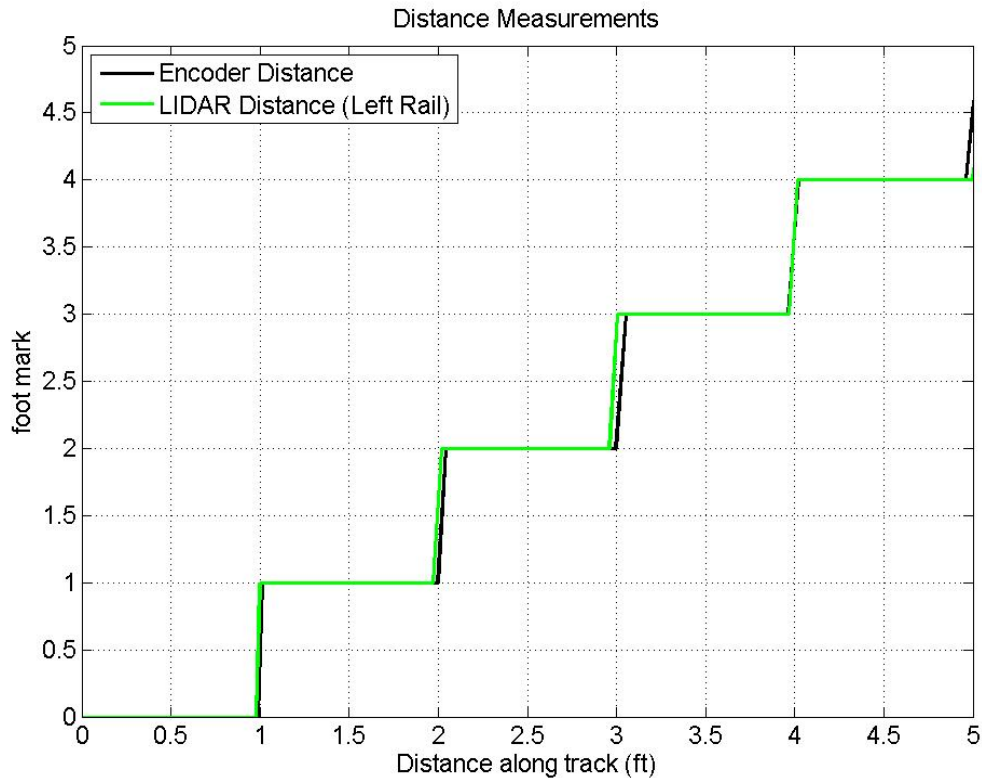


Figure 56: A close-up of simulated LIDAR foot pulse signal versus encoder signal for 5 ft of travel

Figures 55 and 56 show the foot pulses by the encoder and the LIDAR system to be nearly identical, with occasional small deviations. A closer inspection of the signal in Figure 56 indicates that the two signals deviate slightly from each other. However, this deviation is different from the overall accuracy of the two systems, which was evaluated during the ground-truth calibration in Section 3.3.2. The small difference (or jitter) in the foot pulses is caused by the data save rate of the LIDAR and encoder data on the PXI computer and not by the inaccuracy of either system. If the data had been saved at a higher rate, then the foot count jitters would not have been perceptible. The error would have been within the total distance difference measured during the ground-truth calibration runs (i.e., less than 0.4 percent). In a production system, a dedicated voltage-to-frequency counter or a digital counter system would easily enable replacement of the encoder foot pulse with the same from the LIDAR system. Further investigating and demonstrating the circuitry needed to generate the foot pulse signal from the LIDAR system is part of a follow-on study that has been proposed to FRA and is currently under evaluation. The demonstration will include replacing the encoder foot pulse signal with LIDAR systems and proving that the latter can serve as a direct retrofit to the existing foot pulse signal on a track geometry car.

5. Carbody-Mounted LIDAR System Revenue Service Testing

During the previous round of tests, the LIDAR system was truck-mounted. In order to evaluate the suitability of a carbody-mounted system and further verify earlier test results, the system installation was changed and a new round of tests were performed for nearly 5 months onboard a track geometry car that was operated on various revenue service tracks.

The primary conclusions reached during these tests were the same as the earlier PXI system tests discussed in Section 4. The results confirmed the LIDAR system's performance in a different mounting configuration (carbody mounted) and over significantly more miles of track.

5.1 Test Setup

The PXI-based LIDAR system mounting was changed from the truck (previous tests) to the carbody. Recall that the LIDAR lenses were body-mounted during the initial round of testing that included the laboratory grade system, as discussed in Section 3. This round of tests was intended to repeat the initial tests with a field-hardy system over a much longer period of time.

Figure 57 displays the system installation onboard the carbody. The lenses were encased in the same explosion-proof housings that were used earlier. The housing cover, however, was modified to include a metal cover with a cutout (about the size of a quarter coin) for the laser beam. These LIDAR housings were connected to a positive airflow supply to push out dirt and debris from the housing and keep the lenses clean. Figure 58 provides a close-up view of the housing and air supply.

The orientation of the lenses was changed so that the LIDAR beams would point at the gauge corner, as this orientation proved effective in earlier tests.



Figure 57: Body-mounted LIDAR system onboard the track geometry car with the gauge corner beam alignment



Figure 58: LIDAR lens housing attached to an air supply to create positive air pressure inside the housing

5.2 Test Results

The LIDAR system was tested on a variety of tracks in various locations during the 5 months that it was installed onboard a track geometry car. A sample of the collected data has been analyzed to determine distance and curvature. Additionally, a preliminary attempt has been made to measure track alignment from the data.

A summary of the primary findings is presented in the following sections.

5.2.1 Speed Testing

Figure 59 shows the speed comparison for approximately 40 miles of travel. Figure 60 depicts a close-up of the same data over 1 mile of track. The results in Figure 60 reaffirm the earlier findings in that the speed measured by the LIDAR system is nearly identical to the encoder measurements. A closer look at the data in Figure 60 shows a stair-step characteristic in the encoder data, which may be caused by the differentiation computations (note that the encoder distance data is differentiated to obtain velocity), or the dynamics of the encoder itself. Nonetheless, LIDAR shows a smoother measurement of speed (LIDAR measures speed directly) than the encoder, although they both follow the same trend.

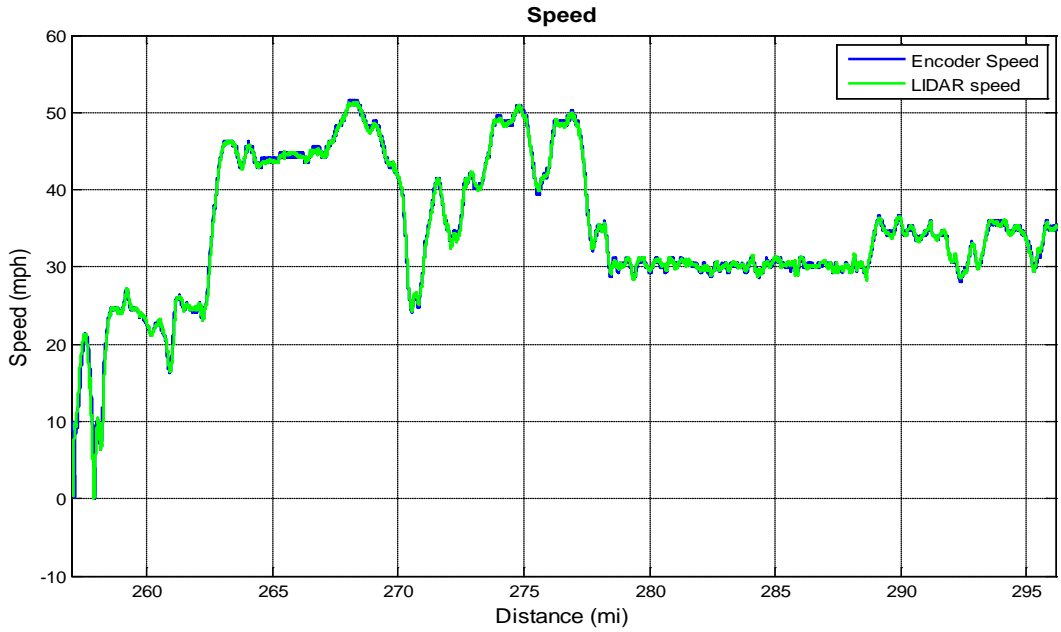


Figure 59: A comparison of encoder and LIDAR speed measurements for 40 miles of revenue service track



Figure 60: A close-up of encoder and LIDAR speed measurements from 1 mile of revenue service track

5.2.2 Curvature Track Testing

The track curvature measurements by the LIDAR system and the IMU onboard the track geometry car also confirm the ability of the LIDAR system to accurately measure track curvature in various degree curves and in real time. Figures 61 and 62 show a comparison between the two systems over a long (40 miles) and short (1 mile) section of track, respectively. Figure 61 shows that the measurements of the LIDAR system and the IMU system are the same. A close-up of the results in Figure 62 for more than 1 mile of track further shows that the curvature measurements by the two systems are nearly identical. As with the previous tests, the LIDAR system measurements show slightly greater variations in the main body of the curve, which requires further evaluation. The source of the variations may be the carbody dynamics in the curve or variations in track geometry. Proving that the variations are due to the track geometry is significant because it allows the LIDAR system to be used simultaneously for track speed and curvature measurements and track geometry assessment.

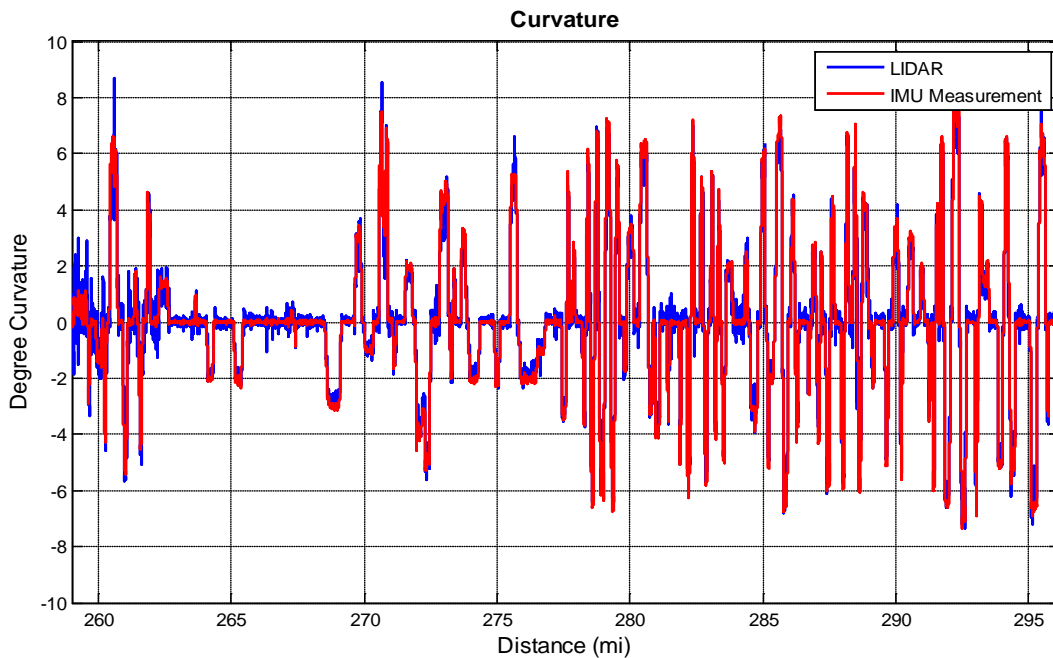


Figure 61: A comparison of IMU vs. LIDAR curvature measurements on 40 miles of revenue service track

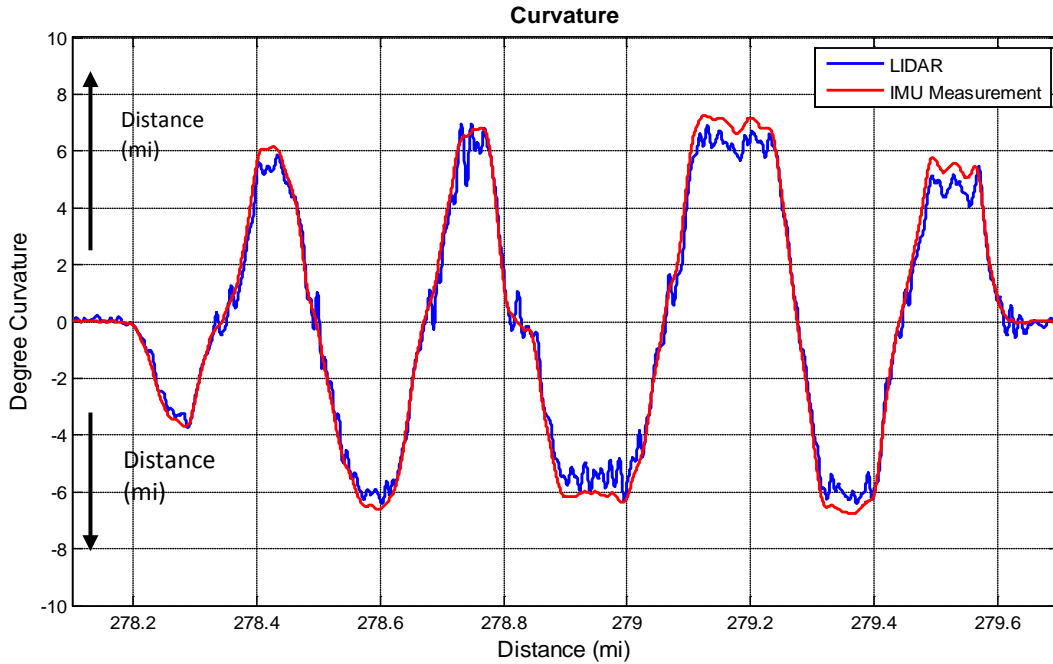


Figure 62: A comparison between LIDAR and Inertial Measurement Unit (IMU) curvature measurements on approximately 1 mile of revenue service track

5.2.3 Individual Left and Right Rail Track Measurements

The rail geometry car measurement systems can be used to individually measure the right and left rail curvature. For this calculation, the left and right alignment measurements are overlaid on top of the IMU curvature data to produce individual curve measurements for the left and right rail. The alignment measurements presented here refer to a style of curvature measurement using chord length data. That is, the curvature of the track is determined by observing the deviation (alignment offset) of the track from a reference string line 62 ft in length. For every inch of separation between the reference rail and string midpoint, the track is rated at 1 degree of curvature. Figure 63 shows the LIDAR curvature and the “IMU alignment” data. The LIDAR data shows oscillations similar to “IMU alignments,” but the curves are not an exact match. The discrepancy between the LIDAR and these alignment readings may be due to the fact that the IMU used on the track geometry car measures alignment in a different manner from LIDAR. Also, the LIDAR result consists only of one line for the right and left rail alignment, generating variation between the LIDAR and IMU data.

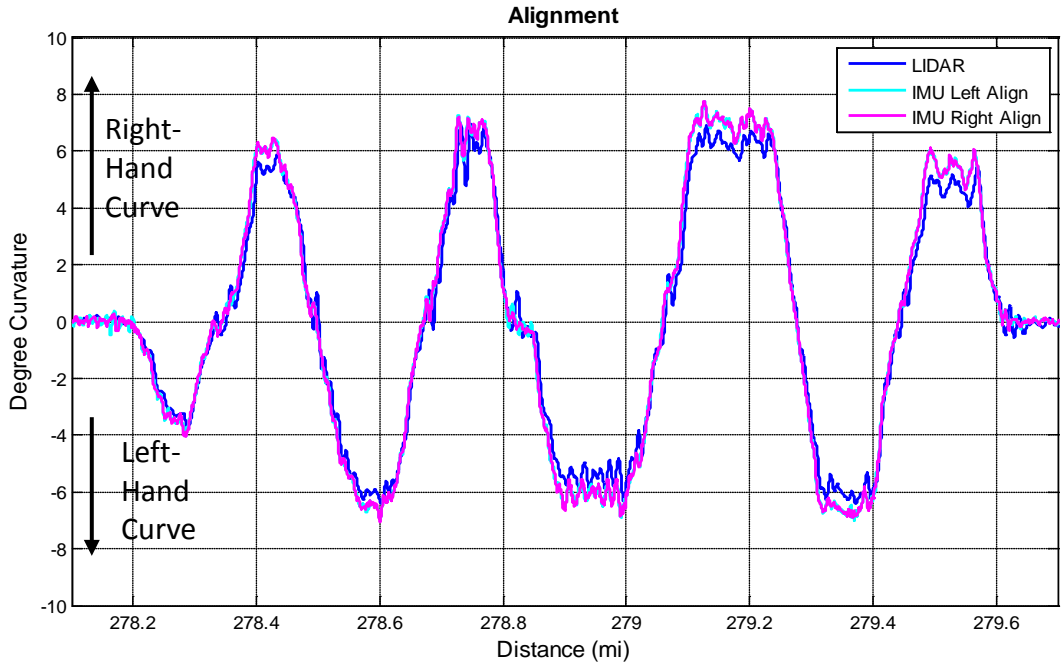


Figure 63: A comparison between LIDAR and Inertial Measurement Unit (IMU) alignment measurements on approximately 1 mile of revenue service track

6. Summary

The results of an extensive series of tests were presented in this report to evaluate the viability and applicability of LIDAR systems for measuring track speed, distance, and curvature in revenue service. The tests proved that a LIDAR system can successfully provide the intended measurements with a higher degree of accuracy than wheel-mounted encoders and IMUs that are commonly used onboard track geometry railcars. The primary advantage of the LIDAR system over the existing practice is that it can provide multifunctional, noncontact speed, distance, and curvature measures, eliminating many of the shortcomings of encoders and IMUs. Additionally, it can operate over a wider range of speeds than other measurement methods. LIDAR can provide accurate measurements at speeds between 0.5 and 100 mph, substantially extending the reliable speed range of encoders, IMUs, and other devices such as GPS.

The tests were initially conducted on the FRA's R4 Hy-Rail vehicle to assess the feasibility of the LIDAR technology and to determine the most suitable system installation configuration on a railcar. The success of the initial tests motivated a long series of tests on a track geometry measurement railcar operated by NS. The railcar tests included both a laboratory-grade system designed and developed at the RTL of VT, and a field-hardy, unmanned system jointly developed by RTL and YES. Both systems were successfully tested over several months and thousands of revenue service miles. Different system configurations and LIDAR lens arrangements were evaluated during tests that primarily included measuring track speed, distance, and curvature on revenue service tracks. Additionally, the tests included ground-truth measurements to establish the accuracy of LIDAR measurements compared with encoders.

The main findings of the study include the following:

1. The LIDAR system can successfully measure track speed and curvature in a noncontact manner in revenue service.
2. The LIDAR system can match or improve the performance of encoders that are commonly used for speed measurements, without some of the difficulties that are commonly experienced with encoders, such as susceptibility of the measurements to wheel-track induced vibrations and wheel diameter change due to wear.
3. The LIDAR system performs at least as accurately as IMUs, which are commonly used for track curvature measurement.
4. The LIDAR system can measure both track speed and curvature at train speeds as low as 0.5 mph, far below that possible with the IMUs that are currently used in track measurement railcars.
5. The LIDAR system installation onboard a track geometry car can be operated for weeks in an unmanned manner, without any need for daily maintenance of the LIDAR lenses (mounted underneath the railcar) or the central processing unit (CPU).
6. The LIDAR system can be mounted successfully to the railcar truck or body without loss of measurement sensitivity, and without requiring any changes to the railcar.

7. The measurements by the LIDAR system exhibit certain dynamics that need to be further investigated to conclusively determine if they are caused by the railcar dynamics, variations in track geometry, or both.
8. The LIDAR speed data can be converted to distance measurements that would provide the TTL foot pulse that is generally available from wheel-mounted encoders.
9. It is possible to replace the field-hardy experimental platform that is developed in this program with an analog, digital, or hybrid circuit that is application-specific to track geometry cars, as a direct retrofit to the wheel-mounted encoders that are commonly used for distance measurements.

The current study successfully demonstrated the applicability and suitability of LIDAR speeds for track measurements, however, additional efforts are needed to further investigate some of the study's findings and to possibly explore additional railroad applications. VA Tech recommends the continued research and development of the LIDAR system, including:

1. Further assessment of system accuracy. Although ground-truth calibration of the LIDAR system was performed during this study to assess the accuracy of travel distance measurements, it would be beneficial to perform a more rigorous assessment of the system for distance, track curvature, and track speed measurements. The tests must be arranged such that the LIDAR measurements can be compared against known data.
2. Evaluation of the LIDAR system's applicability for measuring track geometry. Although the data collected on revenue service track indicates that the LIDAR system could be capable of measuring some aspects of track geometry simultaneously with track speed and curvature, a more formal evaluation of the system is needed to answer the following questions:
 - a) Do the LIDAR measurements include information about track geometry?
 - b) What aspect(s) of track geometry is (are) included in LIDAR measurements?
 - c) What is the best method of processing the data to extract track geometry information in addition to track speed and curvature measurements?
3. Generate TTL foot pulse. A preliminary analysis of the LIDAR measurements indicates that it is possible to generate a foot pulse demarcation every foot, much the same as the TTL pulse by wheel-mounted encoders. A more rigorous analysis must be done to incorporate the hardware and software necessary to make the LIDAR signal mimic the TTL pulse from encoders. The work must be such that it allows LIDAR systems to ultimately become a direct retrofit to track geometry measurement systems, without the need for any major redesigns.
4. Operate the LIDAR system onboard a track geometry car. On a trial basis, install the LIDAR system with the TTL foot pulse output onboard a track geometry car (operated by FRA or one of the railroads) to assess its:
 - a) ability to work as a direct retrofit to existing encoders,
 - b) accuracy of measurements, and

c) long-term performance.

5. Provide a path to a commercially viable system. A workable and successful path to a commercially viable LIDAR system must be put in place to provide speed, TTL foot pulse, and track curvature data in a noncontact manner. The commercialization path must have sufficient details that allow FRA to contract with a suitable company to acquire the LIDAR system for its ATGMS, which is intended as the launch platform.

Appendices

Appendix A. LIDAR Beam Configurations

As shown in Figure 4, the LIDAR beams can be set up to face the gauge corner, top of rail (TOR), or web of the rail. Each of these beam configurations was used during separate tests to analyze the effect on the results. Several R4 tests used the LIDAR beam facing the web of the rail, which resulted in significant signal dropouts during special track work. Dropouts were caused by wide swing in the focal length when the lens was positioned to face the web of the rail. TOR and gauge corner lens configurations showed good performance during initial Hy-Rail testing, and therefore, each of these orientations was tested on the rail geometry cars.

During the May 2012 geometry car testing, the beams were configured for TOR with the lenses truck mounted. This configuration provided curvature readings comparable to those from the rail geometry car readings (both are shown in Figure A-1). In some sections, however, the LIDAR data appears to oscillate significantly more than the track geometry car data. This oscillation may be due to the fact that the LIDAR system is truck-mounted in this test and its output is affected by the truck dynamics in the curves. Figure A-2 displays curvature data over the same section of track with the LIDAR system carbody mounted and with the lenses facing the gauge corner. When the beams are facing the gauge corner, the LIDAR curvature results correlate well with the track geometry car measurements. Both the LIDAR TOR (truck mounted system) and the LIDAR gauge corner (body mounted system) measurements are plotted in Figure A-3. The graph shows that body mounting the LIDAR system may also contribute to smoother curvature results. The body-mounted lenses with gauge corner beam placement have resulted in the most accurate results among the various LIDAR beam orientations tested.

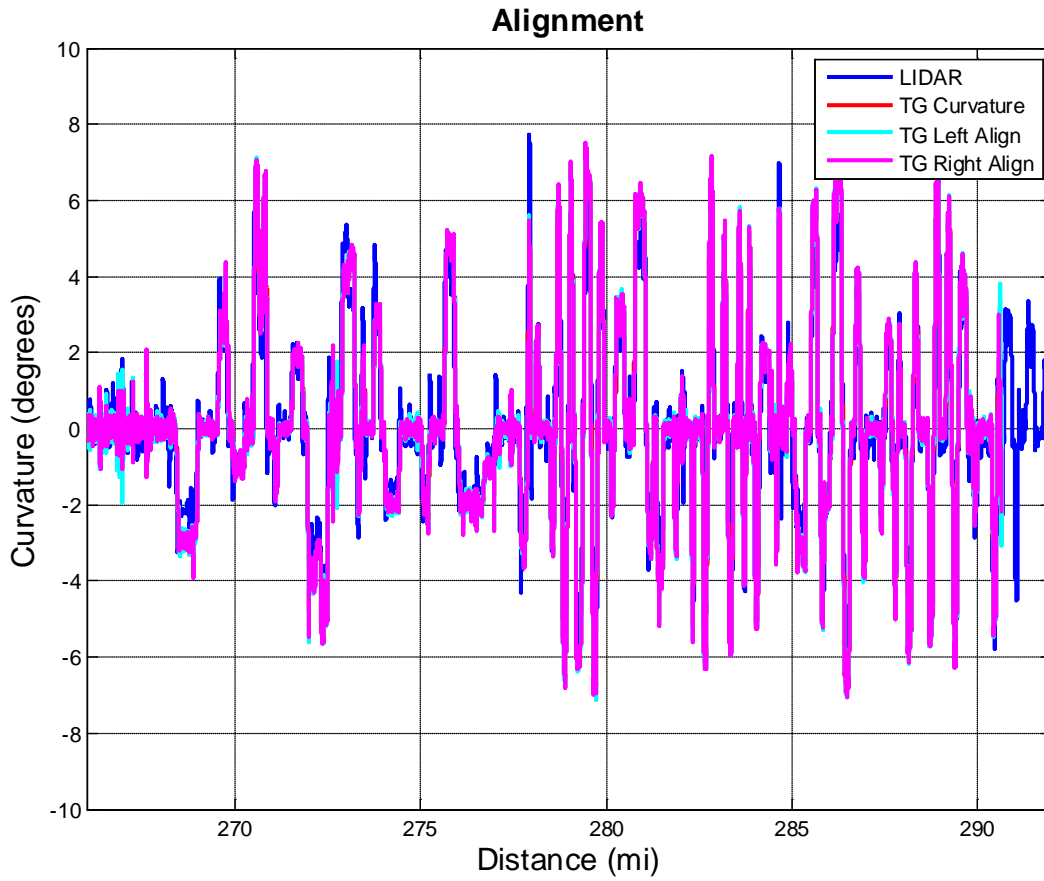


Figure A-1: Comparison of the truck mounted LIDAR facing TOR vs. track geometry car readings of curvature and left and right rail curvature readings (alignments) from May 2012

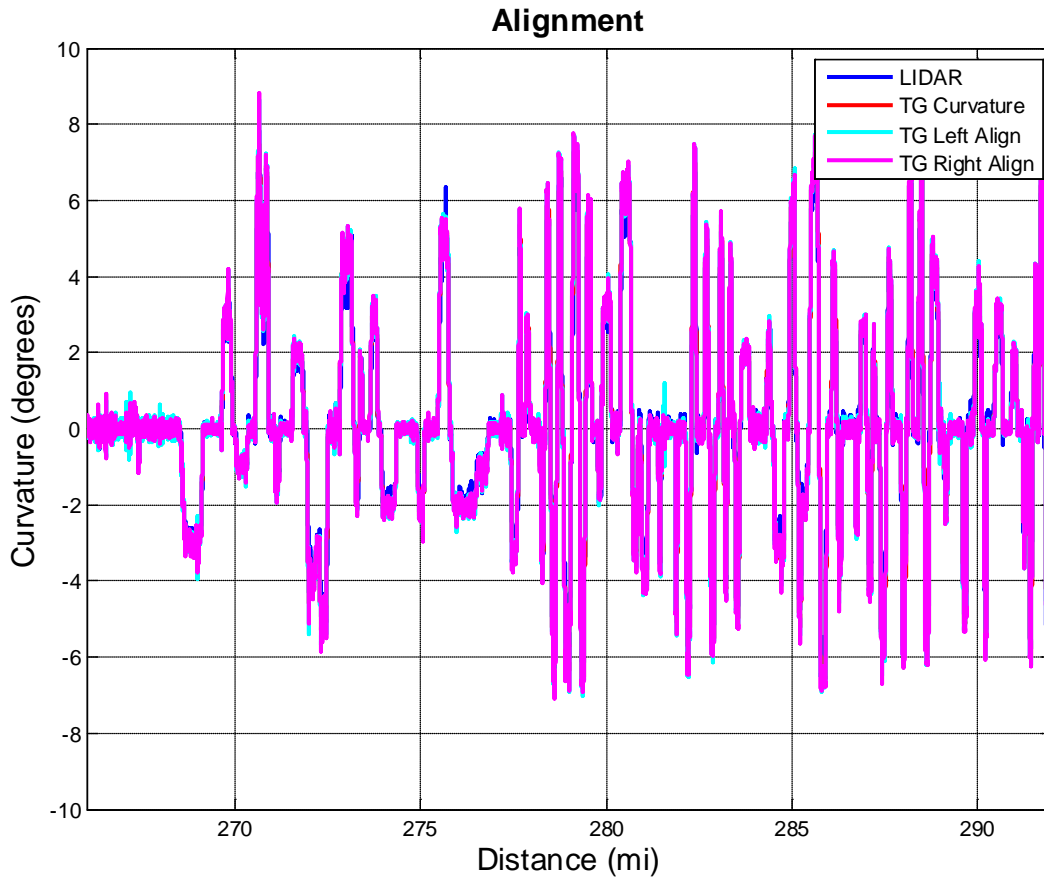


Figure A-2: Comparison of the body mounted LIDAR facing gauge corner vs. the track geometry car readings of curvature and left and right rail curvature readings (alignments) from July 2012

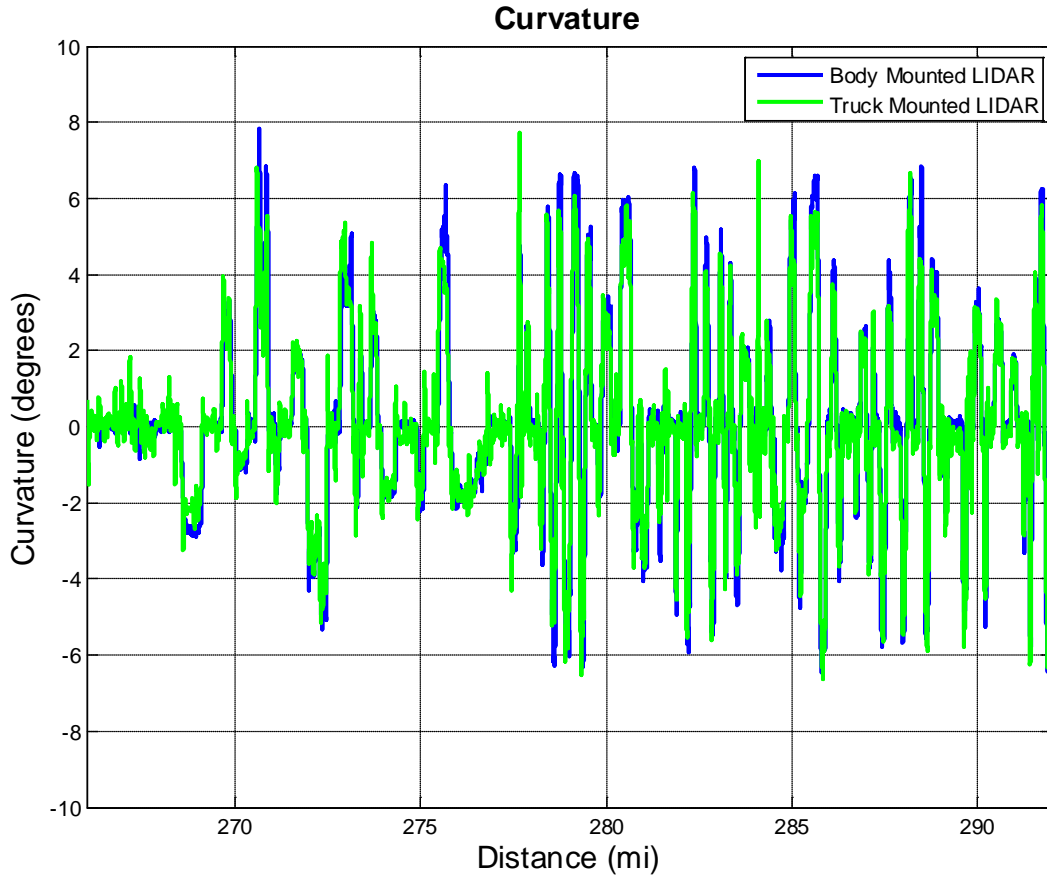


Figure A-3: A comparison of the truck mounted, TOR LIDAR and the body mounted, gauge corner LIDAR curvature measurements (approximately two months between readings)

Appendix B. Analysis of Encoder Noise in Encoder Measurements

In Section 3.3.1, the LIDAR speed data is compared with the encoder data. In Figure 24, the encoder speed data is much noisier than the LIDAR data. The unfiltered data for the 1.5-mile tangent track in Figure B-1 clearly shows that the encoder speed variation greatly increases with track speed, while the LIDAR speed variation does not suffer similar degradation. In fact, compared with encoder data, the LIDAR output contains hardly any noise.

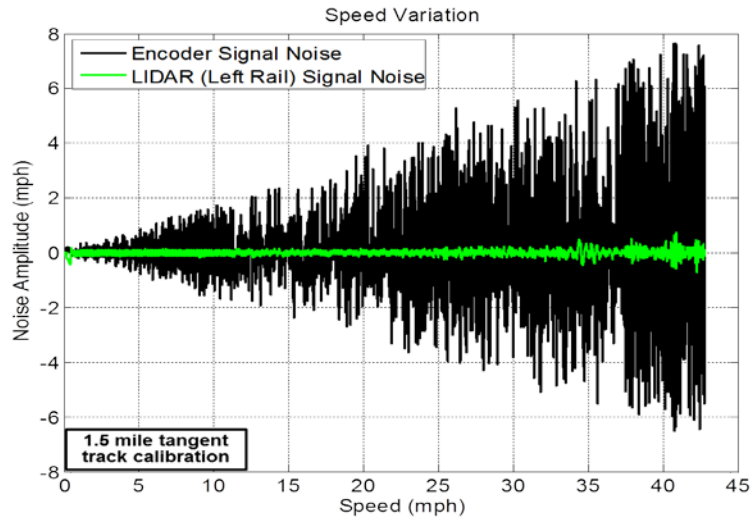


Figure B-1: Speed variation over track speed for the encoder and the LIDAR system

In an effort to decrease signal noise, the encoder was filtered with a third-order Butterworth filter with a cutoff frequency of 0.5 Hz. At 40 mph, 0.5 Hz filtering corresponds to a distance of approximately 30 ft. Figure B-2 below shows the effect of the filter to reduce noise.

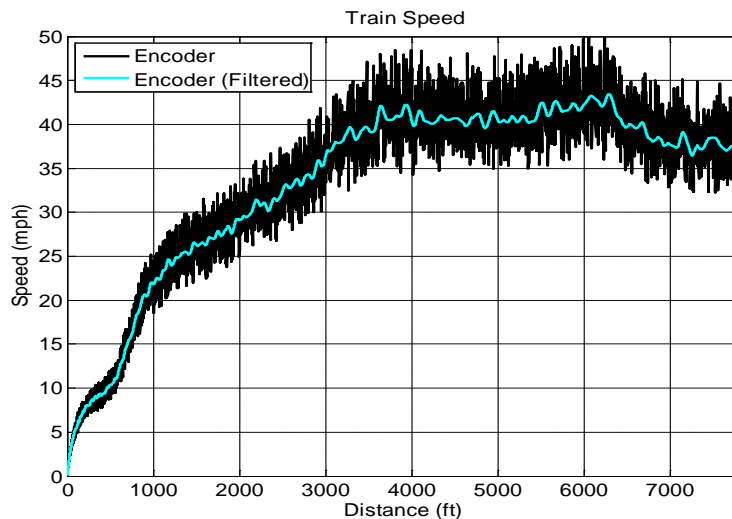


Figure B-2: Encoder filtered with third-order Butterworth with 0.5 Hz cutoff frequency

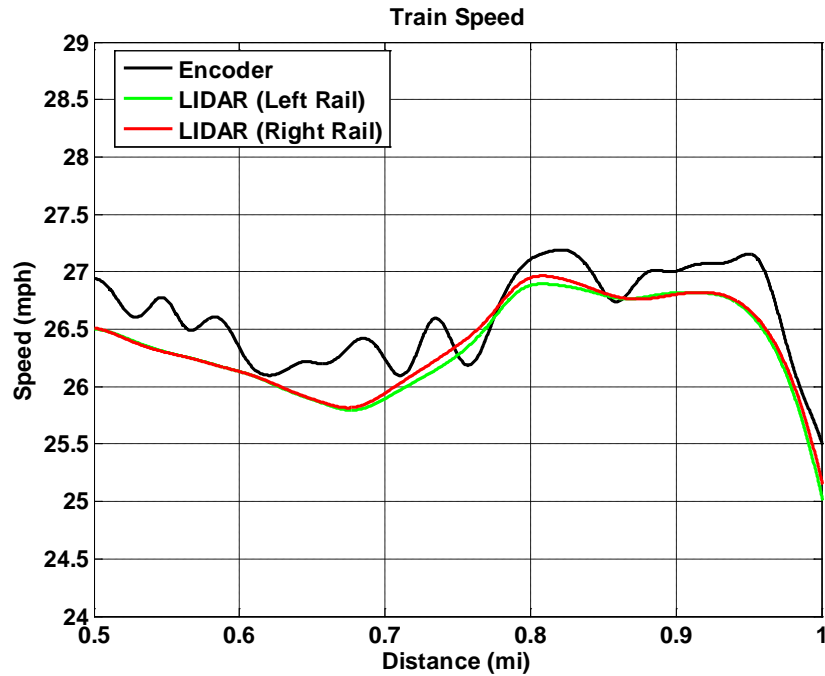
Appendix C. Rail Geometry Car Testing—Weather Summary Table

Table C-1: NOAA weather summary (Farmville) for the 4-hour inclement weather test period

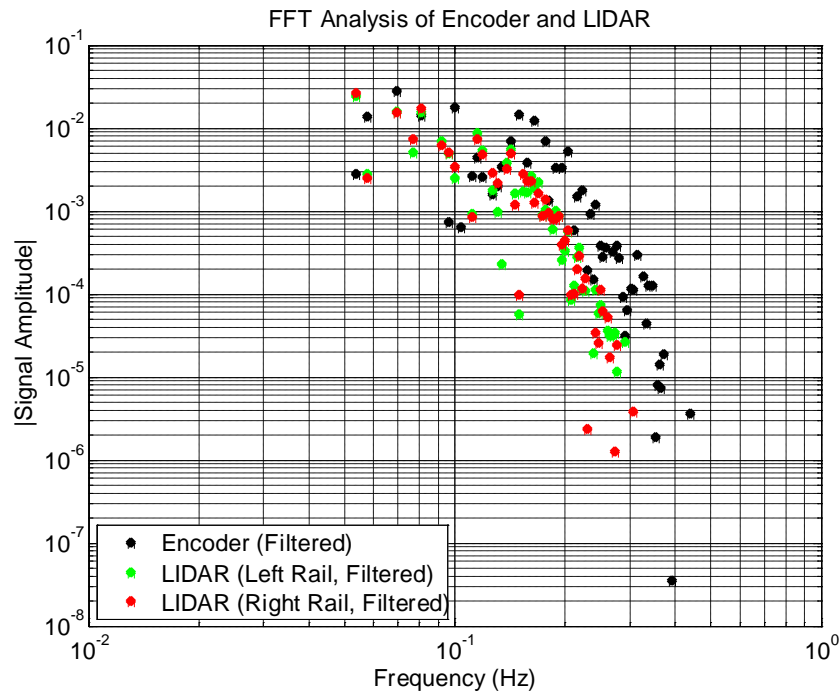
<i>Time (24hr)</i>	<i>Wind (mph)</i>	<i>Weather</i>	<i>Temperature</i>		<i>Relative Humidity</i>	<i>Precipitation 1hr</i>
			<i>Air</i>	<i>Dew point</i>		
4:35	SE 6	Light Rain	64	61	88%	0.03
4:55	SE 8 / G 16	Rain	64	61	88%	0.05
5:15	SW 16 / G 25	Heavy Rain	61	57	88%	0.14
5:35	SW 13 / G 24	Heavy Rain	57	55	94%	0.2
5:55	SW 10	Rain	55	54	94%	0.04
6:15	SW 8	Rain	55	54	94%	0.1
6:35	SW 9	Rain	55	54	94%	0.17
6:55	SW 8	Rain	55	52	88%	0.04
7:15	SW 9	Rain	54	52	94%	0.1
7:35	SW 8	Rain	54	52	94%	0.19
7:55	S 3	Rain	54	52	94%	0.01
8:15	S 6	Rain	52	52	100%	0.06
8:35	S 7	Rain	52	48	88%	0.08
8:55	S 9	Rain	52	48	88%	0.01
9:15	S 8	Rain	50	48	94%	0.05
9:35	S 9	Rain	52	48	88%	0.07
9:55	S 6	Rain	52	48	88%	0.01
10:15	S 7	Light Rain	52	48	88%	0.01
10:35	S 6	Overcast	52	48	88%	0.02

Appendix D. PXI System Testing—Frequency Content Analysis

Analyzing the frequency content of high-fidelity data records is useful for (1) quantifying the behavior of a dynamic system by identifying the major vibratory sources of the system and (2) studying the impact of those vibrations. In this study, the recorded LIDAR and encoder signals from the truck-mounted system discussed in Section 4.3.2 were put through an FFT analysis to break down the signals in terms of frequency content for a typical section of track. Figure D-1 shows the speed signals of the LIDAR and encoder systems overlaid during a half-mile section of track containing one 3.1-degree left-hand curve (from distance 0.7 to 0.85 mile) and also shows the FFT analysis of the filtered speed data.



(a)



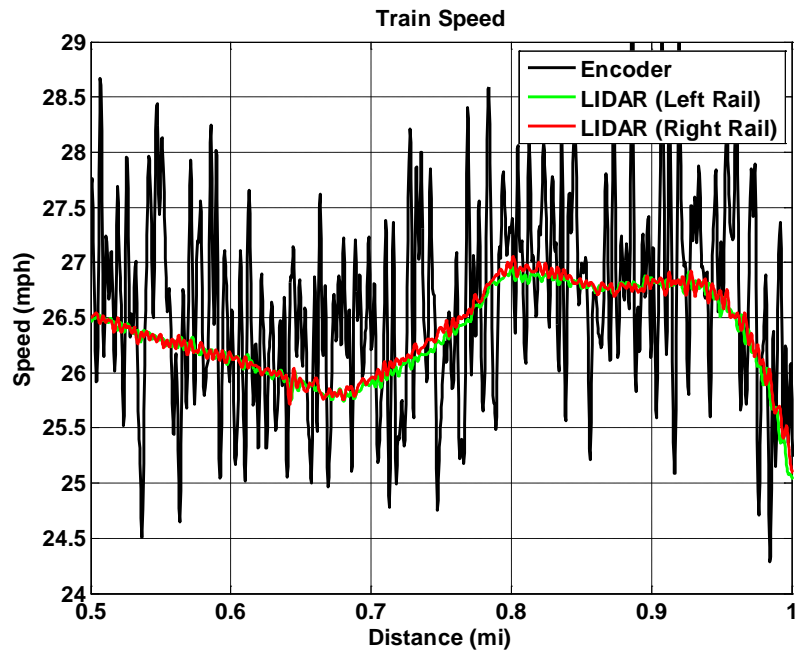
(b)

Figure D-1: LIDAR and encoder train speed on a tangent 3.1-degree left-hand curve tangent section of track (low-pass, third-order Butterworth filtered at 0.15 Hz): (a) the FFT frequency spectrum analysis of this filtered data; (b) showing a higher frequency content in the encoder data at all but the lowest frequencies

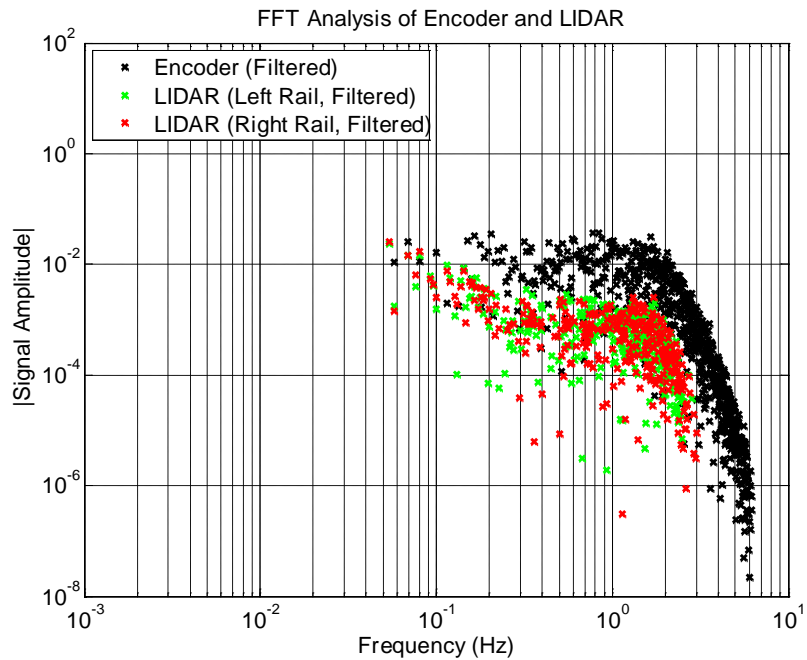
Figure D-2(a) shows the filtered data (0.15 Hz, low-pass, third-order Butterworth filter used for generating the speed plots shown in Figure 51) for the encoder, left rail LIDAR, and right rail LIDAR. In Figure D-2(b), the encoder frequency content is higher for almost all frequencies, with the exception of very low frequencies. Higher signal amplitudes at localized frequencies would typically indicate harmonic vibrations. However, for the encoder, the frequency spectrum is distributed equally across a broad range of frequencies, indicating no distinct vibration of frequency, although the encoder has a broadband noise floor significantly higher than the LIDAR system's. Because the speed in Figure D-2(a) is heavily filtered, it is beneficial to evaluate the filtered data using a higher frequency filter cutoff (see Figure D-2(a)).

Figure D-2(a) shows far more fluctuations in the encoder speed than the LIDAR over the selected 0.5 mile of track, including the 3.1-degree left-hand curve. The wheel-rail interference dynamics during curving is believed to be the primary factor contributing to the wide variations seen in the encoder output

Finally, an FFT frequency spectrum analysis is presented for the unfiltered speed signal data for the same section of track (Figure D-3). This frequency analysis shows that the broadband frequency content is significantly higher for the encoder sensor than for the LIDAR (from upward of 1 Hz). The wheel-rail interference dynamics during curving is believed to be the primary factor contributing to the broadband noise seen in the encoder output. The encoder and LIDAR speed data also covers a broad frequency spectrum, with no particular resonance peak.



(a)



(b)

Figure D-2: LIDAR and encoder train speed on a 3.1-degree left-hand curve tangent section of track (low-pass, third-order Butterworth filtered at 2 Hz): (a) the FFT frequency spectrum analysis of this filtered data; (b) again showing a higher frequency content in the encoder data at all but the lowest frequencies

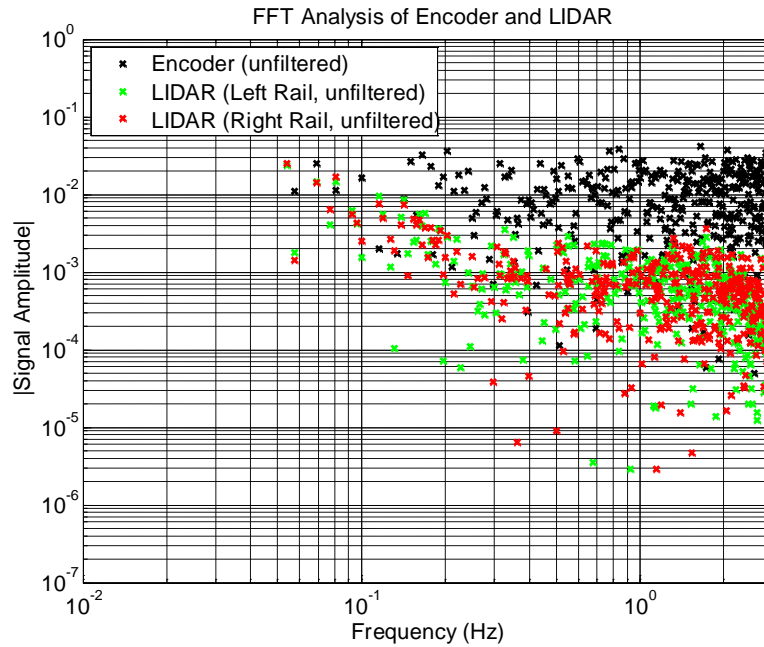


Figure D-3: A close-up of the frequency spectrum of LIDAR and encoder speed data along a 0.5-mile section of track including a 3.1-degree left-hand curve, unfiltered. This frequency analysis shows that the broadband frequency content is significantly higher for the encoder sensor (from 1 Hz upwards).

Abbreviations and Acronyms

ATGMS	Autonomous Track Geometry Measurement Systems
CPU	Central Processing Unit
CVeSS	Center for Vehicle Systems and Safety
FFT	Fast Fourier Transform
FRA	Federal Railroad Administration
GPS	Global Positioning System
IMU	Inertial Measurement Unit
KVM	Keyboard, Video, and Mouse
LDV	Laser Doppler Velocimetry
LIDAR	Light Detection and Ranging
MTTF	Mean Time to Failure
NI	National Instruments
NS	Norfolk Southern
PTC	Positive Train Control
RTL	Railway Technologies Laboratory
SNR	Signal-to-Noise Ratio
TTL	Transistor-Transistor Logic
TOR	Top of Rail
VT	Virginia Tech
YES	Yankee Environmental Systems, Inc.